NWL
TR-2796

Tech Lib

NWL TECHNICAL REPORT TR-2796
November 1972

Dr. J. E. Danberg, LFD, BRL
x4280

BODY ALONE AERODYNAMICS OF GUIDED AND UNGUIDED PROJECTILES AT SUBSONIC, TRANSONIC AND SUPERSONIC MACH NUMBERS

Frank G. Moore

U.S. NAVAL WEAPONS LABORATORY
DAHLGREN, VIRGINIA

DISTRIBUTION APPROVED FOR PUBLIC RELEASE;
DISTRIBUTION UNLIMITED.

NAVAL WEAPONS LABORATORY
Dahlgren, Virginia
22448

R. F. Schniedwind, Capt., USN
Commander

Bernard Smith
Technical Director

NWL Technical Report TR-2796
November 1972

BODY ALONE AERODYNAMICS OF GUIDED
AND UNGUIDED PROJECTILES AT SUBSONIC,
TRANSONIC AND SUPERSONIC MACH NUMBERS

by

Frank G. Moore
Surface Warfare Department

FOREWORD

This work was performed in support of the guided projectile and 5"/54 ammunition improvement programs. In additon to the above programs, support for this work was provided by the Naval Ordnance Systems Command under ORDTASK 35A-501/090-1/UF 32-323-505.

This report was reviewed by Mr. D. A. Jones, III, Head of the Aeroballistics Group, Mr. L. M. Williams, III, Head of the Ballistics Division and Mr. W. R. Chadwick, Research Aerodynamicist.

Released by:

Arthur L. Jones

Arthur L. Jones, Head
Surface Warfare Department

ABSTRACT

Several theoretical and empirical methods are combined into a single computer program to predict lift, drag, and center of pressure on bodies of revolution at subsonic, transonic, and supersonic Mach numbers. The body geometries can be quite general in that pointed, spherically blunt, or truncated noses are allowed as well as discontinuities in nose shape. Particular emphasis is placed on methods which yield accuracies of ninety percent or better for most configurations but yet are computationally fast. Theoretical and experimental results are presented for several projectiles and a computer program listing is included as an appendix.

CONTENTS

LIST OF FIGURES

LIST OF FIGURES (Cont'd)

INTRODUCTION

In the past, designers have relied on wind tunnel and ballistic range tests to predict static forces and moments on projectiles. This is not only very expensive but also quite time consuming because of the man hours required in scheduling and performing a test of the above nature. At most test facilities, there is also a backlog of work of about three to six months.

It is believed that a large portion of wind tunnel and ballistic range tests could be eliminated (particularly for preliminary and intermediate design) if an accurate theoretical method were available to compute static forces and moments throughout the Mach number range. More important though, is the practical use of such a method to the design engineer in determining the configuration which is the most optimum from a lift, drag, and pitching moment standpoint for his given design goals. Quite often, due to the lack of such a method or the funds for wind tunnel testing, less than optimum aerodynamic configurations are used to accomplish a given task. A typical example is the external shape of the 5"/38 projectile. According to the work of reference 1, the range of that projectile could have been increased by more than fifty percent with proper design.

It is the purpose then of the present work to develop a general program which can be applied to the body of the guided or unguided projectile to predict lift, drag, pitching moment, and center of pressure over the Mach number range of current interest, $0 \leq M_\infty \leq 3$. The methods used in the development of the program should be accurate enough to replace preliminary and intermediate wind tunnel tests (accuracy of ninety percent or better for most configurations) but yet should be computationally fast enough so it can be used as an efficient design tool.

There are many methods available in any particular Mach number region to compute static forces and moments on various body shapes. These methods range in complexity from exact numerical to semi-empirical and the body shapes vary from simple pointed cones to complex multi-stage launch vehicles. However, attempts at combining the various methods above into an accurate and computationally fast computer program have been scarce. Saffell, et al[2] developed a method for predicting static aerodynamic characteristics for typical missile configurations with emphasis placed on large angles of attack. However, the drag was computed by handbook techniques[3] and slender body theory was used for the lift and pitching moment. As a result, limited accuracy for body alone aerodynamics was obtained using this method.

Another method which computes forces and moments throughout the Mach number range is the GE "Spinner" program[4] designed specifically for projectiles. This program, which is based on empirical correlations as a function of nose length, boattail length, and overall length, gives very good accuracy for most standard shaped projectiles. However, its use as a design tool is somewhat limited in that the drag of a given length nose is the same no matter what ogive is present or if there are discontinuities present along the nose. The same statement applies to the boattail since a conical boattail of from 5° to 9° is assumed no matter what the boattail shape is. Moreover, no pressures can be computed by the GE program and no attempt has been made to include nonlinear angle of attack effects.

It is apparent then, from the above discussion, that there is a definite need for an analytical method which can take into account nose bluntness and ogive shape, discontinuities along the body surface, as well as nonlinear angle of attack effects. The method presented herein for accomplishing this task relies heavily on analytical work and to a lesser degree on empirical data. As such it is believed to be the first such program with major emphasis on analytical as opposed to empirical procedures.

The body shapes which the program can handle should be general enough so that most projectile and missile configurations could be handled in detail. This means that the nose may be pointed, truncated, or blunted with a spherical cap and that the nose may have two ogives present. For example, on a typical projectile the fuze has one contour and the ogive between the fuze and shoulder has a different contour with a discontinuity in between. The afterbody should consist of a cylinder followed by a boattail or flare. A typical body shape along with the coordinate systems used is shown in Figure 1.

ANALYSIS

A. Wave Drag

Wave drag results from the expansion and compression of the air as it flows over the body surface. Compression of the air is seen in the form of shock waves which first occur around Mach number 0.7 to 0.9 depending on the body shape. The methods used to calculate this form of drag differ significantly in transonic and supersonic flow and thus will be discussed individually below.

Supersonic Flow

There are several methods available for calculating the supersonic pressure distribution but only two of these methods hold promise of meeting our requirements on speed of computation and accuracy as set forth in the introduction. These methods are the second order perturbation theory of Van Dyke[5,6] and the second order shock expansion theory[7] modified for blunt bodies in reference 8. Since the major portion of the flight of most projectiles is in the lower supersonic speed regime the perturbation approach is chosen because it is more accurate than shock expansion theory at these Mach numbers. However, Van Dyke's theory can only be applied directly to bodies where the slope is less than the slope of the free-stream Mach lines. Thus for blunt-nosed configurations, the perturbation theory is combined with the modified Newtonian Theory (the means for combining the two will be discussed shortly).

Before discussing the combined perturbation Newtonian approach a brief discussion of Van Dyke's theory is helpful.

The general first order perturbation problem is: (see reference 9 for the details of the derivation):

$$\phi_{rr} + \phi_r/r + \phi_{\theta\theta}/r^2 - (M^2 - 1)\,\phi_{xx} = 0$$

$$\phi\,(0,r,\theta) = \phi_x\,(0,r,\theta) = 0 \qquad (1)$$

$$\phi_r\,(x,R,\theta) + \sin\alpha\cos\theta = R'\,[\cos\alpha + \phi_x\,(x,R,\theta)]$$

where the subscripts indicate partial differentiation. The first order problem is satisfied exactly by

$$\phi\ (x,r,\theta) = \psi\ (x,r) \cos\alpha + \zeta\ (x,r) \sin\alpha \cos\theta \tag{2}$$

where the first term corresponds to the axial flow solution and the second term to the cross flow solution. The first order problem eq. (1) can then be separated into an axial problem:

$$\begin{aligned} &\psi_{rr} + \psi_r/r - \beta^2\psi_{xx} = 0 \\ &\psi\ (0,r) = \psi_x\ (o,r) = 0 \\ &\psi_r\ (x,R) = R'\ [1 + \psi_x\ (x,R)] \end{aligned} \tag{3}$$

and a cross flow problem:

$$\begin{aligned} &\zeta_{rr} + \zeta_r/r - \zeta/r^2 - \beta^2\zeta_{xx} = 0 \\ &\zeta\ (0,r) = \zeta_x\ (0,r) = 0 \\ &1 + \zeta_r\ (x,R) = R'\ \zeta_x\ (x,R) \end{aligned} \tag{4}$$

Without going into the details, suffice it to say that the solutions of eqs. (3) and (4) are found numerically by placing a distribution of sources and doublets respectively along the x-axis.

Van Dyke then discovered a second order axial solution in terms of the first order solution ψ. Further, since disturbances in the cross flow plane do not affect the pressure as much as disturbances in the axial flow, Van Dyke reasoned that it would be quite legitimate physically to combine this second order axial solution with the first order cross flow solution of Tsien[18] to form a hybrid theory. Once the perturbation velocities ψ_x, ψ_r (second-order axial), and ζ_x, and ζ_r (first-order crossflow) are computed at each point along the body surface the local velocity components are:

$$\frac{u}{V_\infty} = (\cos\alpha)\,(1 + \psi_x) + (\sin\alpha\cos\theta)\,(\zeta_x) \tag{5a}$$

$$\frac{v}{V_\infty} = (\cos\alpha)\,(\psi_r) + (\sin\alpha\cos\theta)\,(1 + \zeta_r) \tag{5b}$$

$$\frac{w}{V_\infty} = -\,(\sin\alpha\sin\theta)\,(1 + \zeta/r) \tag{5c}$$

The pressure coefficient at each body station is then:

$$C_p\,(x,\theta) = \frac{2}{\gamma M_\infty^2}\left[\left(1 + \frac{\gamma-1}{2}\,M_\infty^2\left(1 - \frac{u^2+v^2+w^2}{V_\infty^2}\right)\right)^{\frac{\gamma}{\gamma-1}} - 1\right] \tag{6}$$

Finally the force coefficients are:

$$C_A = \frac{2}{\pi R_T^2}\int_0^{\ell}\int_0^{\pi} C_p\,(x,\theta)\,\frac{r\,dr}{dx}\;d\theta\;dx \tag{7}$$

$$C_N = -\frac{2}{\pi R_r^2} \int_0^{\ell} \int_0^{\pi} C_p (x,\theta) \cos\theta \; r \; d\theta \; dx \tag{8}$$

$$C_M = \frac{1}{\pi R_r^3} \int_0^{\ell} \int_0^{\pi} C_p (x,\theta) \cos\theta \; x \; r \; d\theta \; dx \tag{9}$$

and the center of pressure in calibers from the nose is

$$x_{cp} = - C_M / C_N \tag{10}$$

It should be pointed out that in the actual numerical integration of eqs. (7), (8) and (9) the integration must be carried out in segments of the body between each discontinuity due to the discontinuous pressure distribution.

If the nose is pointed, one need go no further. But if the nose is truncated or is blunted with a spherical cap then some other method must be used to determine the pressure distribution over the truncated portion. The method used herein is modified Newtonian theory[11]. Although this theory is derived assuming a very large Mach number, reasonable values for the pressure coefficient can be obtained over a portion of the nose even at low supersonic Mach numbers. The modified Newtonian pressure coefficient is

$$C_p = C_{p_o} \sin^2 \delta \tag{11}$$

where δ is the angle between a tangent to the local body surface and the freestream direction and where the stagnation pressure behind a normal shock is:

$$C_{p_o} = \frac{2}{\gamma M_\infty^2} \left\{ \left[\frac{(\gamma+1)\ M_\infty^2}{2} \right]^{\frac{\gamma}{\gamma-1}} \left[\frac{\gamma+1}{2\gamma M_\infty^2 - (\gamma-1)} \right]^{\frac{\gamma}{\gamma-1}} -1 \right\} \tag{12}$$

According to reference 12, if the nose is truncated then the pressure on the truncated portion is only about ninety percent of the stagnation value given by eq. (12) so that for a truncated nose:

$$C_{p_o} = \frac{2}{\gamma M_\infty^2} \left\{ 0.9 \left[\frac{(\gamma+1)\ M_\infty^2}{2} \right]^{\frac{\gamma}{\gamma-1}} \left[\frac{\gamma+1}{2\gamma\ M_\infty^2 - (\gamma-1)} \right]^{\frac{\gamma}{\gamma-1}} -1 \right\} \tag{13}$$

If the nose has a spherical cap then it can be shown that:

$$\delta = \sin^{-1}\left(\sin \beta \cos \alpha - \cos \beta \cos \theta \sin \alpha \right) \tag{14}$$

where $\tan \beta = dr/dx$.

Then combining eqs. (11) and (14) one obtains for a spherical nose cap:

$$C_p\ (x,\theta) = C_{p_o} \left(\sin^2\beta \cos^2\alpha - \sin 2\alpha \sin\beta \cos\beta \cos\theta + \cos^2\beta \cos^2\theta \sin^2\alpha \right) \tag{15}$$

where C_{p_o} is given by eq. (12).

The only question that remains now so far as the supersonic Mach number region is concerned is where does the modified Newtonian theory end on the body and where does the perturbation theory begin. To determine this match point recall that the slope of the body surface must be less than the Mach angle to apply perturbation theory, that is

$$\delta \leq \sin^{-1}\left(\frac{1}{M_\infty}\right) \tag{16}$$

Thus, the upper limit of the perturbation theory is $\delta = \sin^{-1}(1/M_\infty)$.

Using this relation in eq. (14) and assuming a spherical nose cap there is obtained for the coordinates of the point below which Newtonian theory must be applied:

$$r_u = \frac{r_n}{M_\infty}\left(\sqrt{M_\infty^2 - 1}\,\cos\alpha + \sin\alpha\right)$$

$$x_u = r_u \tan\alpha + r_n\left(1 - \frac{1}{M_\infty \cos\alpha}\right) \tag{17}$$

It is important to note here that if $x > x_u$ Newtonian theory may still be applied but if $x < x_u$ perturbation theory cannot be applied.

The limiting angle of eq. (16) corresponding to the coordinates of eq. (17) is shown in Figure 2 as the upper curve. Note that very large cone half angles can be computed using the perturbation theory at the lower Mach numbers. However, as shown by Van Dyke[5] the loss in accuracy of perturbation theory increases rapidly as the angle δ is increased. Realistically, since at an angle of 25° - 30° the error is still slight the maximum angle δ for which perturbation theory is applied should not exceed these values. Based on these

accuracy considerations, the Newtonian theory should be applied for δ values outside the solid line boundary of Figure 2 and perturbation theory within the boundary. Now the match point, which for the present work will be defined as the point where the pressure coefficients of the Newtonian theory and the perturbation theory are equal, can be determined as the solution proceeds downstream. For body stations downstream of the match point, perturbation pressures are used in the force coefficient calculations of eqs. (7), (8) and (9) whereas for x values along the surface less than that at the match point Newtonian pressures must be used.

Transonic Flow

If the flow is transonic, the available theories for the wave drag calculations are again limited. Here the main limitations are in body shape because there does not appear to be a theoretical method available which can handle the blunted nose or the discontinuities along the body surface. Wu and Aoyoma[13,14] have developed a method which handles tangent-ogive-cylinder-boattail configurations at zero angle of attack but no general nose geometries can be used as is the case in supersonic flow. Thus the approach of the present paper will be to calculate the wave drag for tangent ogive noses of various lengths throughout the transonic Mach number range and to estimate the wave drag of the more complicated nose geometry based on these results. It is true that the accuracy here is not consistent with that of the supersonic work but it appears from the results (as will be discussed later) that this approach is justified, at least for noses with slight blunting ($r_n/r_b \leq 0.3$).

For transonic flow the perturbation equation (1) has an additional term so that for $\alpha = 0$, eq. (1) is replaced by:

$$\left[1 - M_\infty^2 - (\gamma+1) M_\infty^2 \phi_x \right] \phi_{xx} + \phi_r/r + \phi_{rr} = 0 \qquad (18)$$

Eq. (18) is now nonlinear as opposed to the linear eq. (1) used in supersonic flow. Eq. (18) is again solved numerically[13] for the velocity potential and the pressure and axial force coefficients calculated by eqs. (6) and (7) for the nose of the nose-cylinder-boattail configuration. Figure 3 gives the wave drag obtained by solving eq. (18) for tangent ogive noses of various lengths throughout the transonic Mach number range. For a given Mach number and nose length, the axial force coefficient can be

obtained from this curve by interpolation. If the pressure coefficients along the body surface are desired, however, the general program of Wu and Aoyoma[13] must be used.

The pressure coefficient on the boattail at zero angle of attack in transonic flow[14] is given by:

$$C_p\,(X) = -\frac{2}{5}\,\frac{(x_1 - C)}{\sqrt{(\gamma+1)}\;M_\infty{}^{2/3}}\left[\frac{1}{25}\;\frac{(x_1 - C)^2}{(\gamma+1)\;M_\infty{}^{2/3}} - \frac{1 - M_\infty^2}{(\gamma+1)\;M_\infty^2}\right]^{1/2} - \left(\frac{dR}{dx}\right)^2 \quad (19)$$

where x_1 is measured from the shoulder of the boattail and

$$C^2 = 25\;(\gamma+1)\;M_\infty^{2/3}\left\{\frac{1}{2}\;\frac{1 - M_\infty^2}{(\gamma+1)\;M_\infty^2} + \left[\frac{5}{4}\left(\frac{1 - M_\infty^2}{(\gamma+1)\;M_\infty^2}\right)^2\right.\right.$$

$$\left.\left. + \frac{2}{M_\infty{}^{2/3}}\left(\frac{1 - M_\infty^2}{(\gamma+1)\;M_\infty^2}\right)\left(\frac{3\;dR/dx}{2\;\sqrt{\gamma+1}}\right)^{2/3} + \left(\frac{3\;dR/dx}{2M_\infty\;\sqrt{\gamma+1}}\right)^{4/3}\right]^{1/2}\right\}$$

In addition to the restriction of zero angle of attack, eq. (19) is to be applied for $1 \leq M_\infty < 1.2$ (for $M_\infty \geq 1.2$, afterbody wave drag is calculated using the previous supersonic theory for the entire body). For $M_\infty < 1$, experiment shows that the shock first occurs on a boattail at $M_\infty \approx 0.95$. Accordingly, wave drag will be assumed to vary linearly from zero at $M_\infty = 0.95$ to its maximum value at $M_\infty = 1.0$ which is calculated using the above equation.

B. Skin Friction Drag

The boundary layer will generally be turbulent over about ninety percent of the projectile body for large caliber projectiles. Since the laminar flow region is usually less than ten percent of the total surface area, it will be assumed the entire boundary layer is turbulent. Under this assumption the total or mean skin-friction coefficient, C_{f_∞}, according to Van Driest[15] must be obtained from:

$$\frac{0.242}{A\,(C_{f_\infty})^{1/2}\,(T_W/T_\infty)^{1/2}}\left(\sin^{-1} C_1 + \sin^{-1} C_2\right) = \log_{10}\left(R_{N_\infty} C_{f_\infty}\right) - \left(\frac{1+2n}{2}\right)\log_{10}\left(T_W/T_\infty\right) \quad (20)$$

where $C_1 = \dfrac{2A^2 - B}{(B^2 + 4A^2)^{1/2}}$; $C_2 = \dfrac{B}{(B^2 + 4A^2)^{1/2}}$

and $A = \left[\dfrac{(\gamma-1)\,M_\infty^2}{2\,T_W/T_\infty}\right]^{1/2}$; $B = \dfrac{1 + (\gamma-1)/2\,M_\infty^2}{T_W/T_\infty} - 1$

The variable n of eq. (20) is the power in the power viscosity law:

$$\frac{\mu}{\mu_\infty} = \left(\frac{T_W}{T_\infty}\right)^n \quad (21)$$

and n for air is 0.76. Eq. (20) assumes a fully developed turbulent boundary layer with zero pressure gradient and Prandtl number equal to one.

In order to solve eq. (20) for the mean skin friction coefficient C_{f_∞}, one must have values for T_w/T_∞, R_{N_∞}, and M_∞. The freestream Reynolds number is simply

$$R_{N_\infty} = \frac{\rho_\infty V_\infty \ell}{\mu_\infty} \tag{22}$$

To relate T_w/T_∞ to the freestream Mach number, assume the wall is adiabatic. Defining a turbulent recovery factor R_T by

$$R_T = \left(\frac{T_w}{T_\infty} - 1 \right) \frac{2}{(\gamma-1)\, M_\infty^2}$$

then

$$\frac{T_w}{T_\infty} = 1 + R_T \frac{\gamma-1}{2} M_\infty^2 \tag{23}$$

It has been shown that the recovery factor varies as the cube root of the Prandtl number (see reference 16) for turbulent flow so that:

$$R_T = \sqrt[3]{P_r} \tag{24}$$

Recall that Van Driest's Method assumes a Prandtl number of unity so if this were used then R_T would also be unity. However, the actual value of $P_r \cong 0.73$ so that the previous assumption of Prandtl number one can be compensated for somewhat by the above recovery factor which for $P_r = 0.73$ would be 0.90. Thus eq. (23) becomes:

$$T_w/T_\infty = 1 + 0.9 \frac{\gamma-1}{2} M_\infty^2 \tag{25}$$

Then for a given set of freestream conditions (M_∞, ρ_∞, μ_∞, V_∞) one can combine eqs. (22) and (25) with (20) to solve for C_{f_∞}. The equation must be solved numerically however, since C_{f_∞} cannot be solved for explicitly. A procedure adaptable to equations of this type is the well known Newton-Raphson method discussed in reference 17.

Once the mean skin friction coefficient has been determined for a given set of freestream conditions, the viscous axial force coefficient is simply:

$$C_{A_f} = C_{f_\infty} \frac{S_w}{S_r} \tag{26}$$

The wetted area S_w is the total surface area of the body which can be integrated numerically given a set of body coordinates.

C. Base Drag

Much theoretical work has been performed to predict base pressure (references 18 - 22). There is still no satisfactory theory available, however, and the standard practice has been to use empirical methods. This is the approach taken here. Figure 4 is a mean curve of experimental data from references 18, 19 and 23 - 29. This data assumes a long cylindrical afterbody with fully developed turbulent boundary

layer ahead of the base. There could be deviations from this curve due to low body fineness ratio, boattails, angle of attack, Reynolds number and surface temperature. Each of these effects will be discussed below.

The minimum length of most projectiles is about four calibers. According to references 23 and 29 the base pressure at low supersonic Mach numbers is essentially unaffected by changes in body length if the fineness ratio is greater than four. This is not true at high supersonic and hypersonic Mach numbers as shown by Love[18]. But since the main interest is for $M_\infty \leq 3$ the effect of overall fineness ratio on base pressure can be neglected.

In addition to the above, Love shows that the nose shape has little effect on base pressure for high fineness ratio bodies. Thus, for bodies of fineness ratio of four or greater the effect of nose shape and total length on base pressure can be neglected.

The base pressure is significantly altered by the presence of a boattail so that this change must be accounted for. Probably the most simple method to do this is an empirical equation given by Stoney[28],

$$C_{A_{BA}} = -C_{p_{BA}} \left(\frac{d_B}{d_r}\right)^3 \tag{27}$$

Eq. (27) can be used throughout the entire Mach number range where $C_{p_{BA}}$ is the base pressure given by the curve of Figure 4. An alternative to this procedure is to find the base pressure as a function of boattail angle and then the diameter of the base would be squared instead of cubed as in equation (27). That is

$$C_{A_{BA}} = -C'_{p_{BA}} \left(\frac{d_B}{d_r}\right)^2 \tag{28}$$

where $C'_{P_{BA}}$ is the base pressure coefficient for a given boattail angle. This requires knowing $C'_{P_{BA}}$ however which is not always available. Because of this, eq. (27) will be used.

It has been shown in many works[21,30] that the base pressure is essentially independent of Reynolds' numbers, R_N, if the boundary layer ahead of the base is fully developed turbulent flow. A turbulent boundary layer usually occurs for R_N of 500,000 to 750,000 depending on the roughness of the body surface. The minimum R_N ahead of the base one would expect to encounter on the present bodies would be about 1,000,000. Moreover, most projectiles have various intrusions and protrusions such as on a fuze which tends to promote boundary layer separation. In view of these practical considerations, Reynolds number effects on base pressure may safely be neglected.

The same arguments as the ones above hold for surface temperature as well. Thus in addition to Reynolds number effects, surface temperature effects on base pressure need not be accounted for.

The effect of angle of attack on base pressure is to lower the base pressure and hence to increase the base drag. For bodies without fins, the amount of this decrease is dependent mainly on freestream Mach number. If α is given in degrees then an empirical relation for the change in base pressure coefficient due to angle of attack is given by

$$\left[\Delta C_{P_{BA}}\right]_{\alpha} = -(.012 - .0036M_{\infty})\ \alpha \tag{29}$$

Eq. (29) was derived from a compilation of experimental data presented in Figures 7 through 15 of reference 23. The base drag coefficient thus becomes, in light of eqs. (27) and (29):

$$C_{A_{BA}} = -\left[C_{P_{BA}} - (.012 - .0036M_{\infty})\alpha\right]\left(\frac{d_B}{d_r}\right)^2 \tag{30}$$

D. Viscous Separation and Rotating Band Drag

Figure 5A is a plot of forebody drag coefficient as a function of cone half angle from data taken from reference 31. Since the skin friction drag coefficient is about 0.02 for this case, it can be subtracted from the curve of Figure 5A to yield the pressure drag coefficient. Note that the freestream Mach number is 0.4, low enough so that no appreciable compressibility effects occur. The question therefore arises as to the origin of this type of drag, since it is not compressibility or skin friction drag. It is in fact viscous separation drag. For very large cone half angles, θ_c, the flow over the cone, instead of remaining attached, separates due to the very strong adverse pressure gradient and reattaches downstream. This separation prevents the pressure from decreasing as much as it would in inviscid flow and produces a drag. Oddly enough, this phenomenon does not occur on ogives or on spherical surfaces, apparently due to body curvature effects on the boundary layer. As a result, one can derive an empirical expression for this viscous separation drag, where the important parameter is the angle δ^* which the nose makes with the shoulder of the afterbody. Based on Figure 5A this relation is

$$C_{A_{vis}} = \begin{cases} .012\,(\delta^* - 10°); & \delta^* \geq 10° \\ 0; & \delta^* < 10° \end{cases} \qquad (31)$$

with δ^* in degrees and with $\delta^* = \theta_c$ for a conical nose.

Reference 1 gives the measured effect of a rotating band on drag. The particular rotating band used in those wind tunnel tests had a mean height of about 0.024 calibers. An expression which functionalizes the above results for drag increment due to a rotating band is given by:

$$C_{A_{RB}} = (\Delta C_A)\ (H)/.01 \qquad (32)$$

where H is the mean height of the band in calibers and ΔC_A is the increment in axial force for an H of 0.01 caliber given in Figure 5B. Although the eq. (32) was derived for a particular band, it checks well with the results of Charters[32] for a different band geometry.

E. Inviscid Lifting Properties

At supersonic Mach numbers the inviscid lift, pitching moment, and center of pressure are calculated using Tsien's first order cross flow theory which was discussed earlier in conjunction with Van Dyke's second order axial solution. This method is adequate for small angles of attack where viscous effects are negligible.

At subsonic and transonic Mach numbers the lifting properties are more difficult to obtain. For subsonic velocities the lift could be calculated by perturbation theory[33] but since projectiles rarely fly at Mach numbers less than 0.7, a formulation on this basis was not justified. An alternative would be slender body theory but the accuracy of this approach is inadequate. In light of the above reasoning, a semi-empirical method for normal force characteristics was derived based on nose length, afterbody length, and boattail shape. This method was then extended through the transonic Mach number range since the state-of-the-art in transonic flow does not allow one to handle the general body shapes or flow conditions.

The total inviscid normal force acting on the body may be written

$$C_{N_\alpha} = (C_{N_\alpha})_n + (C_{N_\alpha})_a + (C_{N_\alpha})_B \qquad (33)$$

where the subscripts n, a, and B stand for nose, afterbody, and boattail respectively. The first term of eq. (33) can be approximated by

$$(C_{N_\alpha})_n = C_1 \tan \delta^* + C_2 \qquad (34)$$

where C_1 and C_2 are given in Figure 6 as a function of Mach number. This relationship was determined empirically from the cone results of Owens[31]. It is approximately correct for $\ell_n \geq 1.5$, cone bluntness up to 0.5, and $M_\infty \leq 1.2$. Note that the angle δ^* in eq. (34) is the same as that discussed previously in eq. (31).

The normal force coefficients of the afterbody and boattail can be obtained from Figures 7 and 8 respectively. Figure 7 was derived analytically in the transonic Mach range from the method of Wu and Aoyoma[13] and in subsonic flow from the experimental data of Spring[34] and Gwin[35]. In the work of Spring and Gwin above, the normal force of the nose plus afterbody was given but the nose component can be subtracted off by the use of eq. (34). The boattail normal force coefficient was given by Washington[36] but he stated that there was not enough data available in subsonic and transonic flow. Hence the data of Washington was supplemented by the 175mm Army projectile[37] and Improved 5"/54 Navy projectile[38] data to derive the general curve of Figure 8.

Although slender body theory may not be adequate for predicting the normal force coefficient it appears to predict the center of pressure of the nose and boattail lift components quite adequately. According to slender body theory the center of pressure of the nose is

$$(x_{cp})_n = \ell_n - \frac{(Vol)_n}{\pi R_r^2} \tag{35}$$

and of the boattail

$$(x_{cp})_B = \ell_n + \ell_a + \ell_B - \frac{(Vol)_B}{\pi R_r^2}$$

or

$$(x_{cp})_B = \ell - \frac{(Vol)_B}{\pi R_r^2} \tag{36}$$

The center of pressure of the afterbody normal force was calculated analytically by the method of Wu and Aoyoma in transonic flow and assumed to have the same value in subsonic flow. Figure 9 is a plot of $(x_{cp})_a/\ell_a$ versus afterbody length measured at the point where the afterbody begins. Now knowing the individual lift components and their center of pressure locations, one can compute the pitching moment about the nose as:

$$C_{M_\alpha} = -\left[(C_{N_\alpha})_n (x_{cp})_n + (C_{N_\alpha})_a (x_{cp})_a + (C_{N_\alpha})_B (x_{cp})_B \right] \tag{37}$$

F. Viscous Lifting Properties

Strictly speaking, the previous discussion on inviscid lifting properties gave C_{N_α} and C_{M_α} at $\alpha = 0$ only. If $\alpha > 0$ then there is a nonlinear contribution to lift and hence pitching moment due to the viscous crossflow of velocity $V = V_\infty \sin \alpha$. Allen and Perkins[39] list these contributions as:

$$(\Delta C_N)_{vis} = \eta c_{d_c} \frac{S_p}{S_r} \alpha^2 \tag{38}$$

$$(\Delta C_M)_{vis} = -\eta \, c_{d_c} \left(\frac{S_p}{S_r} \right) (x_p) \quad \alpha^2 \tag{39}$$

where η and c_{d_c} are given in Figure 10. Note that the cross flow drag coefficient is here taken to be a function of Mach number only and the cross flow Reynolds number dependence is not accounted for. The center of pressure of the entire configuration should then be:

$$x_{cp} = - \frac{C_M + (\Delta C_M)_{vis}}{C_N + (\Delta C_N)_{vis}} \tag{40}$$

G. Summary

Figure 11 gives a summary of the various methods used in each particular Mach number region to compute the static aerodynamics. As may be seen, major emphasis has been placed on analytical as opposed to empirical procedures.

RESULTS AND DISCUSSION

A. Numerical Solutions

A computer program was written in Fortran IV for the CDC 6700 computer to solve the various equations discussed in the analysis section by numerical means. The various methods used for each individual equation are the same as those discussed in the references pertaining to the particular equation and will not be repeated here. However, mention should be made of the fact that the step size used in the hybrid theory of Van Dyke was considerably smaller than he suggested, particularly for a blunt nosed body or behind a discontinuity. For example, for the most complicated body shapes as many as 200 points were placed along the body surface. Also slight oscillations in the second order solution were found behind a corner although Van Dyke does not mention these details.

Quite often, it was necessary to evaluate an integral numerically or to compute the value of a function and its derivative at a given point. The integration was carried out using Simpson's rule; the interpolation and differentiation using a five point Lagrange scheme[17]. Both methods have truncation errors which are consistent with the accuracy of the governing set of flow field equations.

The computational times depend on how complicated the body shapes are and the particular Mach number of interest. The longest computational time for the most general body shape computed was less than half a minute for one Mach number. For most configurations the average time is about fifteen seconds per Mach number for $M_\infty \geq 1.2$ and about five seconds per Mach number for $M_\infty < 1.2$. This assumes of course that a table look-up procedure is used in the transonic region where the curves of Figure 3 are input as data sets as opposed to solving the nonlinear partial differential equation (18) for each Mach number. If the aerodynamic coefficients of a given configuration are desired throughout the entire Mach number range, an average execution time of two minutes is required for most configurations (ten Mach numbers).

A detailed discussion of the computer program is included as Appendix A. The various input and output parameters are defined and a listing of the program along with a sample output are also included for the reader's convenience.

B. Comparison with Experiment

The only new method presented in the current work is the combined perturbation - Newtonian theory for blunt bodies. It is thus of interest to see how the pressure coefficients along the

surface compare with experimental data. Figures 12 and 13 present two typical comparisons at $M_\infty = 1.5$ and 2.96. The experimental data is taken from reference 8 which combined modified Newtonian theory with shock expansion theory to compute forces on blunted cones. The asymptotes of the pressure coefficient in each of the planes computed by the method of reference 8 are also indicated on the figures. As seen in the figures the present theory predicts the aerodynamics much better than shock expansion theory at $M_\infty =$ 1.5 and is about the same as the shock expansion approach at $M_\infty =$ 2.96. The reason for this is that the basic perturbation theory was derived assuming shock free flow with entropy changes slight; hence the theory should be most accurate in the lower supersonic speed regime. On the other hand, shock expansion theory was derived assuming a shock present and so one would expect this method to be better than perturbation theory as M_∞ is increased. Apparently, the crossover point is around $M_\infty = 2.5$ to 3.0 so that for the major portion of the supersonic speed range of interest in the present analysis, perturbation theory is more accurate.

Another interesting point in Figure 12 is the discontinuity in slope of the pressure coefficient curve which occurs at the match point. This is because in the expansion region on the spherical nose the perturbation pressure decreases much more rapidly than the Newtonian theory and as a result the overexpansion region, which occurs at low supersonic Mach numbers, is accounted for quite well. Note that the match point is different in each plane around the surface ($x \cong 0.11$ to 0.14).

One of the questions which arises in the development of a general prediction method pertains to accuracy. To answer this question, force coefficients for several cases were computed embracing variations in nose bluntness, Mach number, angle of attack, nose length, and afterbody length. These cases are presented in Figures 14 through 19 along with experimental data.

The first of these cases (Figure 14) gives the axial force coefficient, normal force coefficient derivative, and pitching moment coefficient derivative as a function of nose bluntness for a simple blunted cone configuration. Note that the axial force coefficient includes only the wave plus skin friction components because the base drag was subtracted out of the given set of experimental data. An important point here is that very good accuracy is obtained- even for large bluntness ratios. For example, with bluntness $r_n/r_B = 0.6$, the force coefficients are in error by less than fifteen percent (this is assuming of course there is no error associated with the experimental data which is not exactly correct). This tends to verify that a combined perturbation-Newtonian theory can be used successfully for blunt configurations even at low supersonic Mach numbers.

The next two figures, Figures 15 and 16, compare the theoretical static aerodynamic coefficients with experiment as a function of Mach number for blunted cones with bluntness ratios of 0.2 and 0.406 respectively. Also included in Figure 15 is the slender body theory. As seen by the error comparisons at the lower part of Figure 15, accuracies of better than 90 percent can be obtained throughout the supersonic Mach number range for the force coefficients. Figure 16 gives the aerodynamic data throughout the Mach number range of interest. Again the comparison is favorable even though the transonic wave drag was computed for a tangent ogive having a length equal to that of the blunted cone. The bluntness causes the transonic drag rise to start at a lower Mach number and to be less abrupt than for the pointed tangent ogive.

The third vairable of interest is angle of attack. Figure 17 presents the results for a tangent ogive cylinder of nose length six calibers and total length fourteen calibers. Two Mach numbers are considered, $M_\infty = 1.5$ and $M_\infty = 2.5$. Again the results are quite good, except at very large angles of attack.

Figure 18 compares the force coefficients of the present theory with experiment for a pointed cone of various lengths. Also shown for comparison with the $M_\infty = 1.5$ case is the slender body theory. Although perturbation theory is usually associated with nose slenderness ratios of two and greater, it may, nevertheless, be seen that fair accuracy is obtained for lengths as low as one. This corresponds to a cone half angle of about twenty-five degrees which is the limiting angle used in the combined perturbation - Newtonian theory as shown in Figure 2. For the $M_\infty = 0.5$ case eq. (31) is used to calculate the viscous separation drag which is added to the skin friction drag to get the total forebody drag coefficient. Using this simple formula, excellent agreement with experimental data is obtained

The final variable of interest, afterbody length, is examined in Figure 19. The nose of the body is a 2.83 caliber tangent ogive. For zero afterbody length, the theory agrees with experiment very well. However, as the afterbody length increases the theory underestimates the afterbody lift at the lower supersonic Mach numbers for short afterbody lengths and at the higher Mach numbers for long afterbody lengths. This loss in lift predicted by the inviscid theory was also found by Buford[40] and he attributed it to boundary layer displacement effects. Even so, the present theory is superior to slender body theory which gives zero lift due to an afterbody.

To summarize the previous five figures, one could say in general that accuracies of ninety percent or better can be obtained for force coefficients of most configurations. However, for extreme cases,

such as very large nose bluntness or angle of attack, the accuracy will be decreased and the amount of this decrease can be approximated from Figures 14 through 19.

The next several figures compare theory with experiment for several spin stabilized projectiles. Figures 20, 21 and 22 are Navy projectiles: the 5"/38 RAP (Rocket Assisted Projectile)[41], the 5"/54 projectile [42], and the improved 5"/54 projectile[38], which has a longer nose and boattail than the standard 5"/54. Figures 23 and 24 are Army shapes: the 175mm[37] and 155mm[43] projectiles respectively. For the detailed drawings and other aerodynamics of these shapes the reader is referred to the references cited above.

The theoretical zero lift drag curve of the 5"/38 RAP projectile along with three sets of experimental data[1] and an NWL empirically derived curve are shown in Figure 20. Note that the experimental data varies by about thirty percent for $M_\infty < 1$ and by ten percent for $M_\infty > 1$. The theoretical curve tends to support the BRL data subsonically and the NOL and NWC data supersonically. The numbers in parenthesis are the factors by which the drag curves must be multiplied throughout the flight of the projectile to match actual range firings. The NWL empirical curve is the curve which is actually used in range predictions due to the failure of experimental data to predict an adequate drag curve. This empirical curve was derived from actual range firings. It should be, therefore, slightly high because of yaw induced effects. The important point here is that for this particular shell, the theory agrees better with actual range firings than any of the sets of experimental data.

Figures 21 and 22 give the static aerodynamic coefficients for the 5"/54 RAP and the improved 5"/54 projectiles. The 5"/54 RAP has a nose length of about 2.5 calibers and a boattail of 0.5 calibers whereas the improved round has a 2.75 caliber nose and a 1.0 caliber boattail. Also the 5"/54 RAP has a rotating band whereas the other shell does not. For both shells, excellent agreement with experimental data is obtained for the drag coefficient throughout the entire Mach number range. Fair agreement is obtained for normal force coefficient and hence pitching moment and center of pressure. The comparison for the lifting properties is Mach number dependent: in the low supersonic region the theory is consistently about ten percent low on normal force whereas at high supersonic speeds it compares very well with experiment. The reason, as already mentioned, is the failure of the inviscid theory to predict afterbody lift correctly at low supersonic Mach numbers. At subsonic and transonic Mach numbers, the theory does about as well as could be expected considering that there was a considerable amount of empirical work in that region.

For boattailed configurations, such as the 5"/54 RAP and the Improved 5"/54, it was found necessary to account approximately for the thick boundary layer on the boattail. This was done by viewing the unpublished shadow graphs obtained in conjunction with the work of reference 38. Apparently, a maximum boattail angle of six degrees can be allowed before boundary layer separation takes place. In addition, the boundary layer displacement thickness accounts for another about 1/4 - 1/2 degree decrease in the effective boattail angle. These two results were used to determine effective boattail angles on all boattailed configurations. Without this approximate accounting of the boundary layer effect on the boattail shape, the lifting properties would have been in error by an additional ten percent for boattailed configurations.

The final two shells, the 175 and 155mm, are considered in Figures 23 and 24. Again, excellent drag predictions are made by the theory and good predictions are made for normal force and center of pressure. Intuitively, one would expect the axial force to agree better with experiment than the lift because a second order approach is used in supersonic flow for the axial forces whereas a first order cross-flow theory is used for the normal forces.

Figure 25 presents theoretical results for the five-inch guided projectile. The nose is about sixty percent blunt with two different ogive sections. The overall length is 10.58 calibers with a 0.66 caliber boattail, 7.24 caliber afterbody and 2.68 caliber nose. Although no experimental data is currently available for this extreme case, it is expected that the theory is accurate to within ten percent on axial force and twenty percent on lifting properties.

CONCLUSIONS

1. A general method has been developed consisting of several theoretical and empirical procedures to calculate lift, drag, and pitching moment on bodies of revolution from Mach number zero to about three and for angles of attack to about twenty degrees.

2. Comparison of this method with experiment for several configurations indicates that accuracies of ninety percent or better can be obtained for force coefficients of most configurations. This is at a cost of about $30. for ten Mach numbers in the range $0 \leq M_\infty \leq 3$.

3. A second order axial perturbation solution can be combined with modified Newtonian theory to adequately predict pressures on general shaped bodies of revolution. This is true for Mach numbers as low as 1.2 even though Newtonian theory was derived for high Mach number flow.

4. A first order inviscid crossflow solution is not sufficient to predict afterbody or boattail lift at low supersonic Mach numbers. However, when account is made for the boundary layer, markedly improved results for boattail lift was obtained.

5. There is still no adequate theory available in transonic flow which is computationally fast and accurate and can consider blunt nosed configurations with discontinuities along the ogive. Thus more research needs to be directed along these lines.

REFERENCES

1. Moore, F. G.: "A Study to Optimize the Aeroballistic Design of Naval Projectiles", NWL TR-2337, September 1969.

2. Saffell, B. F., Jr.; Howard, M. L.; Brooks, E. N., Jr.: "A Method for Predicting the Static Aerodynamic Characteristics of Typical Missile Configurations for Angles of Attack to 180 Degrees", NSRDC Report 3645, 1971.

3. Douglass Aircraft Co., Inc.: USAF Stability and Control DATCOM, Revisions by Wright Patterson Air Force Base, July 1963, 2 vols.

4. Whyte, R. H.: "'Spinner' - A Computer Program for Predicting the Aerodynamic Coefficients of Spin Stabilized Projectiles", General Electric Class 2 Reports, August 1969.

5. Van Dyke, M. D.: "A Study of Second-Order Supersonic Flow Theory", NACA Report 1081, 1952.

6. Van Dyke, M. D.: "Practical Calculation of Second-Order Supersonic Flow Past Nonlifting Bodies of Revolution", NACA TN-2744, July 1952.

7. Syvertson, C. A.; Dennis, D. H.: "A Second-Order Shock-Expansion Method Applicable to Bodies of Revolution Near Zero Lift", NACA Report 1328, 1957.

8. Jackson, C. M., Jr.; Sawyer, W. C.; Smith, R. S.: "A Method for Determining Surface Pressures on Blunt Bodies of Revolution at Small Angles of Attack in Supersonic Flow", NASA TN D-4865, November 1968.

9. Van Dyke, M. D.: "First and Second-Order Theory of Supersonic Flow Past Bodies of Revolution", JAS, Vol. 18, No. 3, March 1951, pp. 161-179.

10. Tsien, H. S.: "Supersonic Flow Over an Inclined Body of Revolution", JAS, Vol. 5, No. 12, October 1938, pp. 480-483.

11. Truitt, R. W.: Hypersonic Aerodynamics, The Ronald Press Company, New York, 1959.

12. Tetervin, Neal: "Approximate Analysis of Effect on Drag of Truncating the Conical Nose of a Body of Revolution in Supersonic Flow", NOL TR 62-111, December 1962.

13. Wu, J. M.; Aoyoma, K.: "Transonic Flow-Field Calculation Around Ogive Cylinders by Nonlinear-Linear Stretching Method", U. S. Army Missile Command Technical Report No. RD-TR-70-12, April 1970. Also AIAA 8th Aerospace Sciences Meeting, AIAA Paper, 70-189, January 1970.

14. Wu, J. M.; Aoyoma, K.: "Pressure Distributions for Axisymmetric Bodies with Discontinuous Curvature in Transonic Flow", U. S. Army Missile Command Technical Report No. RD-TR-70-25, November 1970.

15. Van Driest, E. R.: "Turbulent Boundary Layer in Compressible Fluids", JAS, Vol. 18, No. 3, 1951, pp. 145-160, 216.

16. Truitt, R. W.: Fundamentals of Aerodynamic Heating, The Ronald Press Company, New York, 1960.

17. Carnahan, B.; Luther, H. A.; Wilkes, J. O.: Applied Numerical Methods, John Wiley and Sons, Inc., New York, 1969.

18. Love, E. S.: "Base Pressure at Supersonic Speeds on Two-Dimensional Airfoils and on Bodies of Revolution with and without Turbulent Boundary Layers", NACA TN 3819, 1957.

19. Chapman, D. R.: "An Analysis of Base Pressure at Supersonic Velocities and Comparison with Experiment", NACA TR 1051, 1951.

20. Cartright, E. M., Jr.; Schroeder, A. H.: "Investigation at Mach Number 1.91 of Side and Base Pressure Distributions Over Conical Boattails Without and With Jet Flow Issuing From Base", NACA RM E51F26, 1951.

21. Kurzweg, H. H.: "Interrelationship Between Boundary Layer and Base Pressure", JAS, No. 11, 1951, pp. 743-748.

22. Crocco, L.; Lees, L.: "A Mixing Theory for the Interaction Between Dissipative Flows and Nearly-Isentropic Streams", Report No. 187, Princeton University, Aero. Engr. Lab; 1952.

23. Bureau of Naval Weapons: "Handbook of Supersonic Aerodynamics", NAVWEPS Report 1488, Vol. 3, 1961.

24. Reller, J. O., Jr.; Hamaker, F. M.: "An Experimental Investigation of the Base Pressure Characteristics of Nonlifting Bodies of Revolution at Mach Numbers from 2.73 to 4.98", NACA TN 3393, 1955.

25. Peck, R. F.: "Flight Measurements of Base Pressure on Bodies of Revolution with and without Simulated Rocket Chambers", NACA TN 3372, 1955.

26. Fraenkel, L. E.: "A Note on the Estimation of the Base Pressure on Bodies of Revolution at Supersonic Speeds," Royal Aircraft Establishment TN No. AERO 2203, 1952.

27. U. S. Army Missile Command: Engineering Design Handbook: Design of Aerodynamically Stabilized Free Rockets, AMCP 706-280, 1968.

28. Stoney, W. E., Jr.: "Collection of Zero-Lift Data on Bodies of Revolution from Free-Flight Investigations", NASA TR R-100, 1961.

29. Kurzweg, H. H.: "New Experimental Investigations on Base Pressure in the NOL Supersonic Wind Tunnels at Mach Numbers 1.2 to 4.24", NOL Memo 10113, 1950.

30. Krens, F. J.: "Full-Scale Transonic Wind Tunnel Test of the 8-Inch Guided Projectile", NWL TR-2535, 1971.

31. Owens, R. V.: "Aerodynamic Characteristics of Spherically Blunted Cones at Mach Numbers from 0.5 to 5.0", NASA TN D-3088, December 1965.

32. Charters, A. C.: "Some Ballistic Contributions to Aerodynamics", 14th Annual Meeting of IAS, New York, January 1946.

33. Karamcheti, K.: Principles of Ideal-Fluid Aerodynamics, John Wiley and Sons, Inc., New York, 1966.

34. Spring, D. J.: "The Effect of Nose Shape and Afterbody Length on the Normal Force and Neutral Point Location of Axisymmetric Bodies at Mach Numbers from 0.80 to 4.50", U. S. Army Missile Command Report No. RF-TR-64-13, 1964.

35. Gwin, H.; Spring, D. J.: "Stability Characteristics of a Family of Tangent Ogive-Cylinder Bodies at Mach Numbers from 0.2 to 1.5", U. S. Army Missile Command, Report No. RG-TR-61-1, 1961.

36. Washington, W. D.; Pettis, W., Jr.: "Boattail Effects on Static Stability at Small Angles of Attack", U. S. Army Missile Command Report No. RD-TM-68-5, 1968.

37. Whyte, R. H.: "Effects of Boattail Angle on Aerodynamic Characteristics of 175mm M437 Projectile at Supersonic Mach Numbers", U. S. Army Munitions Command Technical Memorandum 1646, September 1965.

38. Ohlmeyer, E. J.: "Dynamic Stability of the Improved 5"/54 Projectile", NWL Technical Report in publication.

39. Allen, J. H.; Perkins, E. W.: "Characteristics of Flow Over Inclined Bodies of Revolution", NACA RM A 50L07, 1965.

40. Buford, W. D.: "The Effects of Afterbody Length and Mach Number on the Normal Force and Center of Pressure of Conical and Ogival Nose Bodies", JAS, No. 2, 1958, pp. 103-108.

41. Chadwick, W. R.: Sylvester, J. F.: "Dynamic Stability of the 5-Inch/38 Rocket Assisted Projectile", NWL Technical Memorandum No. K-63/66.

42. Donovan, W. F.; MacAllister, L. C.: "Transonic Range Tests of 5-Inch/54 Rocket Asissted Projectile (Inert), BRL MR 2107, July 1971.

43. Karpov, B. G.; Schmidt, L. E.; Krial, K.; MacAllister, L. C.: "The Aerodynamic Properties of the 155mm Shell M101 from Free Flight Range Tests of Full Scale and 1/12 Scale Models", BRL MR 1582, June 1964.

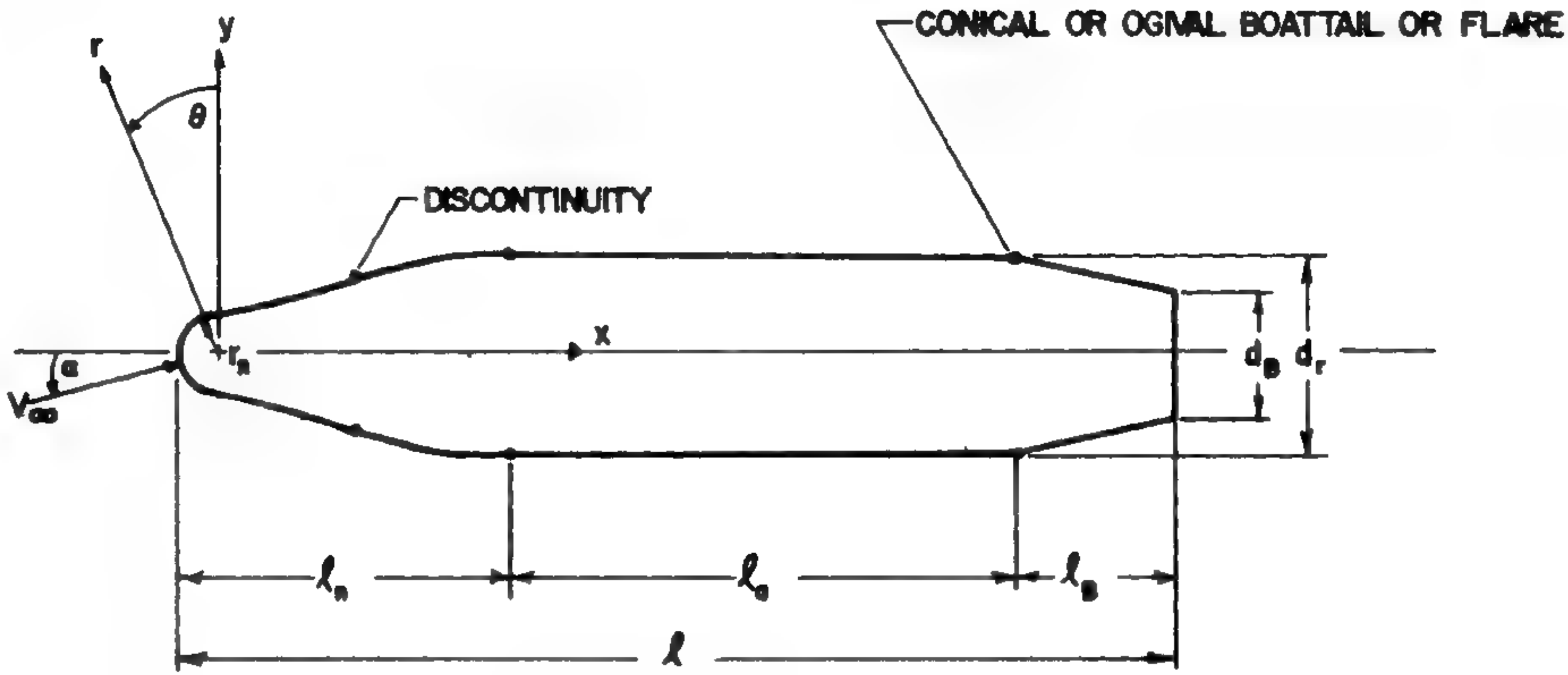

FIGURE 1 TYPICAL BODY GEOMETRY

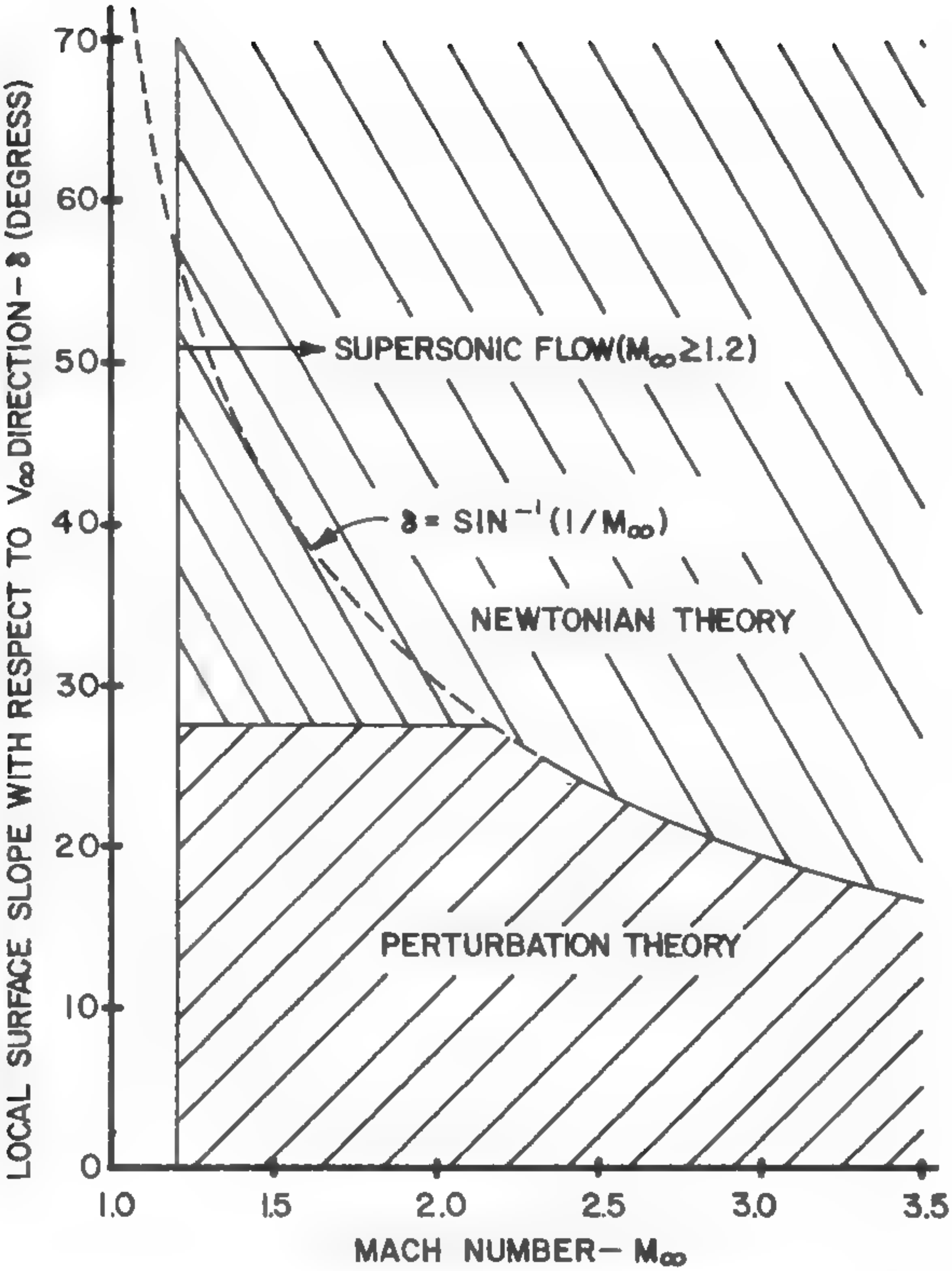

FIGURE 2 BOUNDARIES OF PERTURBATION AND NEWTONIAN THEORY

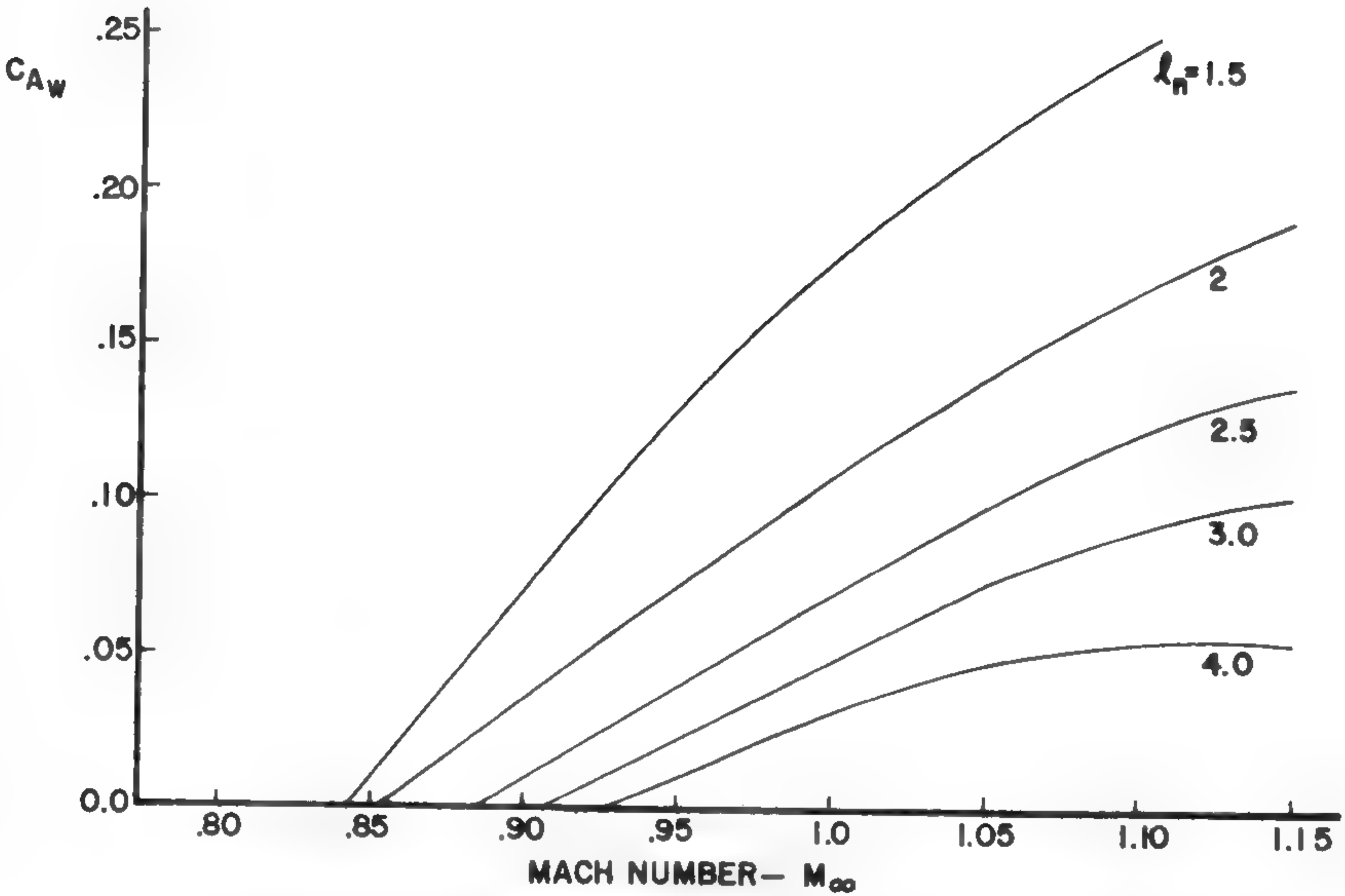

FIGURE 3. TRANSONIC WAVE DRAG OF TANGENT OGIVES.

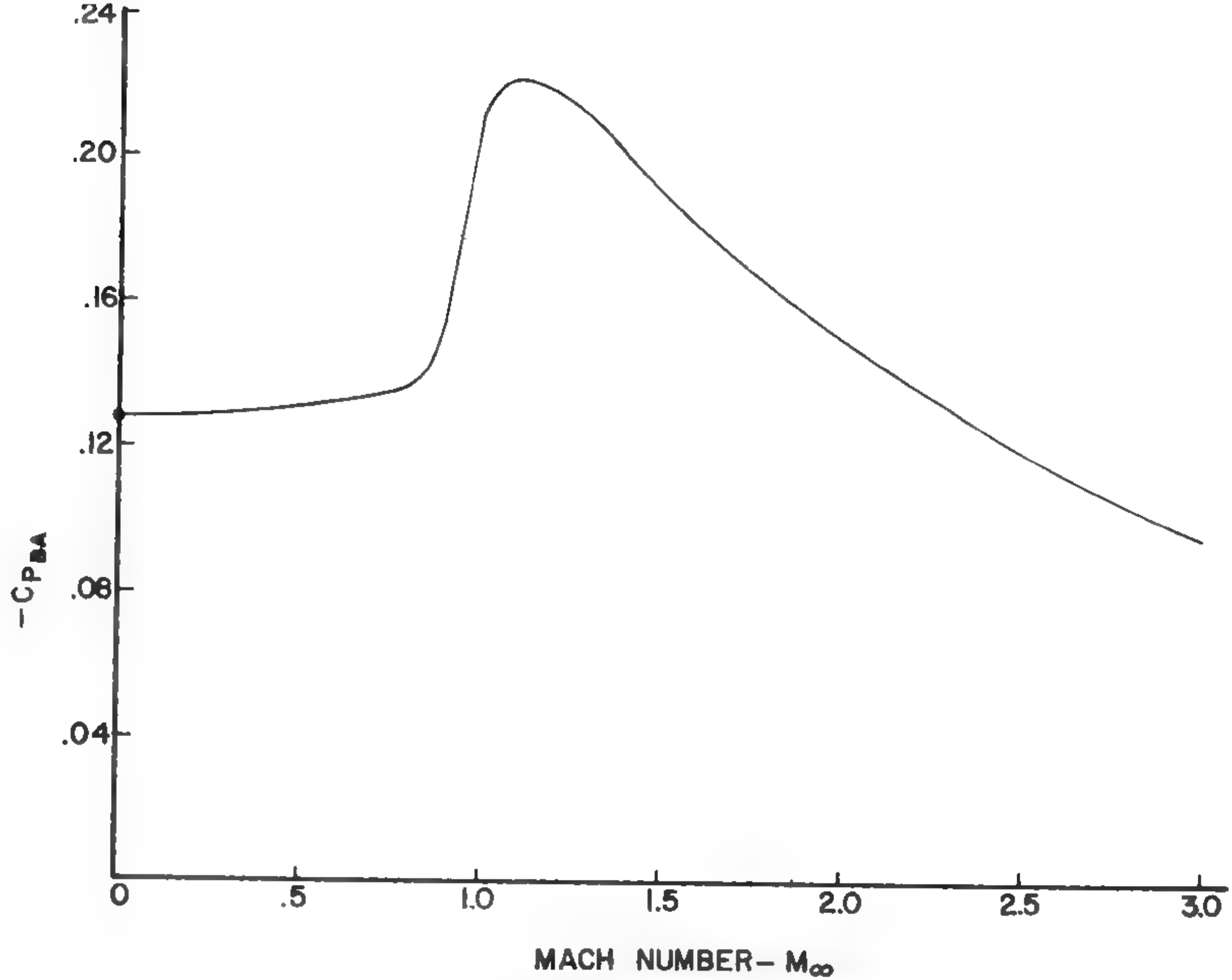

FIGURE 4. MEAN BASE PRESSURE CURVE

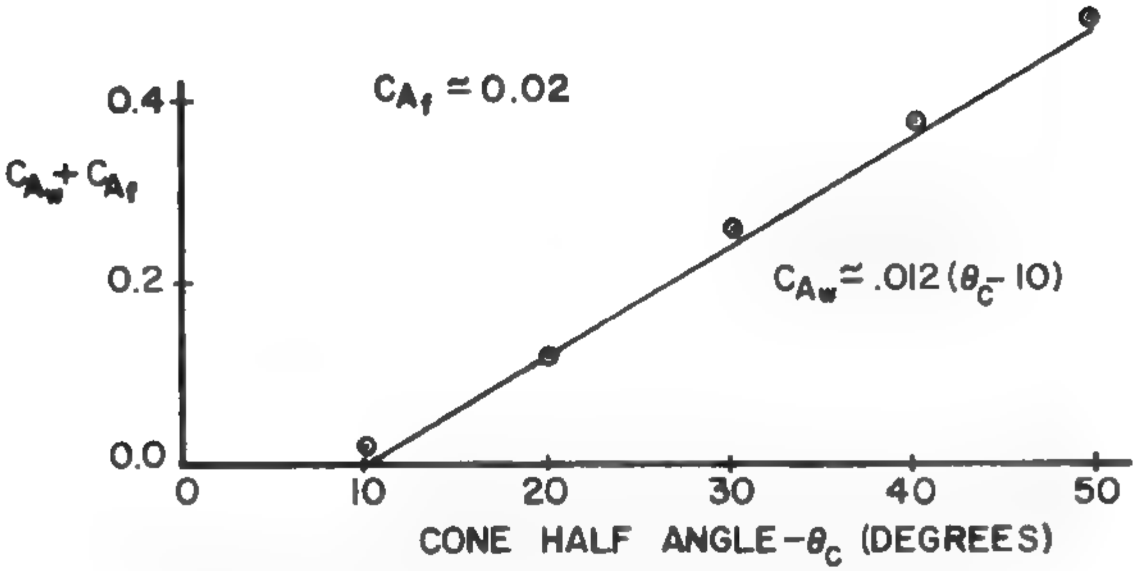

FIGURE 5A. VISCOUS SEPARATION DRAG, $M_\infty = 0.4$

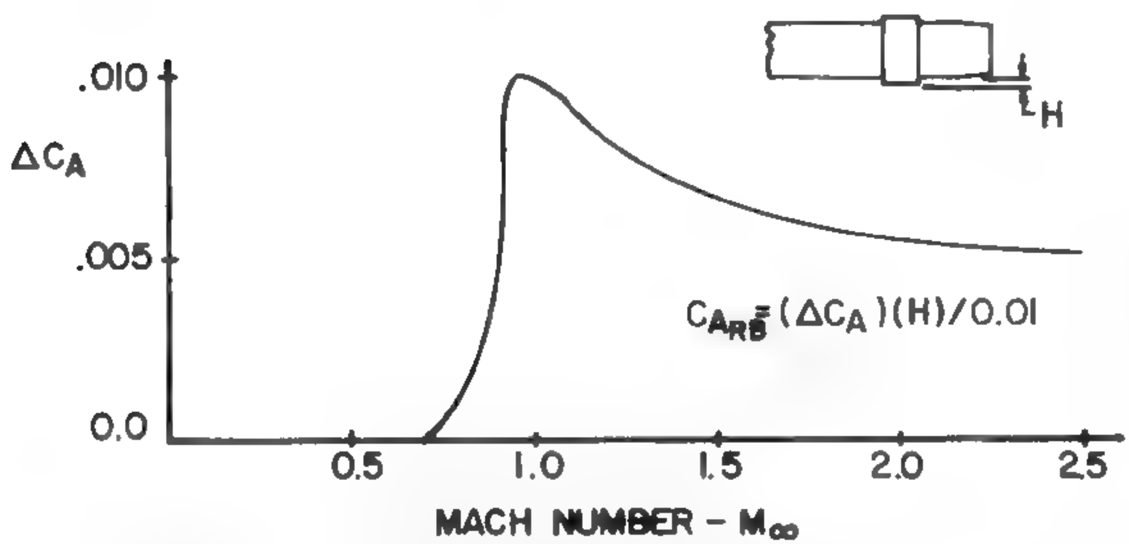

FIGURE 5B. ROTATING BAND DRAG – $C_{A_{RB}}$

FIGURE 5. VISCOUS SEPARATION AND ROTATING BAND DRAG

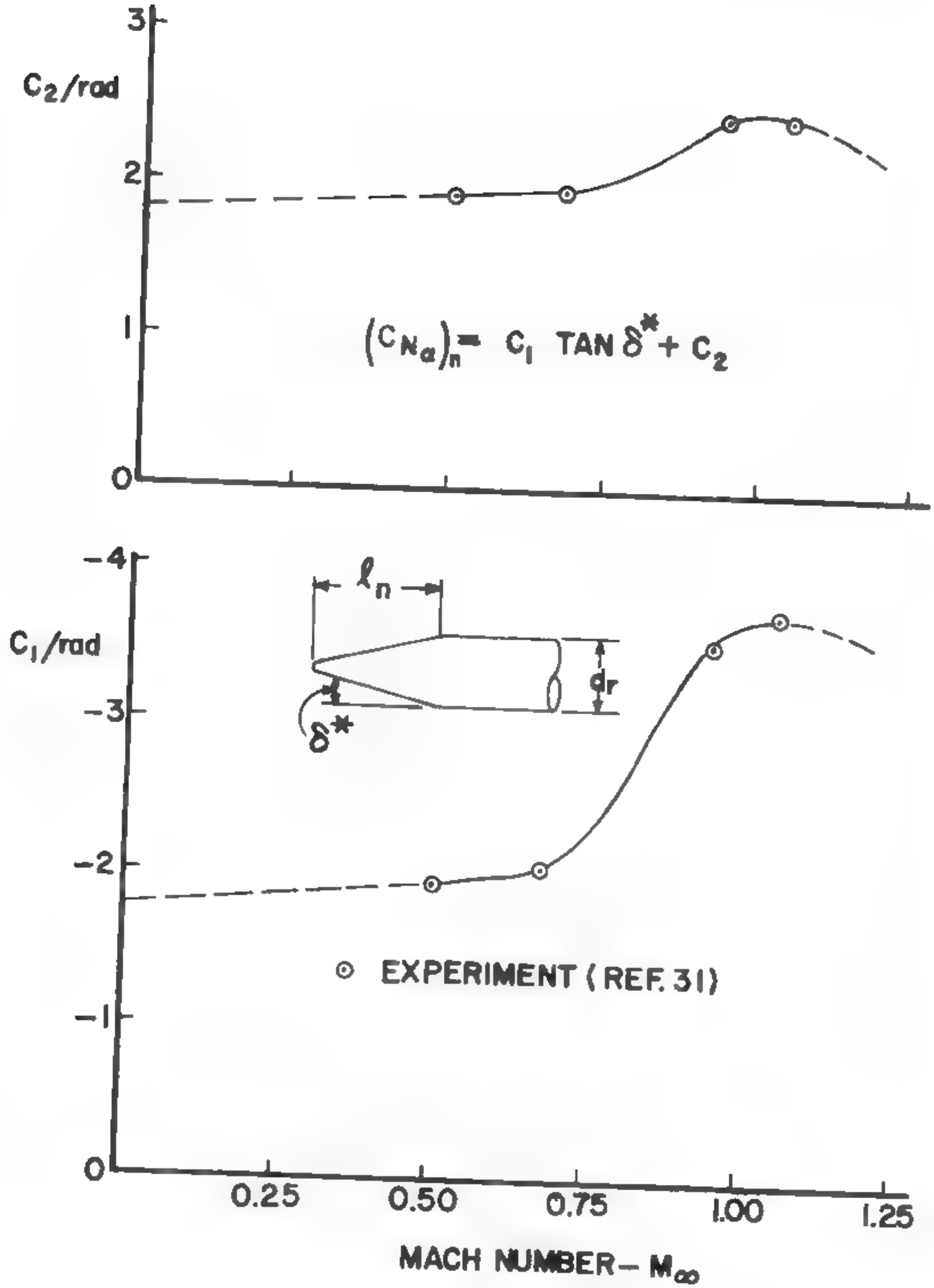

FIGURE 6. CONSTANTS TO DETERMINE $(C_{N_\alpha})_n$ FOR $M_\infty < 1.2$

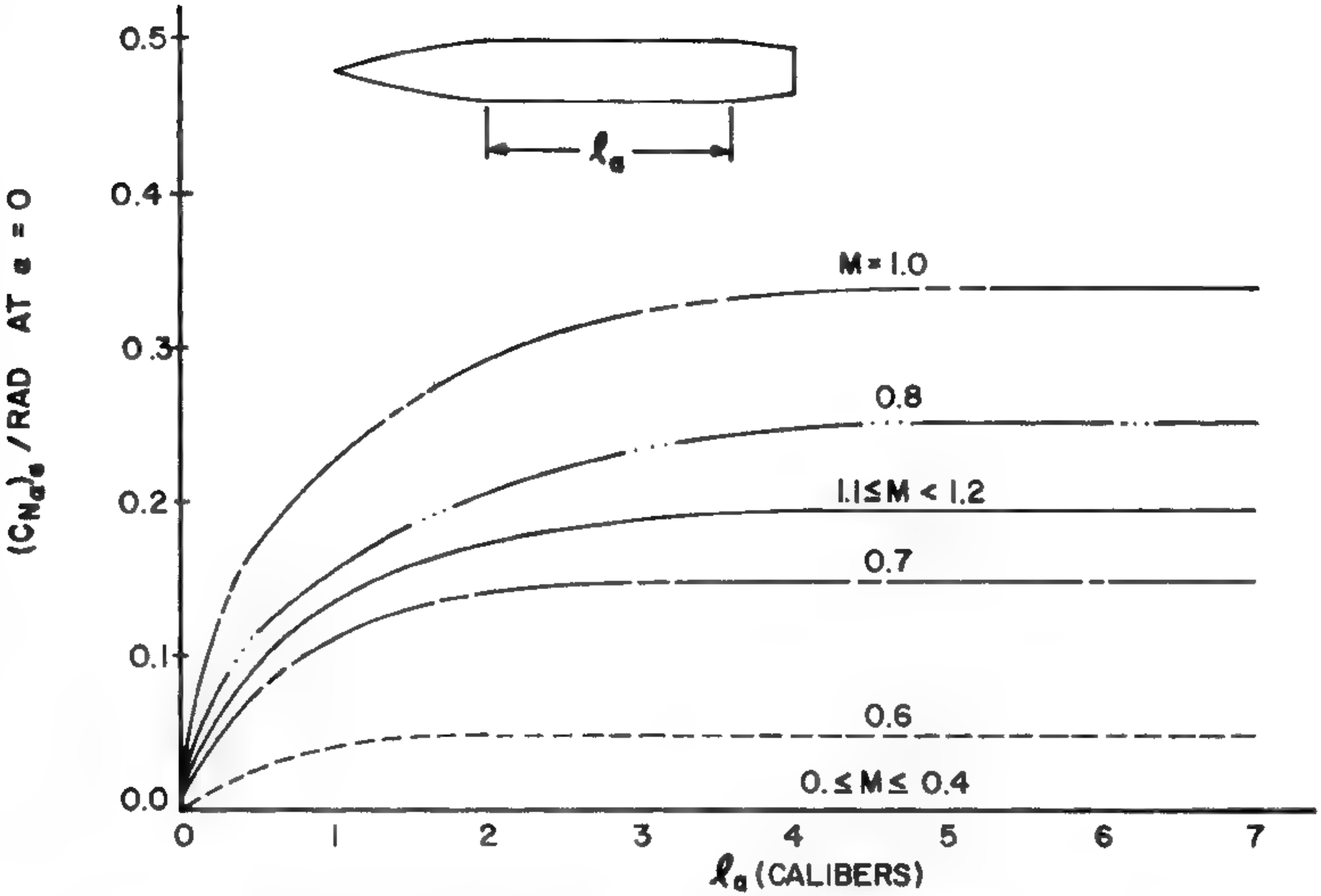

FIGURE 7. INCREASE IN (C_{N_α}) AT SUBSONIC AND TRANSONIC MACH NUMBERS DUE TO AFTERBODY.

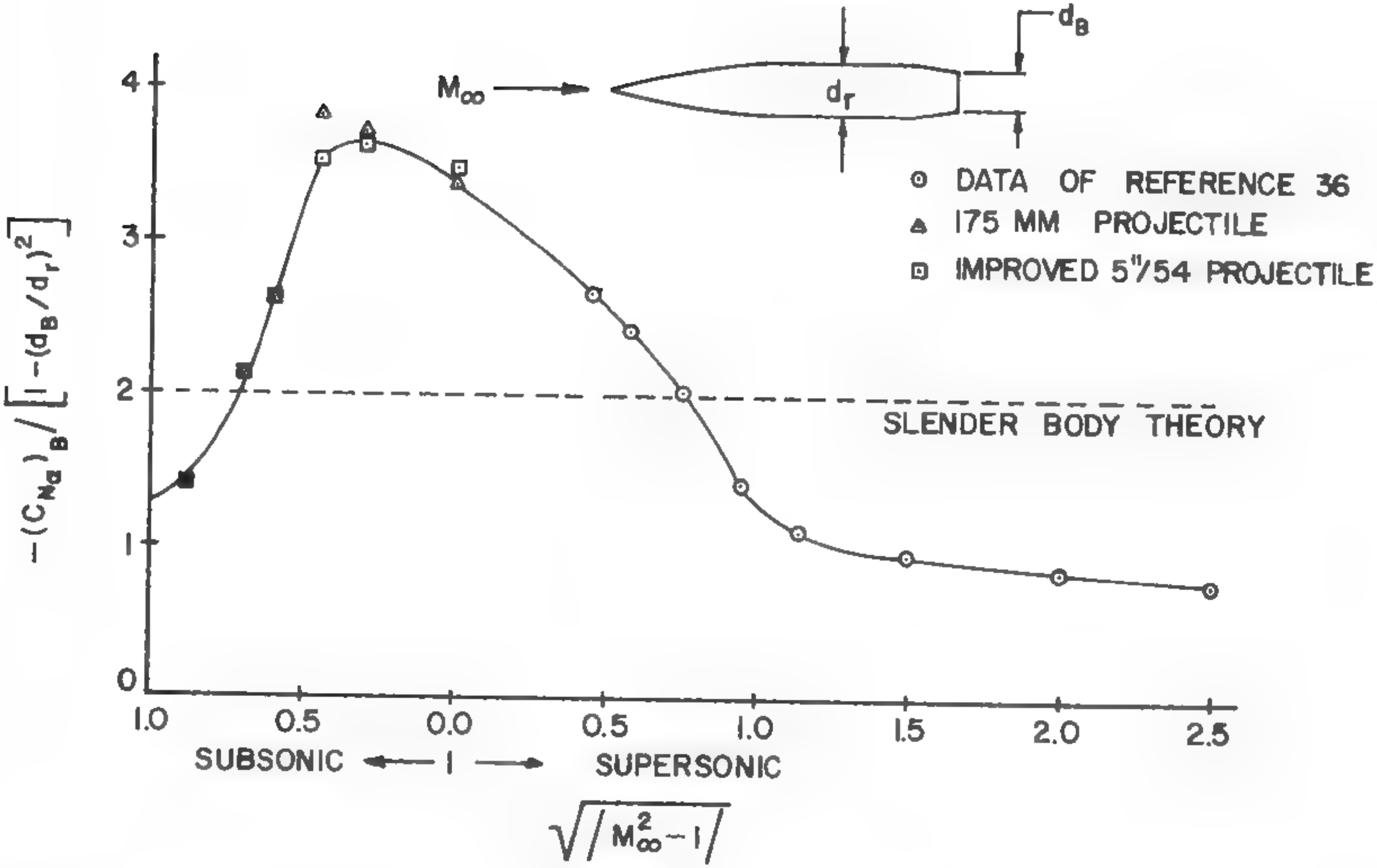

FIGURE 8 DECREASE IN C_{N_α} DUE TO BOATTAIL

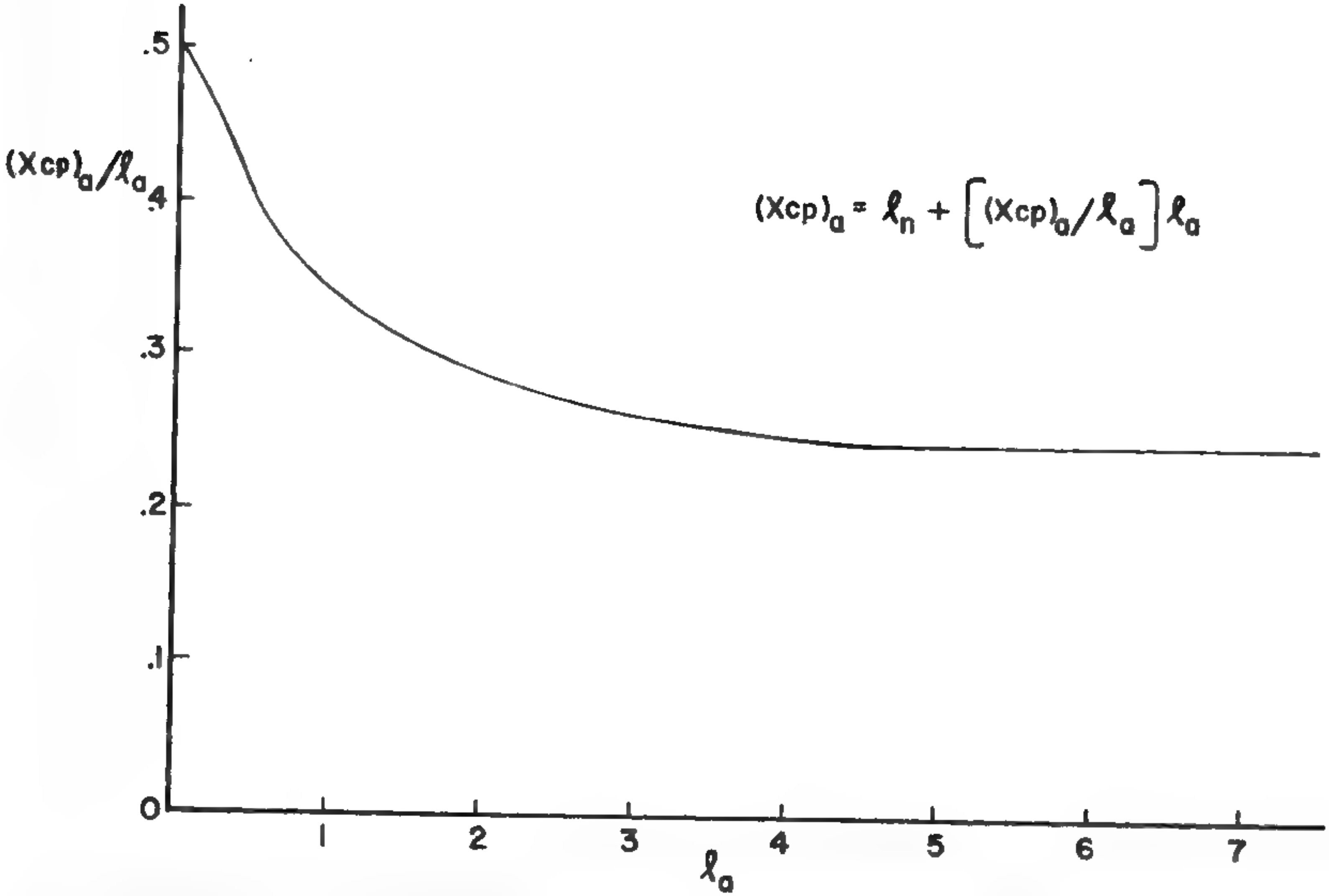

FIGURE 9. CENTER OF PRESSURE OF AFTERBODY LIFT FOR $M_\infty < 1.2$

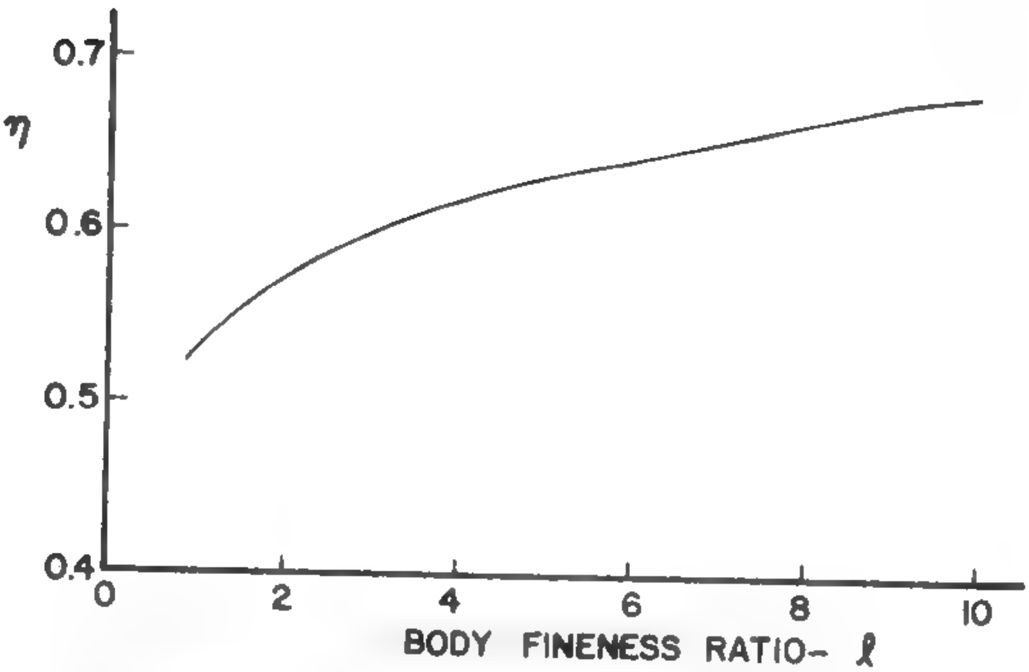

FIGURE 10-A. DRAG PROPORTIONALITY FACTOR–η

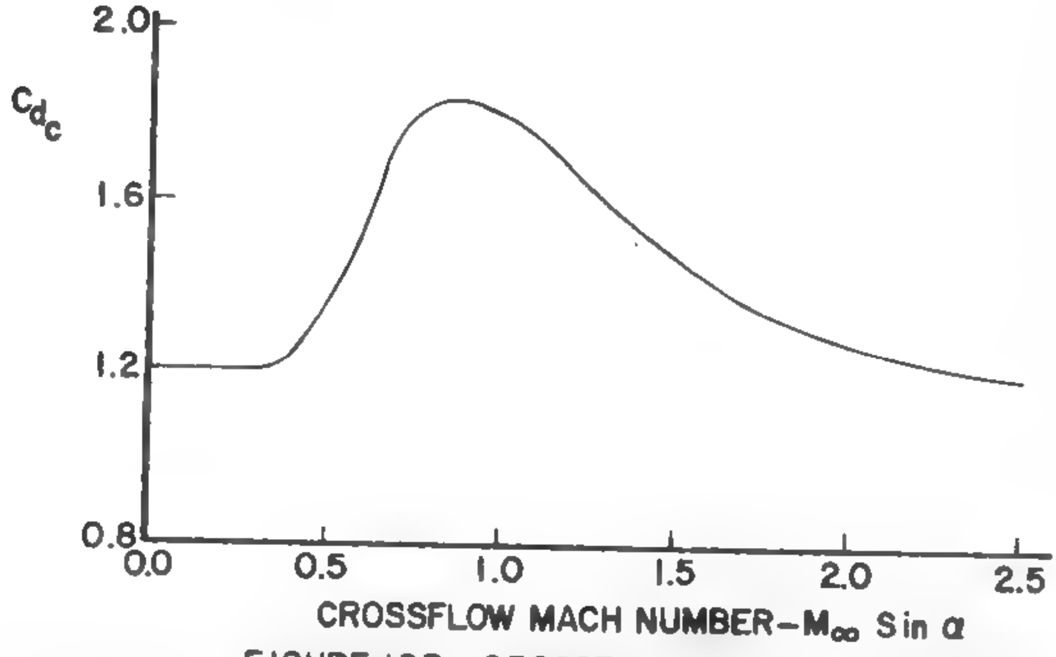

FIGURE 10B. CROSSFLOW DRAG COEFFICIENT

FIGURE 10. DRAG PROPORTIONALITY FACTOR AND CROSSFLOW DRAG COEFFICIENT

COMPONENT \ MACH NUMBER REGION	SUBSONIC	TRANSONIC	SUPERSONIC
NOSE WAVE DRAG	—	Wu and AOYOMA PLUS EMPIRICAL	2^{nd} ORDER VAN DYKE PLUS MODIFIED NEWTONIAN
BOATTAIL WAVE DRAG	—	Wu and AOYOMA	2^{nd} ORDER VAN DYKE
SKIN FRICTION DRAG	VAN DRIEST II		
BASE DRAG	EMPIRICAL		
INVISCID LIFT and PITCHING MOMENT	EMPIRICAL	Wu and AOYOMA PLUS EMPIRICAL	TSIEN 1^{st} ORDER CROSSFLOW
VISCOUS LIFT and PITCHING MOMENT	ALLEN and PERKINS CROSSFLOW		

FIGURE 11 METHODS USED TO COMPUTE BODY ALONE AERODYNAMICS

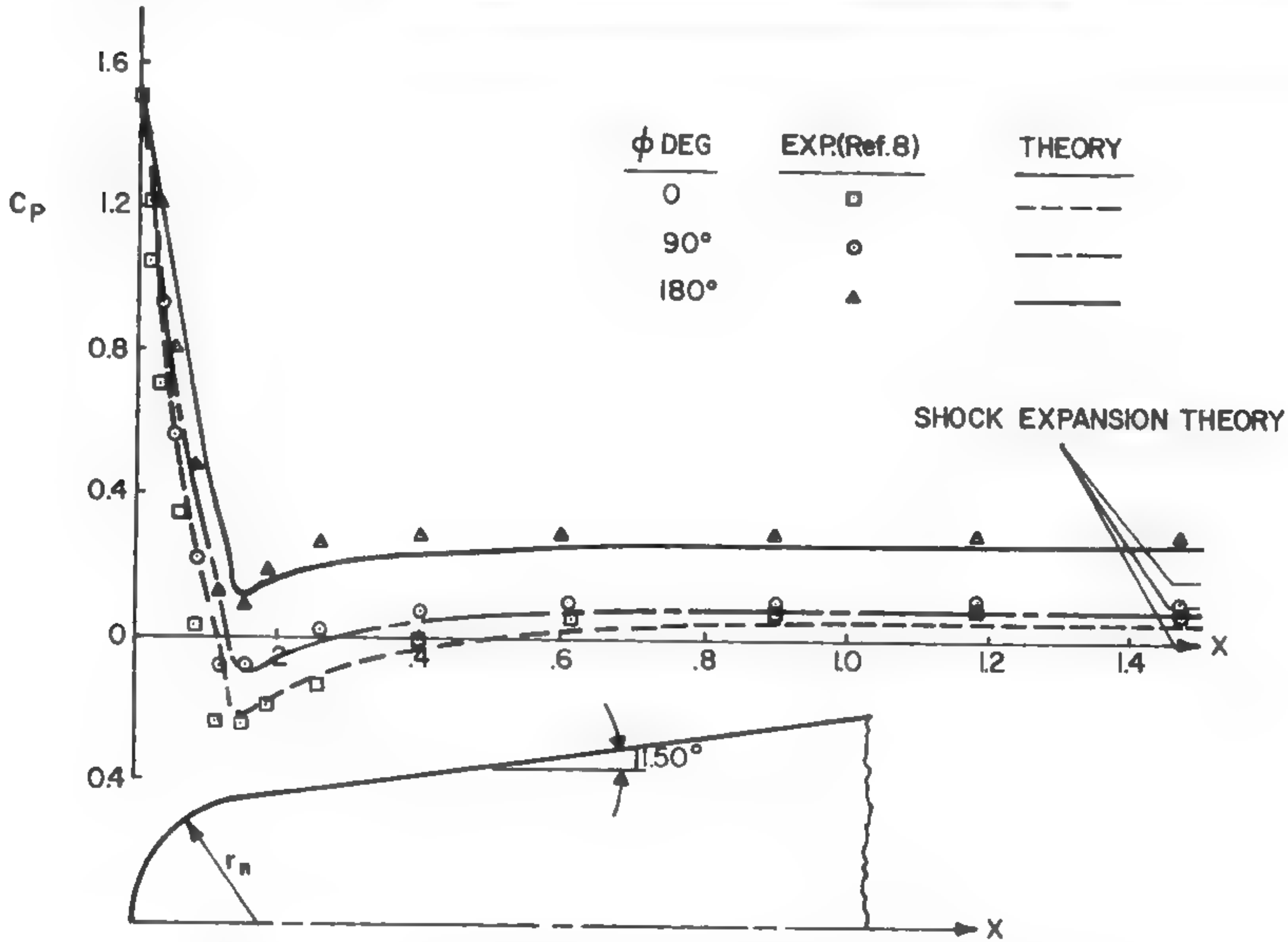

FIGURE 12 COMPARISON OF THEORY AND EXPERIMENT FOR BLUNTED CONE;

$r_n / r_B = 0.35, M_\infty = 1.5, \alpha = 8°$

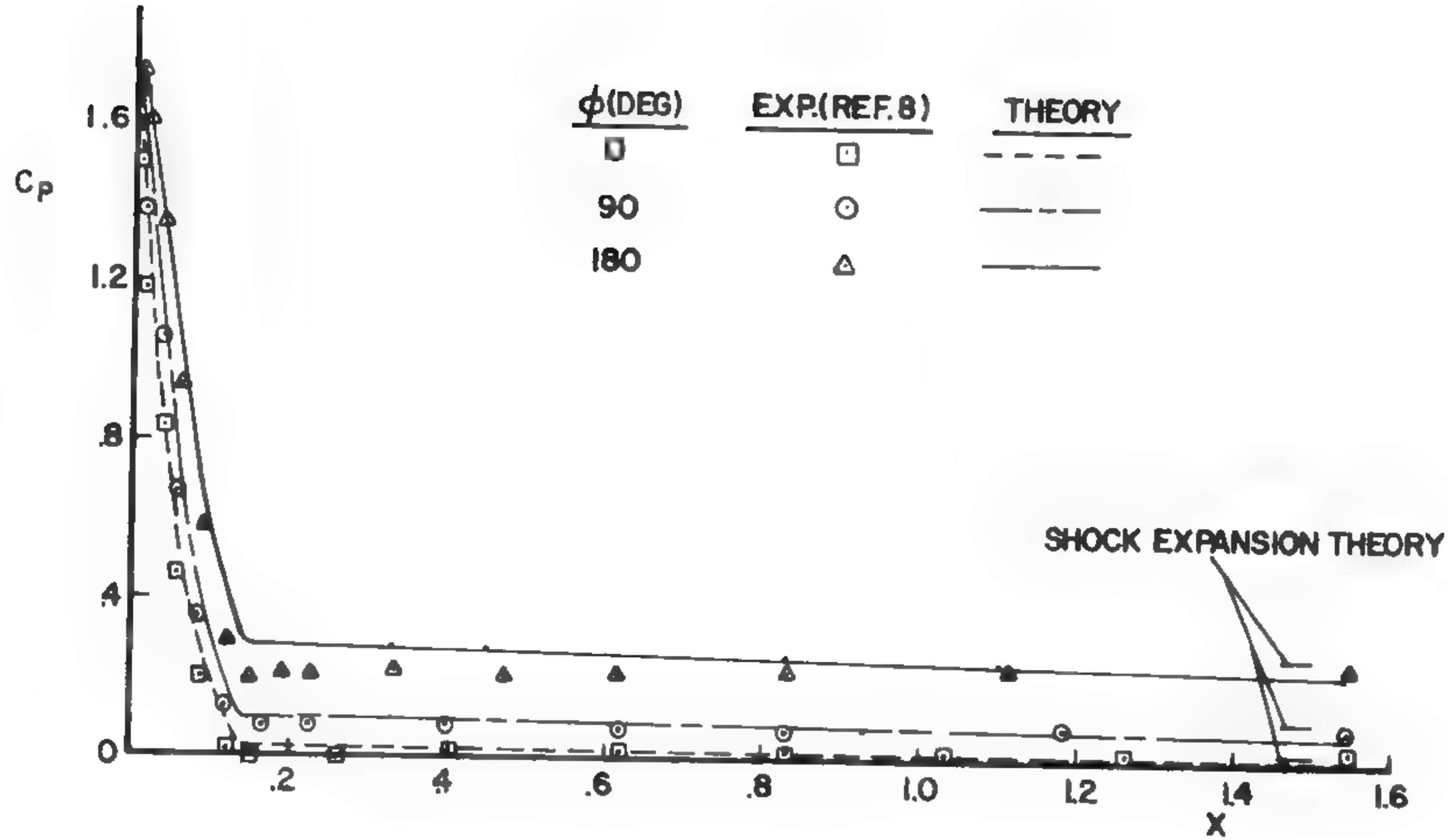

FIGURE 13 COMPARISON OF THEORY AND EXPERIMENT FOR BLUNTED CONE; $r_n / r_B = 0.35$, $M_\infty = 2.96$, $\alpha = 8°$

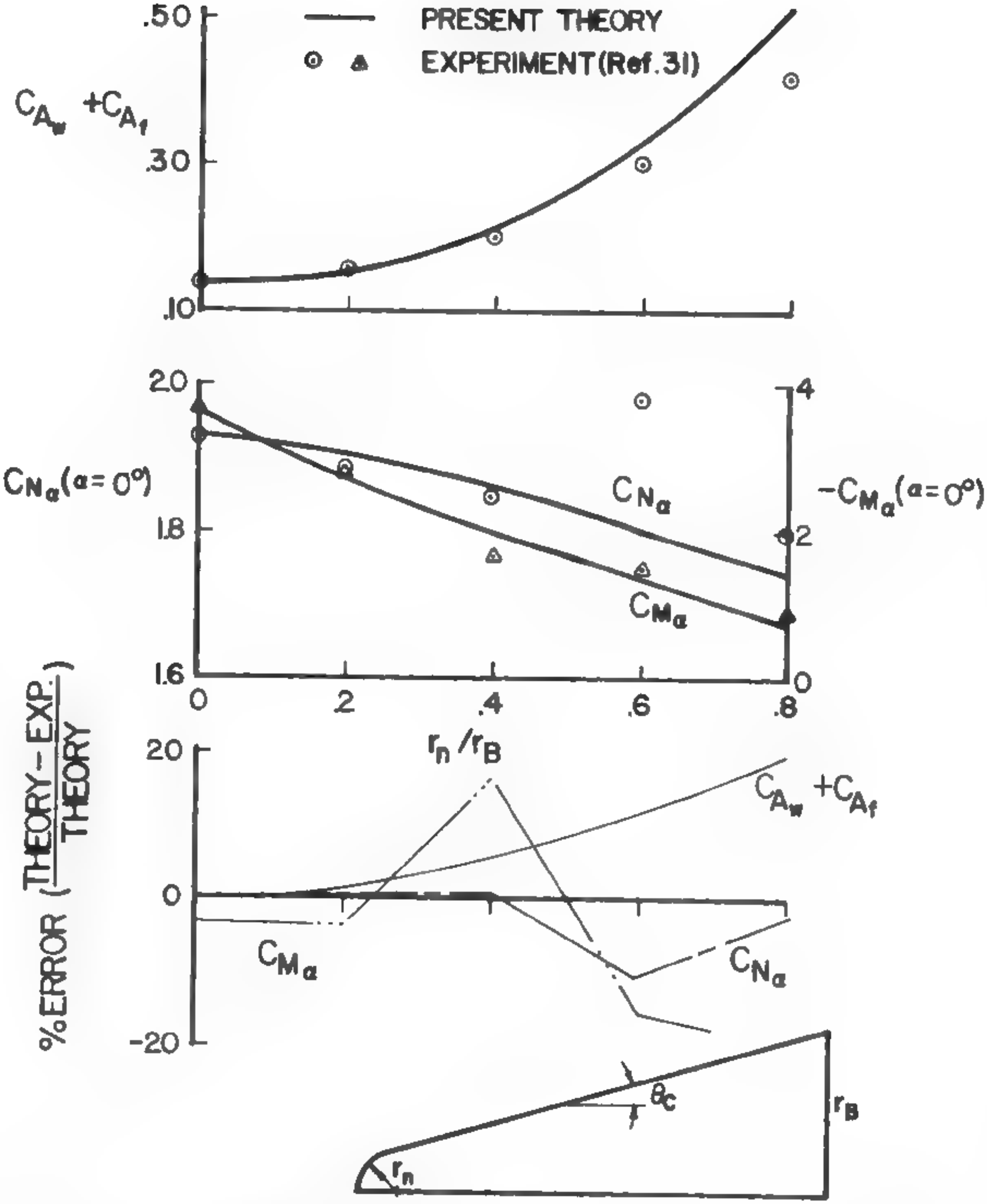

FIGURE 14 COMPARISON OF THEORY AND EXPERIMENT FOR A BLUNTED CONE; $M_\infty = 1.5$, $\theta_C = 10°$.

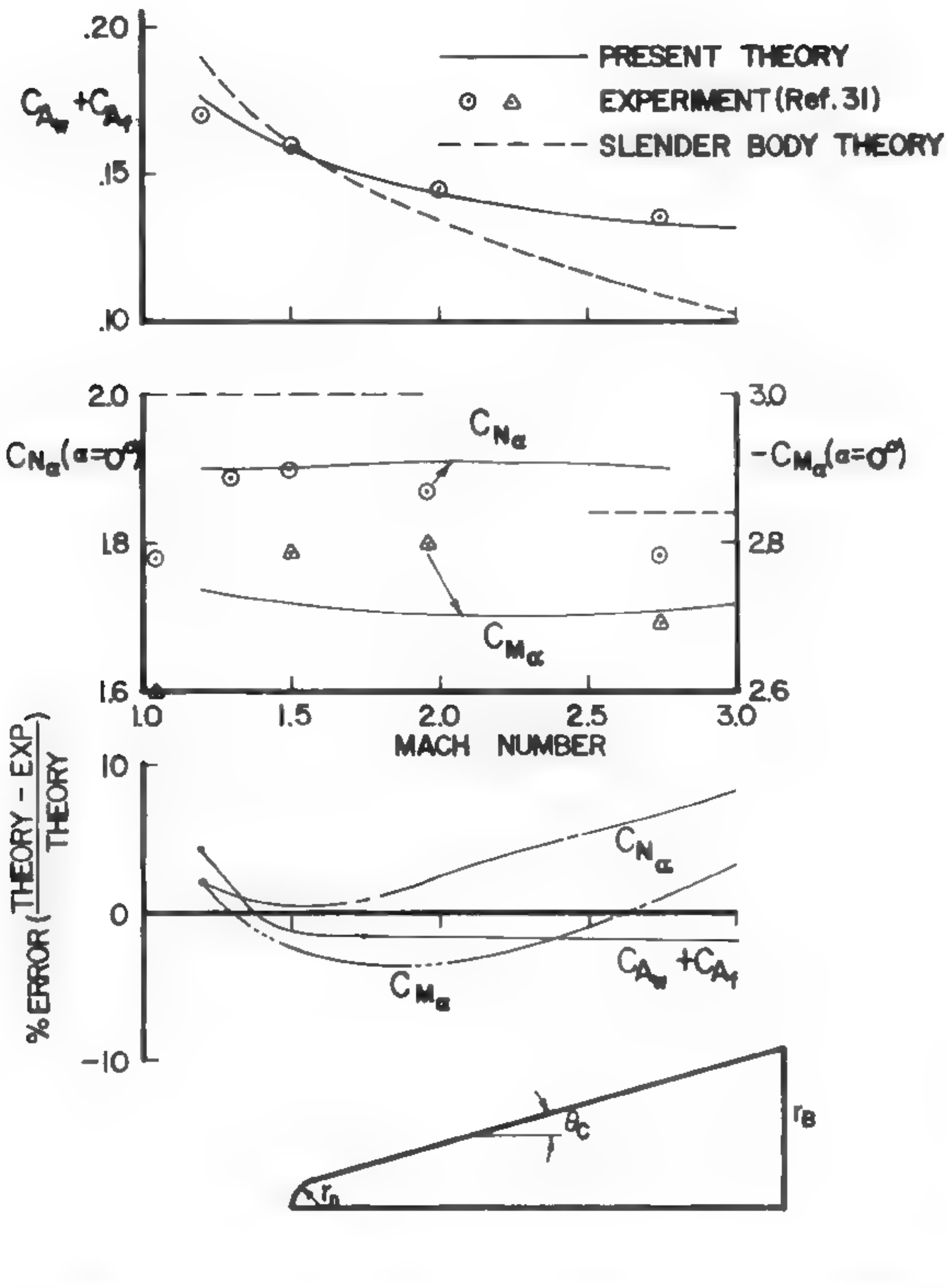

FIGURE 15 COMPARISON OF THEORY AND EXPERIMENT FOR BLUNT CONE; $\theta_C = 10°$, $r_n/r_B = 0.2$.

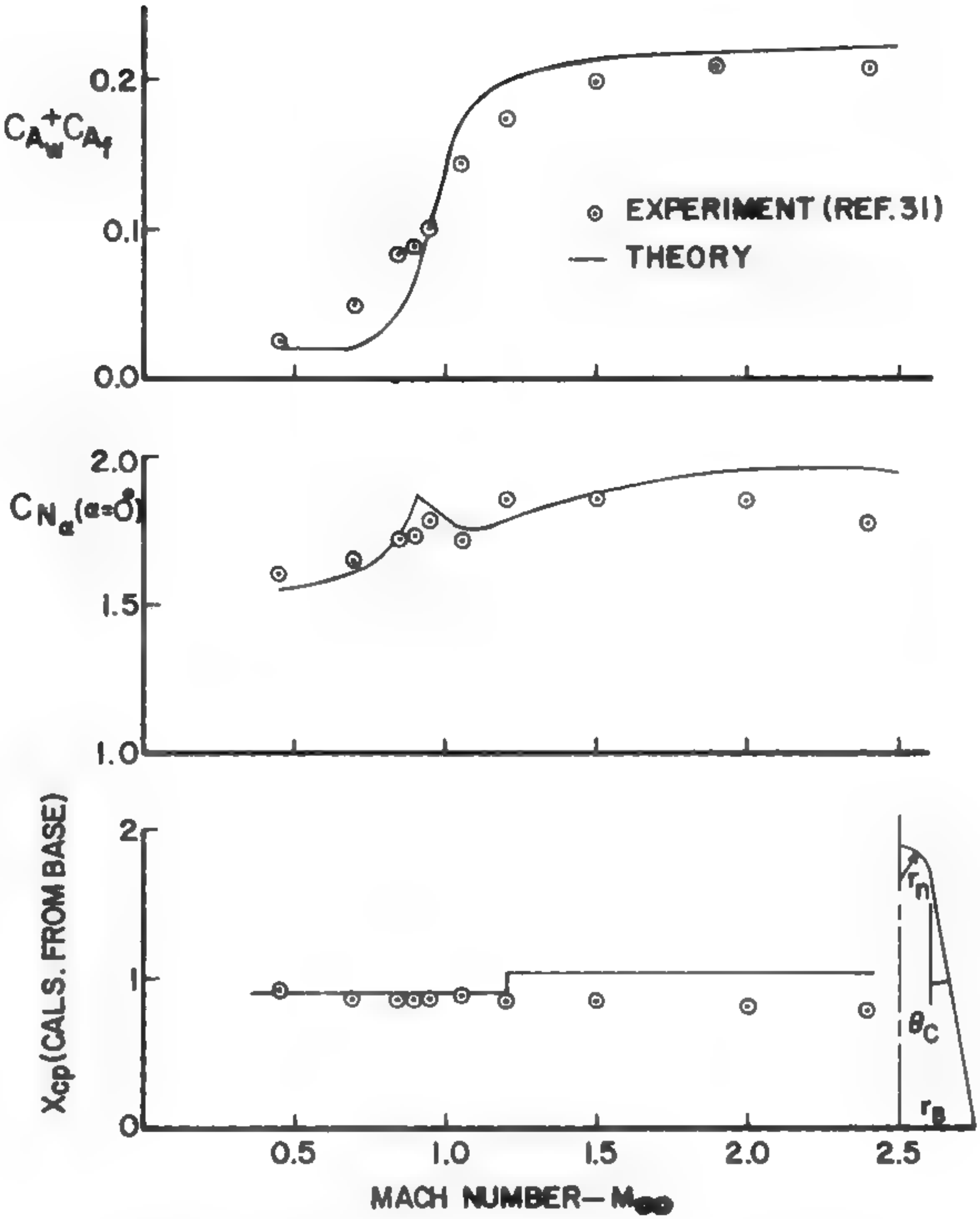

FIGURE 16. COMPARISON OF THEORY AND EXPERIMENT FOR BLUNTED CONE; $\theta_c = 10°$ $r_n / r_B = 0.4$.

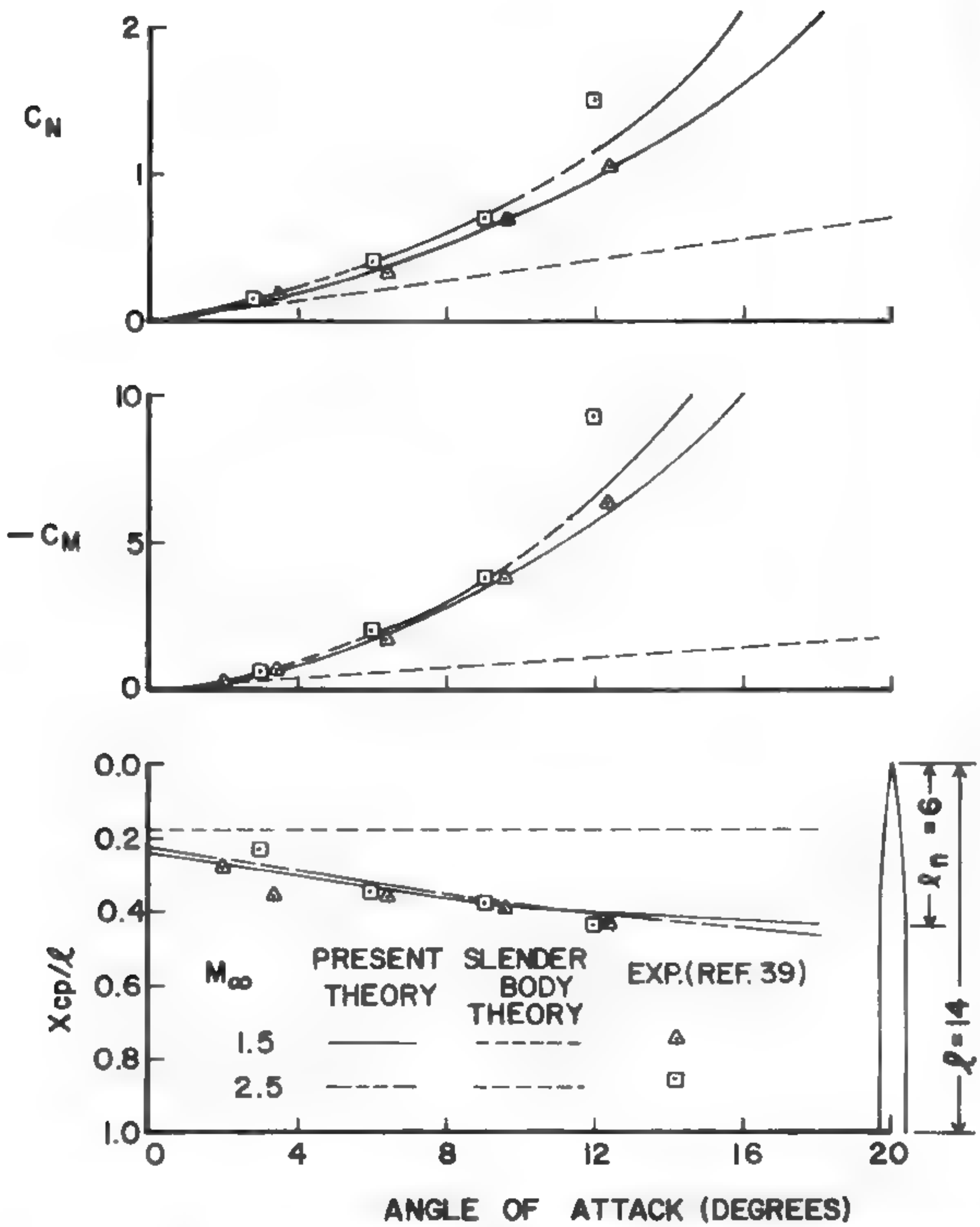

FIGURE 17 COMPARISON OF THEORY WITH EXPERIMENT FOR TANGENT OGIVE-CYLINDER. $\ell = 14$ CALIBERS

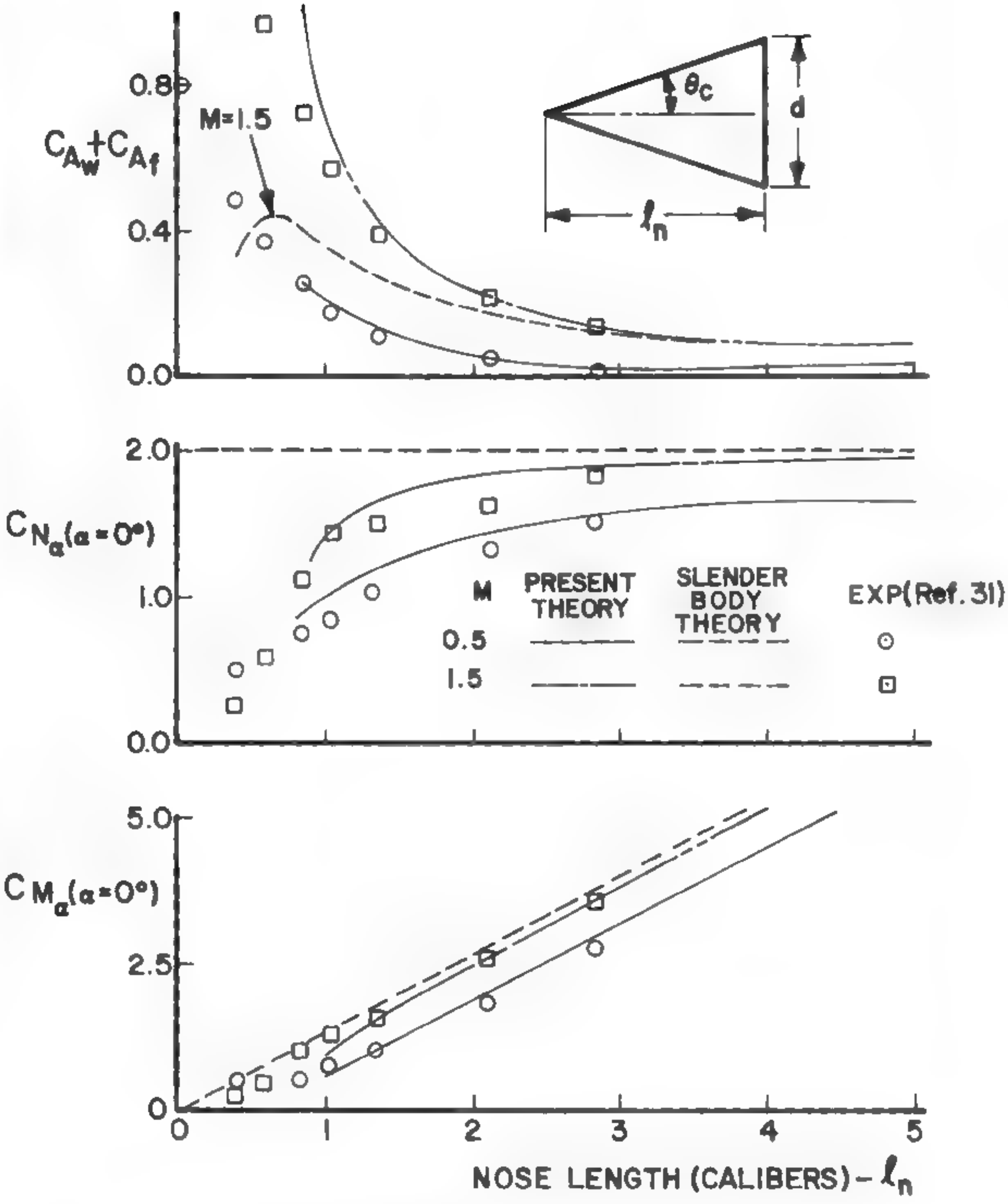

FIGURE 18 COMPARISON OF THEORY AND EXPERIMENT FOR CONES OF VARIOUS LENGTHS.

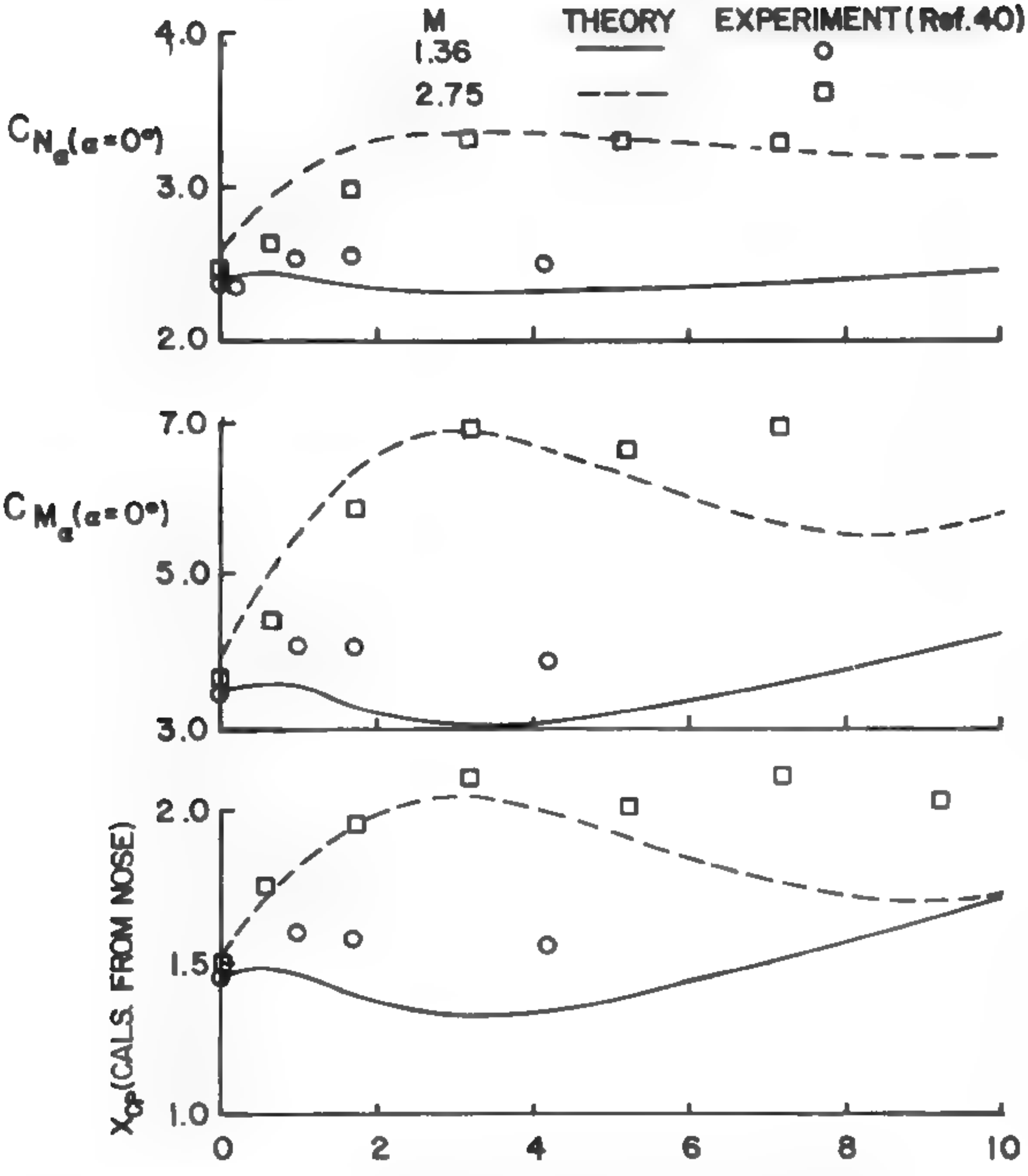

FIGURE 19 COMPARISON OF PRESENT THEORY WITH EXPERIMENT AS A FUNCTION OF AFTERBODY LG. (2.83 CALIBER TANGENT OGIVE NOSE).

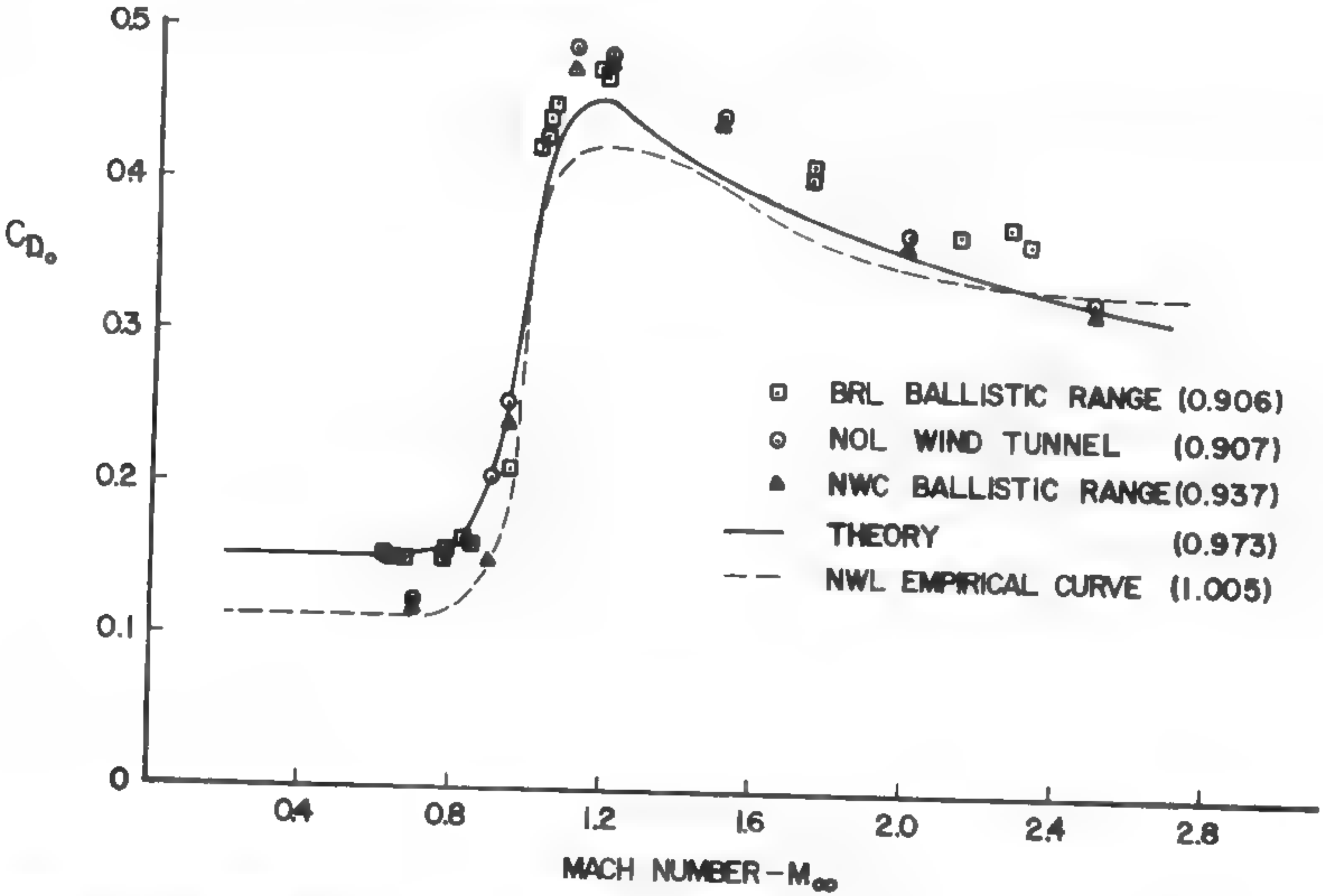

FIGURE 20. ZERO LIFT DRAG CURVE FOR 5"/38 RAP PROJECTILE

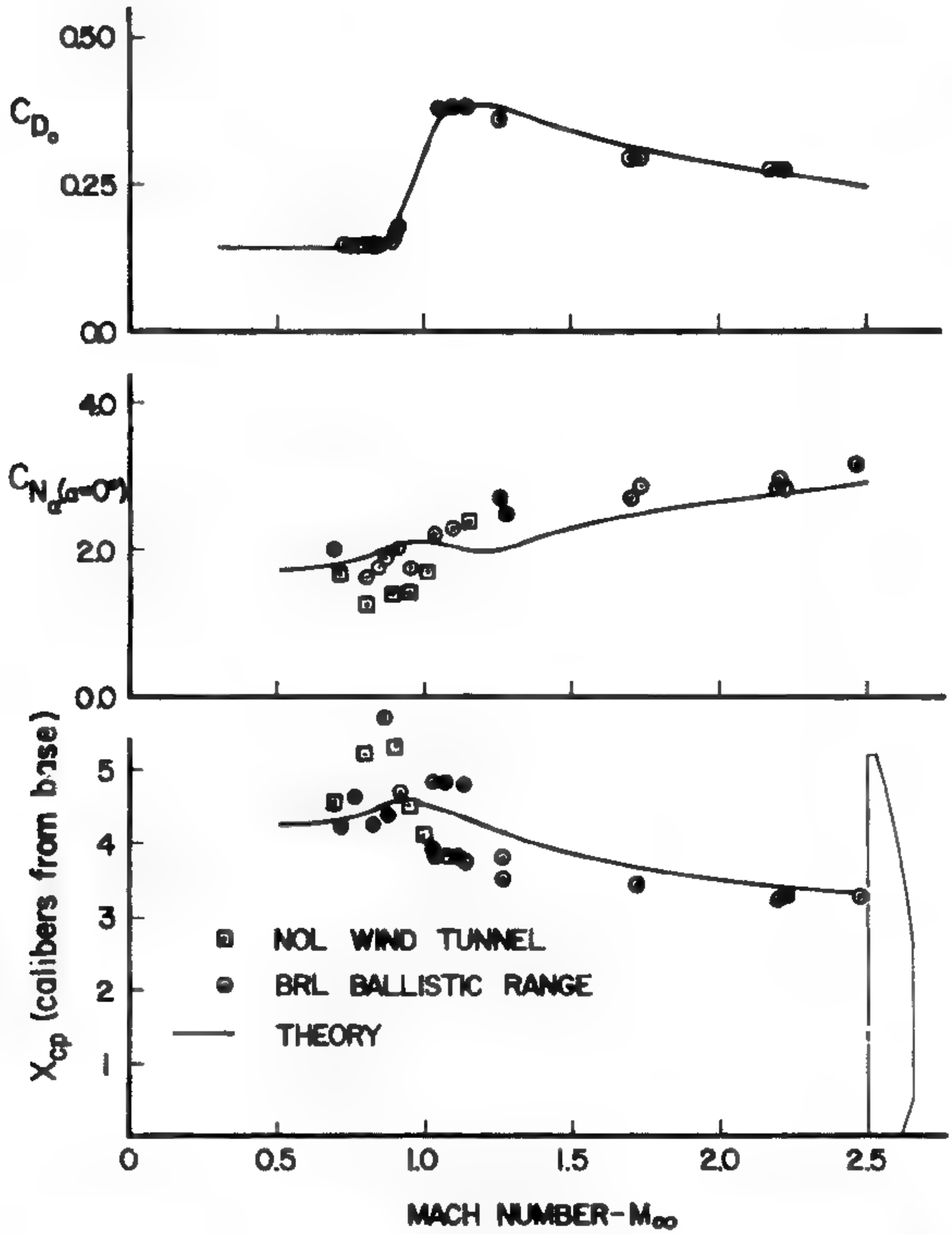

FIGURE 21 COMPARISON THEORY AND TEST DATA FOR 5"/54 RAP PROJECTILE.

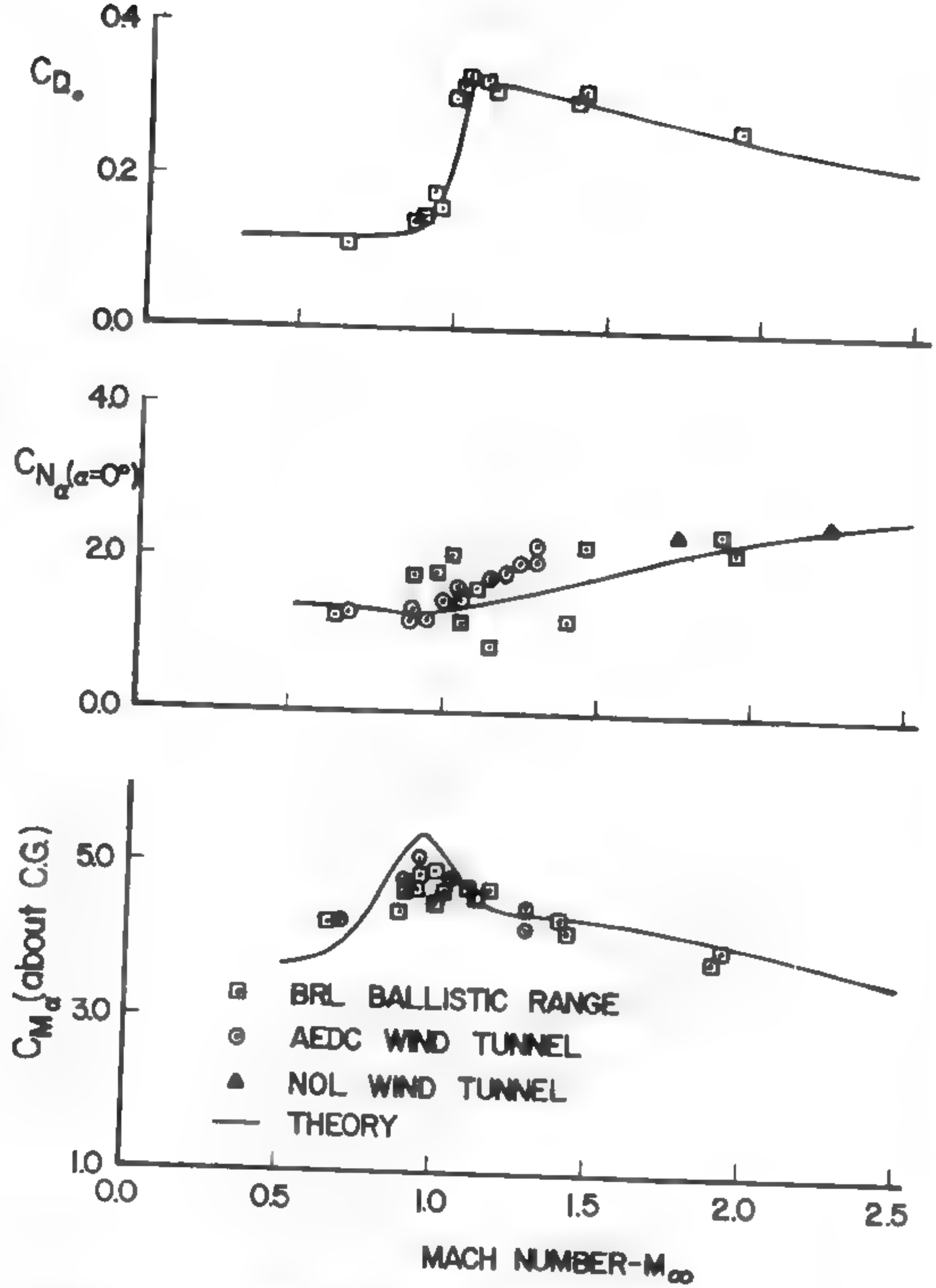

FIGURE 22 COMPARISON OF THEORY AND TEST DATA FOR IMPROVED 5"/54 PROJECTILE.

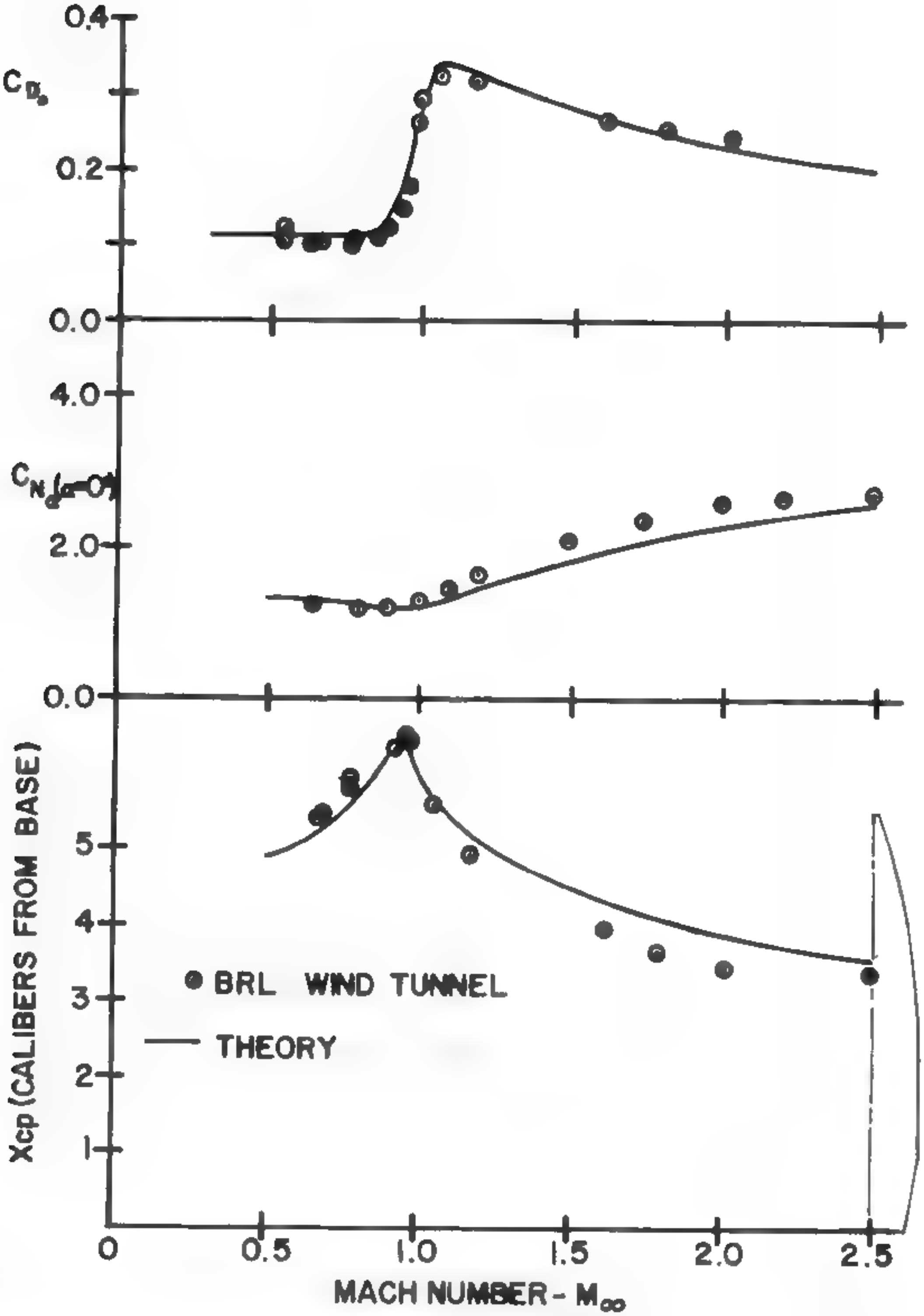

FIGURE 23 COMPARISON OF THEORY AND TEST DATA FOR 175MM XM437 PROJECTILE

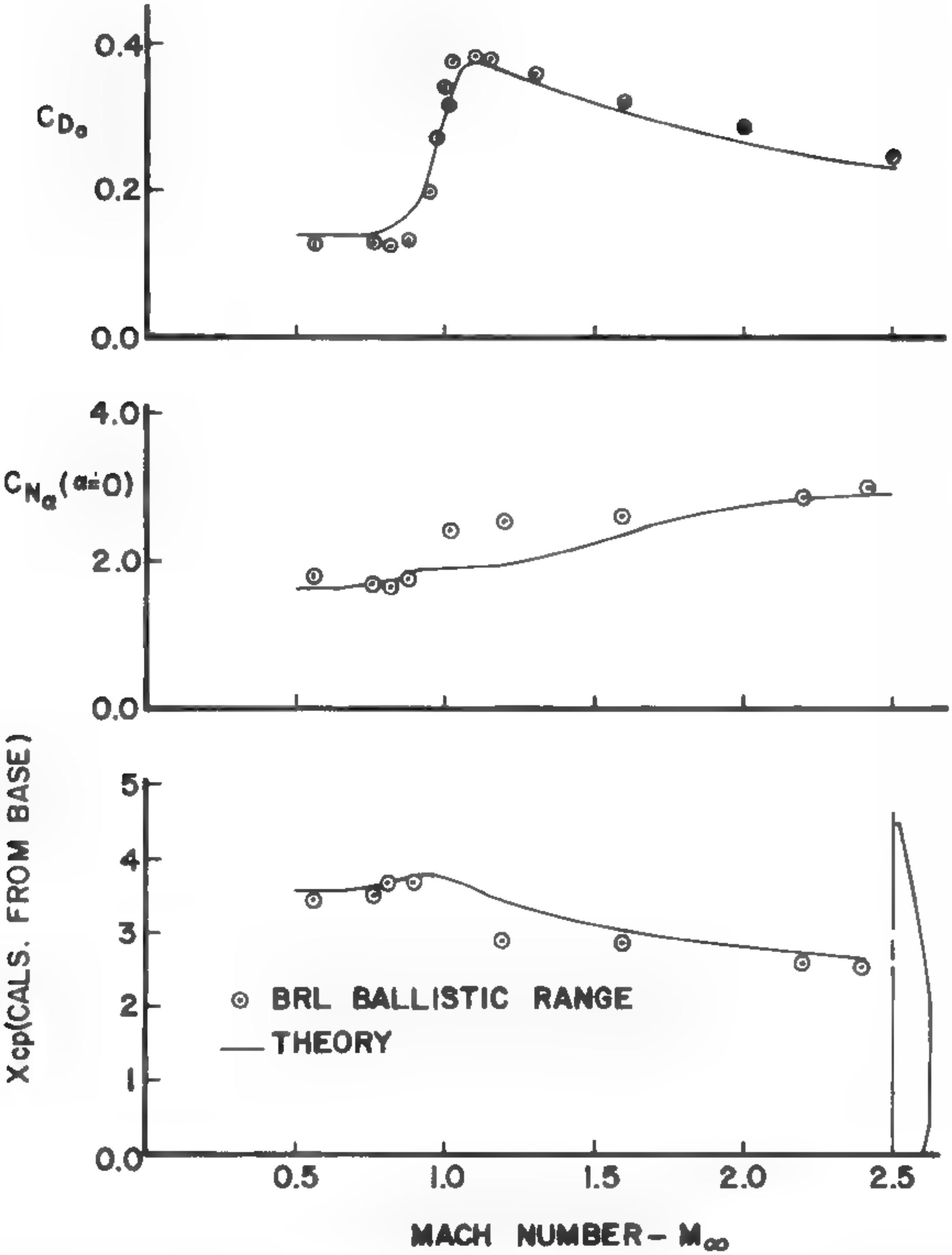

FIGURE 24. COMPARISON OF THEORY AND TEST DATA FOR 155MM PROJECTILE

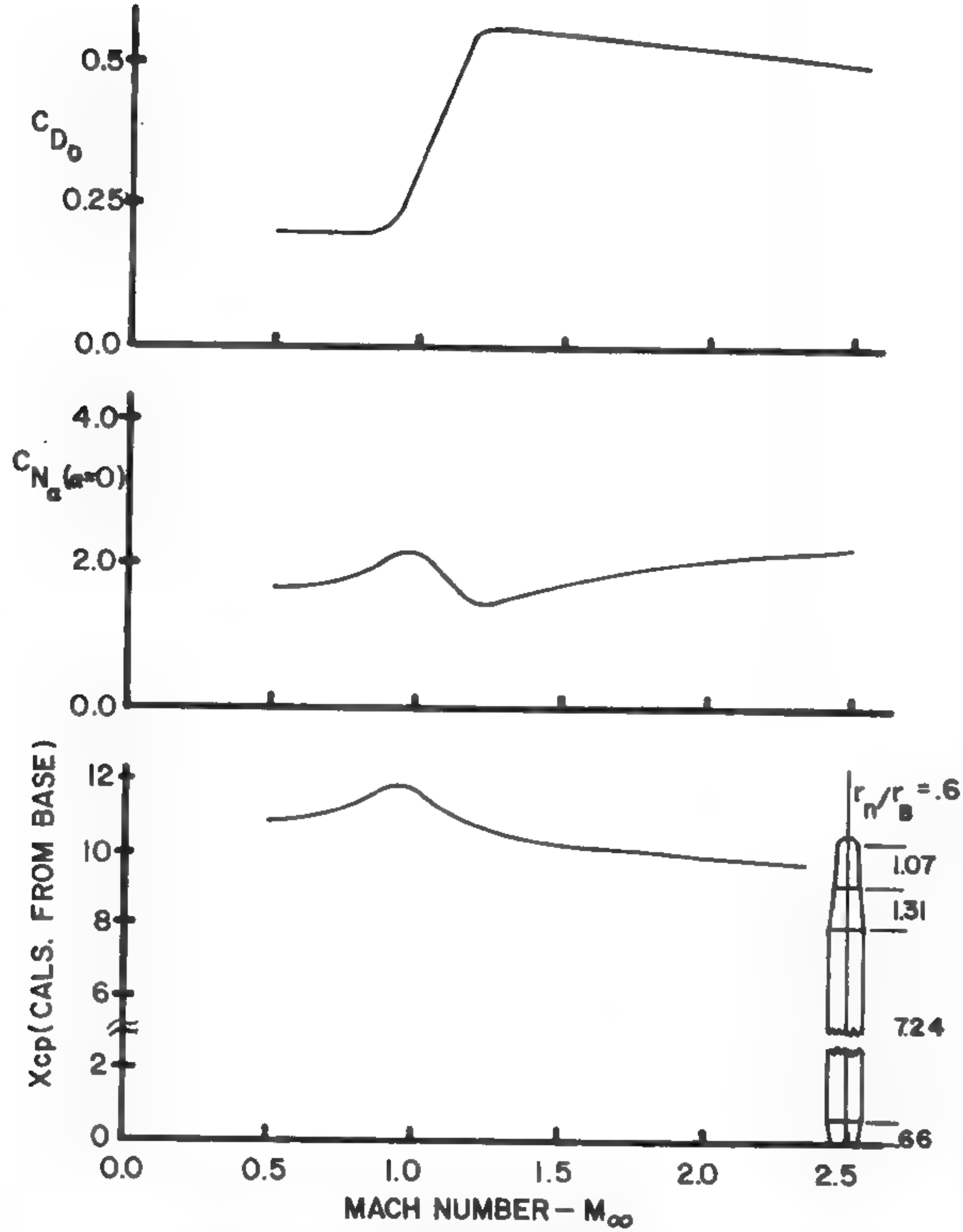

FIGURE 25 AERODYNAMICS OF 5 INCH GUIDED PROJECTILE BODY

APPENDIX A

GLOSSARY

GLOSSARY

C_A	Total axial force coefficient
$C_{A_{BA}}$	Axial force coefficient contribution from base pressure
C_{A_f}	Axial force coefficient contribution from skin friction
$C_{A_{RB}}$	Axial force coefficient contribution from rotating band
$C_{A_{VIS}}$	Axial force coefficient contribution from viscous separation on nose at subsonic Mach numbers
C_{A_W}	Axial force coefficient contribution from expansion and shock waves
C_{D_O}	Zero lift drag coefficient; $C_{D_O} = C_A$
C_{d_c}	Crossflow drag coefficient
C_{f_∞}	Mean skin friction coefficient based on freestream Reynolds number
C_M	Pitching moment coefficient about nose unless otherwise specified (positive nose-up)
C_{M_α}	Pitching moment coefficient derivative - $dC_M/d\alpha$
C_N	Normal force coefficient
C_{N_α}	Normal force coefficient derivative - $dC_N/d\alpha$
C_p	Pressure coefficient; $C_p = (P-P_\infty)/1/2\rho_\infty V_\infty^2$
d	Diameter (calibers)
d_B	Base diameter
H	Mean height of rotating band in calibers
ℓ	Body Length (calibers)
M	Mach number
P_r	Prandtl number
R	Body Radius (calibers)
R'	dR/dx

R_N	Reynolds number - $(\rho V \ell)/\mu$
R_T	Turbulent boundary layer recovery factor
S_w	Wetted surface area of body
S_p	Planform area of body
T_w	Wall temperature
u,v,w	Velocity components in cylindrical coordinate system
V	Total velocity - $V = \sqrt{u^2+v^2+w^2}$
Vol	Volume of body
x,r,θ	Cylindrical coordinates with x along axis of symmetry and in calibers
x,y,z	Rectangular coordinates with x along axis of symmetry and in calibers
x_{cp}	Center of pressure in calibers from nose unless otherwise specified
x_p	Distance to centroid of planform area in calibers from nose
x_u, r_u	Coordinates of point below which perturbation theory cannot be applied
x_1	Distance measured relative to shoulder of boattail
α	Angle of Attack
β	Angle between tangent to body surface and axis of symmetry
γ	Ratio of specific heats (γ = 1.4)
δ	Angle between a tangent to the body surface and freestream direction
δ^*	Angle which the nose makes with the shoulder of the body (degrees)
ζ	Velocity potential in cross flow direction
η	Ratio of drag coefficient of a circular cylinder of finite length to that of a circular cylinder of infinite length
θ	Cylindrical coordinate measured with θ = 0 in leeward plane

θ_c	Cone half angle
μ	Coefficient of absolute viscosity
ρ	Density
ϕ	Total velocity potential which is made up of axial and crossflow velocity potentials
ψ	Velocity potential for axial flow

Subscripts

∞	Freestream conditions
a	Afterbody
B	Boattail
BA	Base
n	Nose
o	Stagnation
r	Reference conditions (reference length is the afterbody diameter = d_r)

APPENDIX B

COMPUTER PROGRAM

COMPUTER PROGRAM TO DETERMINE PRESSURE DISTRIBUTIONS AND FORCES ON UNGUIDED PROJECTILES OR THE BODY ALONE OF THE GUIDED PROJECTILE

The methods described in the report to obtain surface pressures and force coefficients have been programmed for high-speed digital computation. The purpose of this appendix is to provide a general description of the program including a listing of the program and a sample of the required input and resulting output.

A. DESCRIPTION OF PROGRAM

The program reads in the body geometry with $x = 0$ as shown in Figure 1. If the nose is truncated, a conical nose of angle given by Figure 2 is automatically placed on the truncated portion to get the perturbation solution started; but the pressure integration begins at $x = 0$, which is the location of the first point read in. If the nose has a spherical cap, then the program automatically computes this and again the first point read into the computer is at $x = 0$. However, the pressure integration begins at $x = -r_n$.

It is suggested that the description of the body be read in to at least three decimal places if possible because the resulting solution will not be as accurate as it could be otherwise. For example, if the ogive has a formula it is suggested a desk calculator be used to compute the body coordinates as opposed to a slide rule.

Once the coordinates of the body are read in (the various body geometry options are discussed below), the program then computes a new set of body coordinates where the flow field solution will actually be found. These points are unequally spaced along the body to conserve computational time but are also spaced closely enough so an accurate solution can be assured. Once the body geometry has been found, the program checks to see whether the Mach number is subsonic ($M_\infty \leq 0.8$), transonic ($0.8 < M_\infty < 1.2$), or supersonic ($M_\infty \geq 1.2$) and then proceeds to numerically calculate the force coefficients for that particular Mach number.

B. INPUT DATA CARDS

CARD NUMBER	PARAMETERS READ	FORMAT
1	M	I3
2	AL, DIA, HB, AINF, RHOINF, AMUINF, IPRINT	(4F10.4,2F15.12, I5)
3	MN $(MN \leq 16)$	I3
4	AM (I) I = 1,2,3,..., MN-1, MN	16F5.3
5	N, NSHAPE, N1, N2, N3, NBLUNT NFL, NN1A, C2, C4, F, RR	(8I5, 4F10.5)

CARD NUMBER	PARAMETERS READ	FORMAT
6	X(I), R(I) I = 1,2,3,...., N-1, N	2F15.10
.		
.		
.		
N+5		

C. DEFINITION OF PARAMETERS

PARAMETER	USE
M	Specifies number of cases to be run. If M > 1, then only one data card needs to be included for M but cards 2 through (N+5) are included for each additional case
AL	Angle of attack (degrees)
DIA	Body reference diameter (feet)
HB	Mean height of rotating band in calibers
AINF	Freestream speed of sound (ft/sec)
RHOINF	Freestream density (slugs/ft^3)
AMUINF	Freestream absolute viscosity (lb-sec/ft^2)
IPRINT	IPRINT = 1; pressure coefficients are to be printed 2; no pressure coefficients printed
MN	Number of Mach numbers where solutions are computed (MN $\leq$ 16)
AM(I)	Mach number where solution is computed
N	Total number of points read in along body surface (N $\leq$ 30)

PARAMETER	USE
NSHAPE	Parameter which describes body shape 1. Pointed Body NSHAPE = 1; nose only 2; nose plus afterbody 3; nose with discontinuity in it. There may or may not be an afterbody present. 4; nose plus afterbody plus boattail 5; nose with discontinuity in it plus afterbody plus boattail 2. Blunted or Truncated Nose NSHAPE = 3; nose with or without discontinuity. There may or may not be an afterbody present. 5; same as above except afterbody and boattail are present. If NSHAPE = 3 or 5, at least 5 points must be read in along each of the ogives even if the ogive is a straight line.
N1	Number of points read in along first ogive
N2	Number of points read in up through the second ogive (includes first ogive)
N3	N3 = 1; conical boattail 2; ogival boattail (at least 5 points must be given along boattail if N3 = 2)
NBLUNT	NBLUNT = 1; pointed body 2; truncated or spherical cap
NFL	NFL = 1; spherical cap 2; truncated nose
NN1A	NN1A = 1; Blunted nose with no discontinuities present other than the intersection of the nose cap with the ogive (N1 = 1 and N2 $\geq$ 5). 2; Blunted nose with a discontinuity in the ogive so there are two ogives present (N1 $\geq$ 5 and N2 $\geq$ 9).

PARAMETER	USE
C2,C4	Parameters which specify mesh spacing. If nose is pointed, C2 = 0.9 and C2 = 20 are nominal values. For other nose shapes, C2 = .05 and C4 = 1.0 are nominal values.
F	Constant which determines limiting body slope for a given Mach number. F $\leq$ 1.0 with F ≈ 0.95 recommended.
RR	Radius of spherical cap or truncated meplat in calibers.
X(I),R(I)	Body coordinates (in calibers) where I $\leq$ 30.

D. PROGRAM LISTING

The Fortran listing of the source desk currently being used at the Naval Weapons Laboratory is as follows:

```
      PROGRAM MAIN(OUTPUT,INPUT,TAPE5=INPUT,TAPE6=OUTPUT)
      COMMON/GEOM/RP(6),X(30),R(30),C2,N,NSHAPE,N1,N2,XB(225),RB(225)
      COMMON/GEO1/ REP(225),BETA
      COMMON/GEO2/NN1,NN2,NN3,NN4,NFL,NBLUNT,NN,NNI,IPRINT,NN1A
      COMMON/GEO3/VOVS,AL,XM,YM,XINT,YINT,NNIA
      COMMON/GEO4/K,F,RR,RREF
      COMMON/DIS2/ SUM1,SUM2,SUM3,SUM4,SUM5,SUM6
      COMMON/DAT1/ T(100),AK(100),AE(100),C(225),C1(225),C3
      COMMON/DISC/ I,JK,AI2,SUM,JH,PI
      COMMON/BASE/CAB,CNB,CMB
      COMMON/BAND/CAP,CNP,CMP,HB
      COMMON/DIS1/ J1,J3
      COMMON/WAVE/CABL,CNBL,CMBL,CAW,CNW,CMW
      COMMON/VOL/ VOL,CAF,CNF,CMF,RN,DIA,XP,AP,VOLN
      COMMON/ICOU/ ICOUNT
      DIMENSION AM(20),CN(20),CM(20),CL(20),CD(20),XCP(20),CNAL(20),
     1CMAL(20),CA1(20),CAF1(20),CAB1(20),CAW1(20),CAP1(20),ETA(9),
     2ALOD(9),AMC(10),CDC(10)
      DATA(ETA(I),I=1,7)/.53,.57,.613,.64,.665,.70,.765/
      DATA(ALOD(I),I=1,7)/1.,2.,4.,6.,8.,12.,20./
      DATA(AMC(I),I=1,9)/0.,.3,.4,.5,.7,.8,.9,1.,1.4/
      DATA(CDC(I),I=1,9)/1.2,1.2,1.25,1.35,1.74,1.82,1.82,1.8,1.53/
      READ(5,50) M
   50 FORMAT(I3)
C     M=NUMBER OF CASES TO BE COMPUTED.
      DO 27 MM=1,M
      READ(5,43) AL,DIA,HB,AINF,RHOINF,AMUINF,IPRINT
   43 FORMAT(4F10.4,2F15.12,I5)
C     AL=ANGLE OF ATTACK(DEG) DIA=REFERENCE DIAMETER OFF BODY(FT).
C     AINF,RHOINF,AMUINF ARE THE FREESTREAM REFERENCE CONDITIONS FOR
C     SPEED OF SOUND(FT/SEC), DENSITY(SLUGS/FT**3),AND ABSOLUTE
C     VISCOSITY(LB-SEC/FT**2) RESPECTIVELY AT THE GIVEN ALTITUDE
C     IPRINT=1 IF PRESSURE COEFFICIENTS ARE TO BE PRINTED =2 OTHERWISE
C HB=MEAN HEIGHT OF ROTATING BAND IN CALIBERS, IF NO BAND PRESENT HB=1.
      WRITE(6,6)  MM,AL,DIA
    6 FORMAT(//,60X,*CASE NO.*,I3,//,30X,*ANGLE OF ATTACK =*,F6.2,
     1*DEGS*,10X,*REFERENCE DIAMETER =*,F6.3,*FT*,//)
      WRITE(6,7) AINF,RHOINF,AMUINF
    7 FORMAT(54X,*REFERENCE  CONDITIONS*,//,54X,*SPEED OF SOUND      =*,
     1F9.3,* FT/SEC*,/,54X,*DENSITY              =*,F10.7,*  SLUGS/FT**3
     2   *,/,54X,*ABSOLUTE VISCOSITY =*,F15.12,*  LB-SEC/FT**2*,//)
      AL=AL/57.29583
      ICOUNT=0
      READ(5,50) MN
C     MN=NUMBER OF MACH NUMBERS TO COMPUTE THE FORCE COEFFICIENTS OF
C     A PARTICULAR CASE.
      READ(5,15) (AM(I),I=1,MN)
   15 FORMAT(16F5.3)
      DO 1 J=1,MN
      ICOUNT=ICOUNT+1
      VOVS=AM(J)
      RREF=0.5
      BETA=SQRT(ABS(VOVS**2-1.))
      IF(BETA.LE.0.5) BETA=0.5
      CALL [illegible]
```

```
         AM(J)=VOVS
         IF(J.GT.1) GO TO 17
   10    IF(N1.NE.2) GO TO 17
         THEC=ATAN(RP(1))
         THETA=THEC*57.29583
         WRITE(6,30) THETA
   30    FORMAT(1X,17HCONE HALF ANGLE =,F10.5,/)
   17    CONTINUE
         VINF=VOVS*AINF
         RN=RHOINF*VINF/AMUINF
         CALL SKINF
         CALL BASEP
         CALL RBAND
         IF(AL.LT.0.0001) GO TO 18
         IF(VOVS.LT.1.2) CALL NORMFO
   18    IF(VOVS.GE.0.81) GO TO 19
         ICT=NN1
         IF(NSHAPE.EQ.3) ICT=NN2
         IF(NSHAPE.EQ.5) ICT=NN2
         THE1=ATAN(RBP(ICT))*57.293
         IF(THE1.GE.10.) GO TO 51
         CAW=0.
         GO TO 5
   51    CAW=0.012*(THE1-10.)
         GO TO 5
   19    IF(VOVS.LT.1.19) GO TO 2
         CALL HYBRID
         GO TO 5
    2    CALL TRANS
    5    CA=CAF+CAB+CAW+CAP
         CA1(J)=CA
         CAF1(J)=CAF
         CAB1(J)=CAB
         CAW1(J)=CAW
         CAP1(J)=CAP
         XT=XB(NN)+RR
         CALL INTERP(ALOD,ETA,XT,ETA1,7,3)
         AREF=3.14159*RREF**2
         AMC1=VOVS*SIN(AL)
         CALL INTERP(AMC,CDC,AMC1,CDC1,9,3)
         CNV=CDC1*ETA1*AP*AL**2/AREF
         CMV=-ETA1*CDC1*AP*AL**2*XP/(AREF*2.*RREF)
         IF(AL.GT.0.0175) GO TO 52
         CNV=0.
         CMV=0.
   52    CN(J)=CNF+CNB+CNW+CNP+CNV
         CM(J)=CMF+CMB+CMW+CMP+CMV
         CL(J)=CN(J)*COS(AL)-CA*SIN(AL)
         CD(J)=CN(J)*SIN(AL)+CA*COS(AL)
         IF(ABS(AL).LT.0.0001) GO TO 1
         CMAL(J)=CM(J)/AL
         XCP(J)=-CM(J)/CN(J)
         CNAL(J)=CN(J)/AL
    1    CONTINUE
         WRITE(6,8)
```

```
  8   FORMAT(//,53X,*AXIAL FORCE CONTRIBUTIONS*,//,1X,*MACH NO.*,14X,*SK
     1IN FRICTION*,14X,*BASE PRESSURE*,13X,*PRESSURE*,14X,*PROTRUSIONS*
     2,14X,*TOTAL*,//)
      DO 31 L=1,MN
      WRITE(6,9) AM(L),CAF1(L),CAB1(L),CAW1(L),CAP1(L),CA1(L)
  9   FORMAT(3X,F6.3,18X,F6.4,20X,F6.4,17X,F6.4,16X,F6.4,17X,F6.4)
 31   CONTINUE
      WRITE(6,12)
 12   FORMAT(//,56X,*FORCE COEFFICIENTS*,//,10X,*MACH NO.*,10X,*CD*,
     110X,*CN*,10X,*CL*,10X,*CM*,10X,*CNAL*,10X,*CMAL*,10X,*XCP/D*,//)
      DO 14  L=1,MN
      WRITE(6,13) AM(L),CD(L),CN(L),CL(L),CM(L),CNAL(L),CMAL(L),XCP(L)
 14   CONTINUE
 13   FORMAT(12X,F5.3,9X,F6.4,6X,F6.4,6X,F6.4,6X,F6.3,6X,F6.3,8X,F7.3,
     18X,F7.4)
 27   CONTINUE
      END
```

```
      FUNCTION ARSECH(Z)
      ARSECH=ALOG(1./Z+SQRT(1./Z**2-1.))
      RETURN
      END
```

```
      SUBROUTINE BASEP
      COMMON/GEOM/RP(6),X(20),R(20),D2,N,NSHAPE,N1,N2,XB(225),RB(225)
      COMMON/GEO1/ RBP(225),BETA
      COMMON/GEO2/NN1,NN2,NN3,NN4,NFL,NCOUNT,NN,NNI,IPRINT,NN1A
      COMMON/GEO3/VOVS,AL,XM,YM,XINT,YINT,NNIA
      COMMON/GEO4/ K,F,RP,RREF
      COMMON/BASE/ CA3,CNB,CMB
      DIMENSION  TCP3D(20),TXM1(20)
      DATA(TCP3D(I),I=1,19)/.120,.124,.130,.135,.142,.154,.209,.219,.221
     1,.218,.211,.191,.173,.157,.143,.131,.114,.104,.095/
      DATA(TXM1(I),I=1,19)/0.,.5,.7,.8,.85,.90,1.0,1.05,1.1,1.2,1.3,1.5,
     11.7,1.9,2.1,2.3,2.5,2.8,3.0/
      CAAW=0.
C     THIS SUBROUTINE CALCULATES BASE DRAG THROUGHOUT THE MACH NUMBER RANGE
      DCPBA=0.
      CALL INTERP(TXM1,TCP3D,VOVS,CP3D,19,3)
      CDBP = CP3D*(RB(NN)/RREF)**3
      IF(AL.LE.0.0175) GO TO 3
      DCPBA=(.512-.0036*VOVS)*AL*57.295*(RB(NN)/RREF)**3
    3 CONTINUE
      CAB= CDBP + DCPBA + CAAW
      CNB=0.
      CMB=0.
      RETURN
      END
```

```
      SUBROUTINE BLUNT
      COMMON/GEOM/PF(6),X(30),R(30),C2,N,NSHAPE,N1,N2,XB(225),RB(225)
      COMMON/GEO1/ RBP(225),BETA
      COMMON/GEO2/NN1,NN2,NN3,NNL,NFL,NBLUNT,NN,NNI,IPRINT,NN1A
      COMMON/GEO3/VOVS,AL,XM,YM,XINT,YINT,NNIA
      COMMON/GEO4/K,F,RR,RREF
      COMMON/GEO5/ C3
      CALL FDS(X(1),X(1),X(2),X(3),X(4),X(5),R(1),R(2),R(3),R(4),R(5),
     1DRB)
      VOV=VOVS
      IF(VOVS.LE.1.19) VOV=1.0001
      AMU=ASIN(1./VOV )*F
      IF(DRB.LE.AMU) GO TO 21
      AMU=F    *DRB
      VOVS=1./SIN(AMU)
      BETA=SQRT(ABS(VOVS**2-1.))
   21 J=1
      TH1=ATAN(DRB)
      RR=R(1)*COS(TH1)
    2 IF(VOVS.GT.2.1) GO TO 14
      THET1=27.5/57.295
      D=TAN(THET1)
      IF(D.LT.DRB) D=DRB
      THET1=ATAN(D)
      XM=-RR*SIN(THET1)
      YM= RR*COS(THET1)
      XB(1)=XM-YM/TAN(THET1)
      GO TO 15
   14 YM=RR*BETA/VOVS
      XM=-RR/VOVS
      XB(1)=RR**2/XM
      THE  =ATAN(YM/(XM-XB(1)))
      THET1=THE*F
      XM=-RR*SIN(THET1)
      YM= RR*COS(THET1)
      XB(1)=XM-YM/TAN(THET1)
   15 RP(1)=TAN(THET1)
      THE=THET1*57.295
      RB(1)=0.
      XB(2)=XM
      RB(2)=YM
      RBP(1)=TAN(THET1)
      RBP(2)=RBP(1)
      Z=SQRT(1.+DRB**2)
      XI=-DRB*RR/Z
      RI=RR/Z
      XINT=XI
      YINT=RI
      XIXM=ABS(XI-XM)
      NNIA=2
      IF(XIXM-.001) 18,18,19
   18 K=1
      NN1=2
      GO TO 16
   19 F=16./VOV**2
```

```
          IF(F.LT.3.) F=3.
          XB(3)=XB(2)+.01/VDV **F*RB(2)*(THE/30.)**2
          DO 3 K=3,150
          A=K-2
          RB(K)=SQRT(RR**2-XB(K)**2)
          XB(K+1)=XB(K)+.01/VDV **F*RB(K)*A**0.5)*(THE/30.)**2
          RBP(K)=-XB(K)/-B(K)
          IF(XB(K+1).GE.XI) GO TO 10
    3     CONTINUE
   10     XB(K+1)=XI
          RB(K+1)=RI
          RBP(K+1)=DRB
          IF(NN1A.EQ.2) GO TO 16
          NN1=K+1
          NN2=NN1+10
          K=K+1
          XB(K+1)=XI
          RB(K+1)=RI
          RBP(K+1)=RBP(K)
          IF(NFL.EQ.2) NNI=K+1
          IF(RI.GE.RR) GO TO 99
   16     DX=-XI/6.
          DR=(R(1)-RI)/6.
          DO 13 J=1,6
          K=K+1
          XB(K+1)=XB(K)+DX
          RB(K+1)=RB(K)+DR
          RBP(K+1)=DRB
   13     CONTINUE
          IF(NFL.EQ.2) NNI=K+1
          IF(NFL.EQ.2) NN1=K+1
          IF(NN1A.EQ.1) GO TO 99
          K=K+1
          IJ=1
          XB(K+1)=X(1)
          RB(K+1)=R(1)
          CALL FCPS(X,P,XB(K+1),RBP(K+1),N1,3)
   20     BET1=BETA
          IF(BET1.GT.1.) BET1=1.
          K=K+1
          XB(K+1)=XB(K)+C3*BET1*RB(K)
          CALL INTERP(X,P,XB(K+1),RB(K+1),N1,3)
          CALL FCPS(X,P,XB(K+1),RBP(K+1),N1,3)
   17     K=K+1
          IJ=IJ+1
          A=IJ
          C5=A*C3
          BET1=BETA
          IF(BET1.GT.1.) BET1=1.
          XB(K+1)=XB(K)+C5*BET1*RB(K)
          IF(XB(K+1).GE.X(N1)) XB(K+1)=X(N1)
          CALL INTERP(X,P,XB(K+1),RB(K+1),N1,3)
          CALL FCPS (X,P,XB(K+1),RBP(K+1),N1,3)
          IF(XB(K+1).LT.(X(N1)-.0001)) GO TO 17
          ...
```

```
      XR(K+1)=X(N1)
      RR(K+1)=R(N1)
      CALL FDPS(X,R,XB(K+1),R3P(K+1),N1,3)
      NN1=K+1
      GO TO 99
   99 RETURN
      END
```

```
      FUNCTION TSC1
      COMMON/ /T(6),X(  ), (  ), ,N,NS,ARF,N1,N2,XB(225),RB(225)
      COMMON/S 1/ RBP(225),BETA
      COMMON/SOO/NN1,NN2,NN3,NN4,NFL,  UNT,NN,NNI,IPRINT,NN1A
      COMMON/DISC/I,JK,AI2,SUM,JH,PI
      COMMON/DAT1/ T(100),AK(100),AE(100),C(225),C1(225),C3
      D=ABS(RBP(JH)-RBP(JH-1))
      XI=XB(JH)-BETA*RB(JH)
      TAU=BETA*RB(I)/(XB(I)-XI)
      IF(TAU.GE.1.) TAU=0.999999
      CALL INTERP(T,AK,TAU,AKX,100,3)
      CALL INTERP(T,AE,TAU,AEX,100,3)
C     CURVATURE SOLUTION FOR FIRST ORDER FUNCTION
      THR2=C(JH)*BETA*SQRT(XB(I)-XI)*4./3.*SQRT(2.)/PI*SQRT(1.+TAU)*
     1(AEX/TAU-AKX)*SQRT(BETA*RB(JH))
      HALF=0.
      IF(D.LE.0.0001) GO TO 99
      HALF=C(JH)*2.*BETA/PI*SQRT(RB(JH )/RB(I))*SQRT(2.*TAU/(1.+TAU))*
     1((1.+TAU)/TAU*AEX-AKX)
   99 SUM=SUM+THR2+HALF
      RETURN
      END
```

B-13

```
      SUBROUTINE DISC2
      COMMON/GEOM/ R(6),X(30),R(30),C2,N,NSHAPE,N1,N2,XB(225),RB(225)
      COMMON/GEO1/ RBP(225),BETA
      COMMON/DAT1/ T(100),AK(100),AE(100),C(225),C1(225),C3
      COMMON/DISC/I,JK,AI2,SUM,JH,PI
      COMMON/DIS2/ SUM1,SUM2,SUM3,SUM4,SUM5,SUM6
C     CURVATURE SOLUTION.
      XI=XB(JH)-BETA*RB(JH)
      TAU=BETA*RB(I)/(XB(I)-XI)
      IF(TAU.GE.1.) TAU=0.9999999
      CALL INTERP(T,AK,TAU,AKX,100,3)
      CALL INTERP(T,AE,TAU,AEX,100,3)
      A=SQRT(XB(I)-XI)
      B=SQRT(1.+TAU)
      D=2./PI*SQRT(2.         )
      A1=C(JH)*SQRT(BETA*RB(JH))
      B1=SQRT((1.+TAU)*RB(I)/(TAU*RB(JH)))
      SUM1=SUM1-A1    *A**1.5*4./9.*D*B*((3.+TAU)*AKX-4.*AEX)
      SUM2=SUM2-A1    *A*2.*D*B*(AKX-AEX)
      SUM3=SUM3+A1    *BETA*A*2./3.*D*B*(AEX/TAU-AKX)
      SUM4=SUM4-A1    /A*D*AKX/B
      SUM5=SUM5+A1    *BETA/A*D/B*((1.+TAU)/TAU*AEX-AKX)
      SUM6=SUM6-A1    *BETA**2/A*D/B*(2.*(1.+TAU)/TAU**2*AEX-(2.-TAU)/
     1TAU*AKX)/3.
      E=ABS(RBP(JH)-RBP(JH-1))
      IF(E.LT.0.0001) GO TO  99
C     CORNER SOLUTION
      A2=A**2
      F=SQRT(RB(JH)/RB(I))/PI
      G=SQRT(2.*TAU)/B
      IF(TAU.GT.0.999) GO TO 2
      H=1./(1.-TAU)
    2 H1=C(JH)
      SUM1 = SUM1-H1*4.*A2*F*B**2*G*(AKX-AEX)
      SUM2 = SUM2-H1*2.*F*G*AKX
      SUM3 = SUM3+H1*2.*BETA*F*G*(B**2*AEX/TAU-AKX)
      IF(TAU.LT.0.999) GO TO 1
      SUM4=SUM4+H1/(8.*BETA*RB(JH))
      SUM5=SUM5+3.*H1/(8.*RB(JH))
      SUM6=SUM6-7.*BETA*H1/(8.*RB(JH))
      GO TO 99
    1 SUM4 = SUM4+H1*F/A2*H*G*(AKX-AEX)
      SUM5 = SUM5+H1*BETA*F/A2*H*G*(AEX/TAU-AKX)
      SUM6 = SUM6-H1*BETA**2/A2*F*H*G*((2.-TAU**2)/TAU**2*AEX-(2.-TAU)
     1/TAU*AKX)
   99 RETURN
      END
```

```
      SUBROUTINE ISC3
      COMMON/GEOM/PF(6),X(30),R(30),C2,N,NSHAPE,N1,N2,XB(225),RB(225)
      COMMON/GEO1/ RBP(225),BETA
      COMMON/DAT1/ T(100),AK(100),AE(100),C(225),C1(225),C3
      COMMON/DISC/I,JK,AI2,SUM,JH,PI
      D=ABS(RBP(JH)-RBP(JH-1))
      XI=XB(JH)-BETA*RB(JH)
      TAU=BETA*RB(I)/(XB(I)-XI)
      IF(TAU.GE.1.) TAU=0.9999999
      CALL INTERP(T,AK,TAU,AKX,100,3)
      CALL INTERP(T,AE,TAU,AEX,100,3)
C     CURVATURE SOLUTION FOR COMPLIMENTARY FUNCTION
      A=SQRT(2.*TAU*RB(JH)/(RB(I)*(1.+TAU)))
      B=C1(JH)*BETA/PI*SQRT(BETA*RB(JH))
      SUM=SUM+2.*BETA*C1(JH)/PI*A*((1.+TAU)/TAU*AEX-AKX)
      IF(D.LE.0.0001) GO TO 99
C     CORNER SOLUTION FOR COMPLIMENTARY FUNCTION
      B1=-C3*BETA/PI
      IF(TAU.GT.0.995) GO TO 1
      SUM1=B*SQRT(XB(I)-XI)*4./3.*SQRT(2.*(1.+TAU))*(AEX/TAU-AKX)
      SUM2=B1/(XB(I)-XI)*A/(1.-TAU)*(AEX/TAU-AKX)
      GO TO 2
 1    SUM1=0.
      SUM2=-3.*C3    /(8.*RB(I))
 2    SUM=SUM+SUM1+SUM2
 99   RETURN
      END
```

```
      SUBROUTINE DISC4
      COMMON/GEOM/RP(6),X(30),R(30),C2,N,NSHAPE,N1,N2,XB(225),RB(225)
      COMMON/GEO1/ RBP(225),BETA
      COMMON/DAT1/ T(100),AK(100),AE(100),C(225),C1(225),C3
      COMMON/DISC/I,JK,AI2,SUM,JH,PI
      COMMON/DIS2/SUM1,SUM2,SUM3,SUM4,SUM5,SUM6
C     CURVATURE SOLUTION
      XI=XB(JH)-BETA*RB(JH)
      TAU=BETA*RB(I)/(XB(I)-XI)
      IF(TAU.GE.1.) TAU=0.9999999
      CALL INTERP(T,AK,TAU,AKX,100,3)
      CALL INTERP(T,AE,TAU,AEX,100,3)
      A=SQRT(XB(I)-XI)
      B=SQRT(1.+TAU)
      D=2.**1.5/PI
      E=ABS(RBP(JH)-RBP(JH-1))
      F=SQRT(RB(JH)/RB(I))/PI
      G=SQRT(2.*TAU)/B
      A2=A**2
      H1=C1(JH)*F*G
      SUM1=SUM1-H1*4.*A2*B**2*(AKX-AEX)
      SUM2=SUM2-H1*2.*AKX
      SUM3=SUM3+H1*2.*BETA*(B**2*AEX/TAU-AKX)
      IF(E.LT.0.0001) GO TO 2
C     CORNER SOLUTION
      H2=C1(JH)*D*B*SQRT(BETA*RB(JH))
      SUM1=SUM1+H2*A**1.5*4./9.*((3.+TAU)*AKX-4.*AEX)
      SUM2=SUM2-H2*A*2.*(AKX-AEX)
      SUM3=SUM3+H2*BETA*A*2./3.*(AEX/TAU-AKX)
      SUM1=SUM1+C3     *2.*G*F*AKX
      IF(TAU.LT.0.995) GO TO 1
      SUM2=SUM2-C3     /(8.*BETA*RB(JH))
      SUM3=SUM3-3.*C3     /(8.*RB(JH))
      GO TO 2
    1 H=1./(1.-TAU)
      SUM2=SUM2-C3     /A2*F*H*G*(AKX-AEX)
      SUM3=SUM3-C3     *BETA/A2*F*H*G*(AEX/TAU-AKX)
    2 CONTINUE
      RETURN
      END
```

```
      SUBROUTINE FCF (X,X1,X2,X3,X4,X5,F1,F2,F3,F4,F5,FX)                    Q   1
      A1=(X-X4)*(X-X5)*(2.  *X-X2-X3)+(X-X2)*(X-X3)*(2.  *X-X4-X5)
      A2=(X-X4)*(X-X5)*(2.  *X-X1-X3)+(X-X1)*(X-X3)*(2.  *X-X4-X5)
      A3=(X-X4)*(X-X5)*(2.  *X-X1-X2)+(X-X1)*(X-X2)*(2.  *X-X4-X5)        Q
      A4=(X-X3)*(X-X5)*(2.  *X-X1-X2)+(X-X1)*(X-X2)*(2.  *X-X3-X5)
      A5=(X-X3)*(X-X4)*(2.  *X-X1-X2)+(X-X1)*(X-X2)*(2.  *X-X3-X4)        Q
      D1=(X1-X2)*(X1-X3)*(X1-X4)*(X1-X5)                                     Q   7
      D2=(X2-X1)*(X2-X3)*(X2-X4)*(X2-X5)                                     Q   8
      D3=(X3-X1)*(X3-X2)*(X3-X4)*(X3-X5)                                     Q   9
      D4=(X4-X1)*(X4-X2)*(X4-X3)*(X4-X5)                                     Q  10
      D5=(X5-X1)*(X5-X2)*(X5-X3)*(X5-X4)                                     Q  11
      C1=A1/D1                                                               Q  12
      C2=A2/D2                                                               Q  13
      C3=A3/D3                                                               Q  1
      C4=A4/D4                                                               Q  15
      C5=A5/D5                                                               Q  16
      FX=C1*F1+C2*F2+C3*F3+C4*F4+C5*F5                                       Q  17
      RETURN                                                                 Q  18
      END                                                                    Q  19-
```

```
      SUBROUTINE FDP5(TX,TY,X    ,Y,N,J)
      DIMENSION TX(30),TY(30)
      I=0
    1 I=I+1
      IF(TX(I).LE.X    ) GO TO 1
      K=J+2
      IF(I.LE.K) I=K
      IF(I.GT.(N-2)) I=N-2
      CALL FD5(X    ,TX(I-2),TX(I-1),TX(I),TX(I+1),TX(I+2),TY(I-2),TY(I-1)
     1),TY(I),TY(I+1),TY(I+2),Y    )
      RETURN
      END
```

```
      SUBROUTINE GEOM
      COMMON/GEOM/RR(6),X(10),R(10),C2,N,NSHAPE,N1,N2,XB(225),RB(225)
      COMMON/GEO1/ RRB(225),BETA
      COMMON/GEO2/NN1,NN2,NN3,NN4,NFL,NBLUNT,NN,JNI,IPRINT,NN1A
      COMMON/GEO3/VOVS,AL,XM,YM,XINT,YINT,NPIA
      COMMON/GEO4/K,F,RR,RREF
      COMMON/GEO5/ C3
      COMMON/ICOU/ ICOUNT
      COMMON/LENG/BL,ANL,ALA
      IF(ICOUNT.GT.1) GO TO 31
      READ(5,1) N,NSHAPE,N1,N2,N3,NBLUNT,NFL,NN1A,C2,C4,F,RR
    1 FORMAT(8I5,4F10.5)
   31 C3=C2/C4
C  N= TOTAL NUMBER OF POINTS READ IN ALONG BODY.
C   NSHAPE IS A PARAMETER WHICH DESCRIBES THE BODY SHAPE.
C   NN1=NUMBER OF GRID POINTS COMPUTED ALONG FIRST OGIVE?NN2 ALONG 2ND
C      PORTION OF BODY? NN3 ALONG THIRD PORTION AND NN4 ALONG 4TH SEGMENT.
C     MAXUMUM OF 4 SEGMENTS ALLOWABLE.
C     N3=1 FOR CONICAL BOATTAIL,=2 FOR OGIVAL BOATTAIL. IF OGIVAL BOATTAIL
C        IS PRESENT THEN AT LEAST 5 POINTS MUST BE GIVEN ALONG BOATTAIL.
C   C2 IS A FACTOR WHICH DETERMINES STEP SIZE IN X DIRECTION.
C
C               POINTED BODY
C
C  NBLUNT=1
C    C2=0.9 AND C4= 20. ARE NOMINAL VALUES FOR THESE PARAMETERS.
C    NSHAPE=1? NOSE ONLY.
C    NSHAPE=2? NOSE PLUS AFTERBODY.
C    NSHAPE=3? NOSE WITH A DISCONTINUITY IN IT. THERE MAY OR MAY NOT BE
C        AN AFTERBODY PRESENT.
C    NSHAPE =4? NOSE PLUS AFTERBODY PLUS BOATAIL.
C    NSHAPE 5? NOSE WITH DISCONTINUITY IN IT PLUS AFTERBODY PLUS BOATAIL.
C    N1=NUMBER OF POINTS ALONG FIRST OGIVE?N2 = NUMBER OF POINTS THROUGH
C       SECOND OGIVE INCLUDING FIRST OGIVE.
C     IF NSHAPE = 3 OR 5 , AT LEAST FIVE POINTS MUST BE READ IN ALONG
C    EACH OF THE OGIVES, EVEN IF THE OGIVE IS A STRAIGHT LINE.
C
C               BLUNTED BODY
C
C    NBLUNT=2
C   C2=.05 AND C4= 1.0 ARE NOMINAL VALUES FOR THESE PARAMETERS.
C   NFL=1 FOR SPHERICAL CAP? NFL=2 FOR TRUNCATED NOSE.
C    WHEN THE BODY IS BLUNTED NSHAPE MUST BE EITHER 3 OR 5.
C    NSHAPE = 3,NN1A=1? BLUNTED NOSE WITH NO DISCONTINUITIES OTHER THAN THE
C      INTERSECTION OF THE CAP WITH OGIVE.
C    NSHAPE=3, NN1A=2? BLUNTED NOSE WITH A DISCONTINUITY IN THE OGIVE SO THERE
C      ARE 2 OGIVES PRESENT.
C    NSHAPE=5,NN1A=1? SAME AS ABOVE EXCEPT BOATTAIL PRESENT.
C    NSHAPE=5,NN1A =2? SAME AS ABOVE EXCEPT BOATTAIL PRESENT.
C    IF NN1A =1 , THEN N1=1 AND N2.GE.5? IF NN1A=2, THEN N1.GE.5 AND N2. GE.9
C  RR = RADIUS OF SPHERICAL CAP IN CALIBERS(OR TRUNCATED PORTION).
      IJ=1
      IF(ICOUNT.GT.1) GO TO 32
      WRITE(6,34)
   34 FORMAT(24X,*BODY COORDINATES*,//,26X,*X*,11X,*R*,/)
```

```
      DO 2 I=1,N
      READ(5,3) X(I),R(I)
      WRITE(6,33) X(I),R(I)
   33 FORMAT(20X,2F12.4)
    2 CONTINUE
    3 FORMAT(2F15.10)
   32 IF(NBLUNT.EQ.2) CALL BLUNT
      IF(NBLUNT.EQ.2) GO TO 5
      XB(1)=X(1)
      RB(1)=R(1)
      IF(N1.NE.2) GO TO 4
      IF(NN1A.EQ.2) GO TO 4
  510 DO 508 I=2,5
      RP(I)=(R(I)-R(1))/(X(I)-X(1))
      TA=RP(I)
      TABE=BETA*TA
      IF(TABE.LT.0.94) GO TO 509
  508 CONTINUE
  509 XB(2)=X(I)
      RB(2)=R(I)
      RP(1)=RP(I)
      NN1=2
      K=1
      RBP(1)=RP(1)
      RBP(2)=RBP(1)
      GO TO 5
    4 DO 6 J=1,5
      L=1
      CALL FDP5(X,R,X(J),RP(J),N2,L)
    6 CONTINUE
      TA=RP(1)
      TABE=BETA*TA
      RBP(1)=TA
      IF(N1.EQ.2) GO TO 510
      IF(TABE.LT..94) GO TO 503
      DO 505 I=1,5
      TABE=BETA*RP(I)
      IF(TABE.LE.0.94) GO TO 506
  505 CONTINUE
  506 XB(2)=X(I)
      RB(2)=R(I)
      RBP(2)=RP(I)
      RP(1)=RP(I)
      RB(1)=0.
      RBP(1)=RP(1)
      XB(1)=XB(2)-RB(2)/RP(1)
      XB(3)=XB(2)+0.01
      JJ=3
      JK=2
      GO TO 507
  503 CALL FL5(X(1),X(1),X(2),X(3),X(4),X(5),RP(1),RP(2),RP(3),RP(4),
     1RP(5),RPP)
      RHOB=ABS((1.+RP(1)**2)**1.5/RPP)
      XB(2)=0.025*RHOB/BETA**1.5    +XB(1)
      JJ=2
```

```
      JK=1
      JJ=N1
      IF(NN1A.EQ.2) JJ=N2
  567 J=1
      DO 7 K=JJ,F9
      CALL INTERP(X,-,XB(K),RB(K),JU,3)
      CALL FDP5(X,P,XB(K),RPP(K),JU,J)
      BET1=BETA
      IF(BET1.GT.1.) BET1=1.
      XB(K+1)=XB(K)+BET1*(RB(K)--B(JK))*C2
      IF(XB(K+1).GE.X(N1)) GO TO 8
    7 CONTINUE
    8 XB(K+1)=X(N1)
      RB(K+1)=R(N1)
      NN1=K+1
      NN2=NN1+10
      CALL FDP5(X,P,XB(K+1),RBP(K+1),JU,J)
    5 GO TO(9,10,11,12,11) ,NSHAPE
    9 NN=NN1
      ANL=XB(NN)
      BL=0.
      ALA=0.
      GO TO 99
   10 XB(K+2)=X(N1)
      RB(K+2)=R(N1)
      RBP(K+2)=0.
      BET1=BETA
      IF(BET1.GT.1.0) BET1=1.
      XB(K+3)=C3    *BET1*RB(K+2)+XB(K+2)
      RB(K+3)=RB(K+2)
      RBP(K+3)=0.
   14 K=K+1
      IJ=IJ+1
      A=IJ
      CS=A*C3
      BET1=BETA
      IF(BET1.GT.1.0) BET1=1.
      XB(K+3)=CS*BET1*RB(K+2)+XB(K+2)
      RB(K+3)=RB(K+2)
      RBP(K+3)=0.
      IF(XB(K+3).LT.X(N)) GO TO 14
      XB(K+3)=X(N)
      RB(K+3)=R(N)
      NN=K+3
      NN1=K+2
      ANL=XB(NN1)
      BL=0.
      ALA=XB(NN)-XB(NN1)
      NNK=NN +10
      GO TO 99
   11 XB(K+2)=X(N1)
      RB(K+ )=R(N1)
      J=N4
      CALL FDP5(X,P,XB(K+2),RBP(K+2),  ,  )
      BET1=BETA
```

```
          IF(BET1.GT.1.0) BET1=1.
          XB(K+3)=XB(K+2)+C3    *BET1*RB(K+2)
          CALL INTERP(X,R,XB(K+3),RB(K+3),N2,3)
          CALL FDP5(X,R,XB(K+3),RBP(K+3),N2,J)
   15     K=K+1
          IJ=IJ+1
          A=IJ
          C5=A*C3
          BET1=BETA
          IF(BET1.GT.1.0) BET1=1.
          XB(K+3)=XB(K+2)+C5*BET1*RB(K+2)
          IF(XB(K+3).GE.X(N2)) XB(K+3)=X(N2)
          CALL INTERP(X,R,XB(K+3),RB(K+3),N2,3)
          CALL FDP5(X,R,XB(K+3),RBP(K+3),N2,J)
          IF(XB(K+3).LT.(X(N2)-.0001)) GO TO 15
          IJ=1
          XB(K+3)=X(N2)
          RB(K+3)=R(N2)
          NN2=K+3
          ANL=XB(NN2)+RR
          IF(NFL.EQ.2) ANL=XB(NN2)
          BL=0.
          ALA=0.
          CALL FDP5(X,R,XB(K+3),RBP(K+3),N2,J)
          IF(XB(K+3).LT.(X(N)-.0001)) GO TO 30
          NN=K+3
          NN3=K+3
          GO TO 99
   30     RBP(K+4)=0.
          XB(K+4)=XB(K+3)
          RB(K+4)=RB(K+3)
          BET1=BETA
          IF(BET1.GT.1.0) BET1=1.
          XB(K+5)=C3    *BET1*RB(K+4)+XB(K+4)
          XB(K+5)=C3/100.*BET1*RB(K+4)+XB(K+4)
          RB(K+5)=RB(K+4)
          RBP(K+5)=0.
   16     K=K+1
          IJ=IJ+1
          A=IJ
          C5=A*C3
          BET1=BETA
          IF(BET1.GT.1.0) BET1=1.
          XB(K+5)=C5*BET1*RB(K+4)+XB(K+4)
          RB(K+5)=RB(K+4)
          RBP(K+5)=0.
          IF(XB(K+5).LT.X(N2+1)) GO TO 16
          XB(K+5)=X(N2+1)
          RB(K+5)=R(N2+1)
          NN3=K+5
          ALA=XB(NN3)-XB(NN2)
          IF(NSHAPE.EQ.5) GO TO 13
          NN=K+5
          GO TO 99
   12     XB(K+2)=X(N1)
```

```
      RB(K+2)=R(N1)
      RBP(K+2)=0.
      ANL=XB(NN1)
      BET1=BETA
      IF(BET1.GT.1.0) BET1=1.
      XB(K+3)=C3    *BET1*RB(K+2)+XB(K+2)
      X3(K+3)=C3/100.*BET1*RB(K+2)+XB(K+2)
      RB(K+3)=RB(K+2)
      RBP(K+3)=0.
   17 K=K+1
      IJ=IJ+1
      A=IJ
      C5=A*C3
      BET1=BETA
      IF(BET1.GT.1.0) BET1=1.
      XB(K+3)=XB(K+2)+C5*BET1*RB(K+2)
      RB(K+3)=RB(K+2)
      RBP(K+3)=0.
      IF(XB(K+3).LT.X(N1+1)) GO TO 17
      XB(K+3)=X(N1+1)
      RB(K+3)=R(N1+1)
      NN2=K+3
      ALA=XB(NN2)-XB(NN1)
      IJ=1
      XB(K+4)=XB(K+3)
      RB(K+4)=RB(K+3)
      RBP(K+4)=RBP(K+3)
      BET1=BETA
      IF(BET1.GT.1.0) BET1=1.
      XB(K+5)=XB(K+4)+C3    *BET1*RB(K+4)
      IF(N3.EQ.2) GO TO 20
      IF(ICOUNT.GT.1) GO TO 517
      SLOPE=(R(N)-RB(K+4))/(X(N)-XB(K+4)) +1./57.293
      IF(SLOPE.LT.-0.0872) SLOPE=-.0872
      R(N)=SLOPE*(X(N)-XB(K+4))+RB(K+4)
  517 RB(K+5)=RB(K+4)+SLOPE*(XB(K+5)-XB(NN2))
      RBP(K+4)=SLOPE
      RBP(K+5)=SLOPE
      GO TO 21
   20 CALL INTER5(XB(K+5),X(N-4),X(N-3),X(N-2),X(N-1),X(N),R(N-4),
     1R(N-3),R(N-2),R(N-1),R(N),RB(K+5))
      CALL FD5(XB(K+5),X(N-4),X(N-3),X(N-2),X(N-1),X(N),R(N-4),R(N-3),
     1R(N-2),R(N-1),R(N),RBP(K+5))
   21 IF(XB(K+5).LT.X(N)) GO TO 18
      XB(K+5)=X(N)
      RB(K+5)=R(N)
      NN3=K+5
      BL=XB(NN3)-XB(NN2)
      NN=K+5
      GO TO 99
   18 K=K+1
      IJ=IJ+1
      A=IJ
      C5=A*C3
      BET1=BETA
```

```
      IF(BET1.GT.1.0) BET1=1.
      XB(K+5)=XB(K+4)+C5*BET1*RB(K+4)
      IF(N3.EQ.2) GO TO 22
      RB(K+5)=RB(NN2)+SLOPE*(XB(K+5)-XB(NN2))
      RBP(K+5)=SLOPE
      GO TO 23
   22 CALL INTER5(XB(K+5),X(N-4),X(N-3),X(N-2),X(N-1),X(N),R(N-4),
     1R(N-3),R(N-2),R(N-1),R(N),RB(K+5))
      CALL FD5(XB(K+5),X(N-4),X(N-3),X(N-2),X(N-1),X(N),R(N-4),R(N-3),
     1R(N-2),R(N-1),R(N),RBP(K+5))
   23 IF(XB(K+5).LT.X(N)) GO TO 19
      XB(K+5)=X(N)
      RB(K+5)=R(N)
      NN3=K+5
      NN=K+5
      BL=XB(NN3)-XB(NN2)
      GO TO 99
   13 XB(K+6)=XB(K+5)
      RB(K+6)=RB(K+5)
      IJ=1
      BET1=BETA
      IF(BET1.GT.1.0) BET1=1.
      XB(K+7)=XB(K+6)+C3/2.*BET1*RB(K+6)
      IF(N3.EQ.2) GO TO 24
      IF(ICOUNT.GT.1) GO TO 516
      SLOPE=(R(N)-RB(K+6))/(X(N)-XB(K+6)) +1./57.293
      IF(SLOPE.LT.-0.0872) SLOPE=-.0872
      R(N)=SLOPE*(X(N)-XB(K+6))+RB(K+6)
  516 RB(K+7)=RB(K+6)+SLOPE*(XB(K+7)-XB(NN3))
      RBP(K+6)=SLOPE
      RBP(K+7)=SLOPE
      GO TO 25
   24 CALL INTER5(XB(K+7),X(N-4),X(N-3),X(N-2),X(N-1),X(N),R(N-4),
     1R(N-3),R(N-2),R(N-1),R(N),RB(K+7))
      CALL FD5(XB(K+7),X(N-4),X(N-3),X(N-2),X(N-1),X(N),R(N-4),R(N-3),
     1R(N-2),R(N-1),R(N),RBP(K+7))
   25 IF(XB(K+7).LT.X(N)) GO TO 19
      XB(K+7)=X(N)
      RB(K+7)=R(N)
      NN4=K+7
      NN=K+7
      BL=XB(NN4)-XB(NN3)
      GO TO 99
   19 K=K+1
      IJ=IJ+1
      A=IJ
      C5=A*C3
      BET1=BETA
      IF(BET1.GT.1.0) BET1=1.
      XB(K+7)=XB(K+6)+C5*BET1*RB(K+6)
      IF(N3.EQ.2) GO TO 26
      RB(K+7)=RB(NN2)+SLOPE*(XB(K+7)-XB(NN3))
      RBP(K+7)=SLOPE
      GO TO 27
   26 CALL INTER5(XB(K+7),X(N-4),X(N-3),X(N-2),X(N-1),X(N),R(N-4),
```

```
     1R(N-3),R(N-2),R(N-1),R(N),FR(K+7))
      CALL FDS(XF(K+7),X(N-4),X(N-3),X(N-2),X(N-1),X(N),R(N-4),R(N-3),
     1R(N-2),R(N-1),R(N),RRR(K+7))
   27 IF(XB(K+7).LT.X(N)) GO TO 13
      XB(K+7)=X(N)
      RR(K+7)=R(N)
      NN=K+7
      NN4=K+7
      BL=XB(NN)-XB(NN3)
   99 CONTINUE
      RETURN
      END
```

```
      SUBROUTINE HYBRID
      COMMON/GEOM/RH(6),X(50),R(50),R2,N,NSHAPE,N1,N2,XB(225),RB(225)
      COMMON/GEO1/ RBP(225),BETA
      COMMON/GEO2/NN1,NN2,NN3,NN4,NFL,NBCUNT,NN,NNI,IPRINT,NN1A
      COMMON/GEO3/VOVS,AL,XM,YM,XINT,YINT,NNIA
      COMMON/GEO4/K,F,RR,REFF
      COMMON/DIS2/ SUM1,SUM2,SUM3,SUM4,SUM5,SUM6
      COMMON/DAT1/ T(100),AK(100),AE(100),C(225),C1(225),C3
      COMMON/DISC/ I,JK,AI2,SUM,JH,PI
      COMMON/DIS1/J1,J3
      COMMON/WAVE/CABL,CNBL,CMBL,CAW,CNW,CMW
      COMMON/CPV/ CPV(225,20),JA,JB
      DIMENSION PSI(225),PHI(225),ZEOX(225),ZEOR(225),ZED(225),
     1ZEOXX(225),ZEOXR(225),ZEORR(225),PSIX(225),PSIR(225),ZEOP(225),
     2ZEOPX(225),ZEOPR(225),PHIX(225),PHIR(225),B(225),ZE1(225),
     1ZE1X(225),ZE1R(225)
      DIMENSION THET(20),THET1(20)
      DATA(T(I),I=1,99)/.01,.02,.03,.04,.05,.06,.07,.08,.09,.10,.11,.12,
     1.13,.14,.15,.16,.17,.18,.19,.20,.21,.22,.23,.24,.25,.26,.27,.28,
     2.29,.30,.31,.32,.33,.34,.35,.36,.37,.39,.39,.40,.41,.42,.43,.44,
     3.45,.46,.47,.48,.49,.50,.51,.52,.53,.54,.55,.56,.57,.58,.59,.60,
     4.61,.62,.63,.64,.65,.66,.67,.68,.69,.70,.71,.72,.73,.74,.75,.76,
     5.77,.78,.79,.80,.81,.82,.83,.84,.85,.86,.87,.88,.89,.90,.91,.92,
     6.93,.94,.95,.96,.97,.98,.99/
      DATA(AK(I),I=1,99)/3.35902,3.02571,2.83492,2.70218,2.60107,
     12.51987,2.45234,2.39475,2.34473,2.30064,2.26132,2.22592,2.19380,
     22.16445,2.13748,2.11257,2.08946,2.06794,2.04782,2.02896,2.01123,
     31.99451,1.97871,1.96376,1.94957,1.93608,1.92324,1.91099,1.89929,
     41.88811,1.87740,1.86713,1.85727,1.84780,1.83870,1.82993,1.82148,
     51.81331,1.80547,1.79787,1.79053,1.78343,1.77655,1.76989,1.76344,
     61.75718,1.75111,1.74521,1.73948,1.73392,1.72851,1.72324,1.71812,
     71.71313,1.70827,1.70354,1.69892,1.69442,1.69003,1.68575,1.68157,
     81.67748,1.67350,1.66960,1.66579,1.66206,1.65842,1.65485,1.65137,
     91.64795,1.64461,1.64133,1.63813,1.63499,1.63191,1.62889,1.62593,
     A1.62303,1.62018,1.61739,1.61465,1.61196,1.60932,1.60672,1.60418,
     B1.60168,1.59922,1.59680,1.59443,1.59210,1.58981,1.58755,1.58534,
     C1.58316,1.58101,1.57890,1.57683,1.57479,1.57278/
      DATA(AE(I),I-1,99)/1.02836,1.04970,1.06835,1.08526,1.10085,
     11.11541,1.12909,1.14204,1.15433,1.16606,1.17727,1.18802,1.19835,
     21.20828,1.21786,1.22711,1.23604,1.24469,1.25307,1.26119,1.26907,
     31.27672,1.28416,1.29139,1.29843,1.30528,1.31196,1.31847,1.32482,
     41.33102,          1.33707,1.34298,1.34875,1.35439,1.35991,1.36531,
     51.37059,1.37575,1.38082,1.38577,1.39063,1.39539,1.40005,1.40463,
     61.40911,1.41351,1.41783,1.42207,1.42623,1.43032,1.43433,1.43827,
     71.44214,1.44594,1.44968,1.45336,1.45697,1.46053,1.46402,1.46746,
     81.47085,1.47417,1.47745,1.48068,1.48385,1.48698,1.49006,1.49309,
     91.49607,1.49902,1.50192,1.50477,1.50759,1.51036,1.51310,1.51579,
     A1.51845,1.52107,1.52366,1.52621,1.52872,1.53121,1.53365,1.53607,
     B1.53845,1.54081,1.54313,1.54542,1.54769,1.54992,1.55213,1.55430,
     C1.55646,1.55858,1.56068,1.56275,1.56480,1.56682,1.56882/
      PI=3.1415927
      T(100)=1.
      AK(100)=PI/2.
      AE(100)-AK(100)
C     THIS SUBROUTINE COMPUTES THE SECOND ORDER AXIAL AND FIRST
```

```
C          ORDER CROSS FLOW PERTURBATION VELOCITY COMPONENTS. THESE
C           COMPONENTS ARE THEN COMBINED TO YIELD A HYBRID SOLUTION.
      IKK=1
      IK=1
      THET(1)=0.
      THET1(1)=0.
      DO 47 IJ=2,19
      THET1(IJ)=THET1(IJ-1)+10.
      THET(IJ)=THET1(IJ)/57.29593
   47 CONTINUE
   17 TA=RP(1)
      IF(IPRINT.NE.1) GO TO 118
      WRITE(6,140) VOVS
  140 FORMAT(//,1X,*PRESSURE COEFFICIENTS AT M = *,F6.3,//)
      WRITE(6,41)
   41 FORMAT(7X,1HX,10X,1HR,10X,5HDR/DX,7X,3HCP ,/)
  118 TA2=TA**2
      C(1)=TA2/SQRT(1.-BETA**2*TA2)
C    CONICAL SOLUTION , SUBSCRIPT=1
      F11= ARSECH(BETA*TA)
      F22= SQRT(1.-BETA**2*TA2)
      ZE0(1)=(F22-F11)*C(1)
      ZE0X(1)=-C(1)*F11
      ZE0R(1)=C(1)*F22/TA
      ZE0XX(1)=-1./F22*C(1)
      ZE0XR(1)=1./(F22*TA)*C(1)
      ZE0RR(1)=-1./(F22*TA2)*C(1)
C   PARTICULAR SOLUTION AT TIP
      I=1
      AN=1.2*VOVS**2/BETA**2
      PSIX(I)=VOVS**2*((ZE0(I) +AN*TA    *ZE0R(I))*ZE0XX(I) + ZE0X(I)*(
     1ZE0X(I)+AN*TA    *ZE0XR(I))-0.75*TA    *ZE0R(I)**2*ZE0XR(I))
      PSIR(I)=VOVS**2*((ZE0(I)+AN*TA    *ZE0R(I))*ZE0XR(I)+ZE0X(I)*((AN
     1+1.)*ZE0R(I)+AN*TA    *ZE0RR(I))-0.25*ZE0R(I)**2*(ZE0R(I)+3.*TA
     2*ZE0RR(I)))
C    COMPLIMENTARY SOLUTION AT TIP.
      C1(1)=TA*(TA*(1.+ZE0X(1))-PSIR(1))/F22
      AB=C1(1)/C(1)
      ZE0P(1)=AB*ZE0(1)
      ZE0PX(1)=AB*ZE0X(1)
      ZE0PR(1)=AB*ZE0R(1)
C   TOTAL SOLUTION AT TIP= PARTICULAR PLUS COMPLIMENTARY.
      PHIX(1)=PSIX(1)+ZE0PX(1)
      PHIR(1)=PSIR(1)+ZE0PR(1)
      QB=(1.+ZE0X(I))**2+ZE0R(I)**2
      CP01=2./(1.4*VOVS**2)*((1.+0.2*VOVS**2*(1.-QB))**3.5 - 1.)
      QA=(1.+PHIX(I))**2+PHIR(I)**2
      CPV(1,1)=2./(1.4*VOVS**2)*((1.+0.2*VOVS**2*(1.-QA))**3.5-1.)
      CP02=CPV(1,1)
      IF(IPRINT.NE.1) GO TO 119
      WRITE(6,42) XB(I),RB(I),RBP(I),CP02
  119 IF(NN.EQ.2) GO TO 35
C     FIRST ORDER AXIAL FLOW
      DO 7 I=2,NN
      SUM=0.
```

```
      IF(I.LE.2) GO TO 36
      J2=I-1
      DO 8 J=2,J2
      XI=XB(J-1)-BETA*RB(J-1)
      TAU=BETA*RB(I)/(XB(I)-XI)
      IF(TAU.GE.1.0) TAU=.999999
      SUM=SUM+BETA*C(J)*(XB(I)-XI)*(SQRT(1.-TAU**2)/TAU-TAU*ARSECH(TAU))
    8 CONTINUE
      JH=NN1+1
      IF(I.LE.JH) GO TO 36
      CALL DISC1
      J=NN1+1
      XI=XB(J-1)-BETA*RB(J-1)
      TAU=BETA*RB(I)/(XB(I)-XI)
      IF(TAU.GE.1.) TAU=0.999999999
      SUM=SUM-BETA*C(J)*(XB(I)-XI)*(SQRT(1.-TAU**2)/TAU-TAU*ARSECH(TAU))
      JH=NN2+1
      IF(I.LE.JH) GO TO 36
      CALL DISC1
      J=NN2+1
      XI=XB(J-1)-BETA*RB(J-1)
      TAU=BETA*RB(I)/(XB(I)-XI)
      IF(TAU.GE.1.) TAU=0.999999999
      SUM=SUM-BETA*C(J)*(XB(I)-XI)*(SQRT(1.-TAU**2)/TAU-TAU*ARSECH(TAU))
      JH=NN3+1
      IF(I.LE.JH) GO TO 36
      CALL DISC1
      J=NN3+1
      XI=XB(J-1)-BETA*RB(J-1)
      TAU=BETA*RB(I)/(XB(I)-XI)
      IF(TAU.GE.1.) TAU=0.999999999
      SUM=SUM-BETA*C(J)*(XB(I)-XI)*(SQRT(1.-TAU**2)/TAU-TAU*ARSECH(TAU))
   36 XI=XB(I-1)-BETA*RB(I-1)
      TAU=BETA*RB(I)/(XB(I)-XI)
      IF(TAU.GE.1.) TAU=0.999999999
      TAU1=BETA*RB(I)/(XB(I)-XB(1)+BETA*RB(1))
      IF(TAU.GE.1.0) TAU=.999999
      TT=C(1)*BETA*SQRT(1.-TAU1**2)/ TAU1
      DEN=BETA*(XB(I)-XI)*(SQRT(1.-TAU**2)/TAU-TAU*ARSECH(TAU))
      C(I)=(R8P(I)-TT-SUM)/DEN
  502 IF(IKK-2) 62,63,64
   62 JL=NN1
      GO TO 65
   63 JL=NN2
      GO TO 65
   64 JL=NN3
   65 IF(I.LE.JL) GO TO 7
      D=ABS(R8P(JL+1)-R8P(JL))
      IF(D.GE.0.0001) GO TO 68
      C(JL+1)=C(JL)
      IKK=IKK+1
      GO TO 7
   68 C(JL+1)=(R8P(JL+1)-R8P(JL))/(R8P(JL+1)+BETA)
      IKK=IKK+1
    7 CONTINUE
```

```
C     I=2 IS 2ND POINT ON SURFACE
      DO 9 I=2,NN
      SUM1=0.
      SUM2=0.
      SUM3=0.
      SUM4=0.
      SUM5=0.
      SUM6=0.
C  J=1 IS CONICAL SOLN. WHICH WILL BE ADDED IN BELOW.
      DO 10 J=2,I
      XXI=XB(I)+BETA*RB(J-1)-XB(J-1)
      TAU=BETA*RB(I)/XXI
      IF(TAU.GE.1.) TAU=0.999999999
      F1=ARSECH(TAU)
      F2=SQRT(1.-TAU**2)
      SUM1=SUM1-C(J)*XXI**2*((1.+0.5*TAU**2)*F1 -1.5*F2)
      SUM2=SUM2-2.*C(J)*XXI*(F1-F2)
      SUM3=SUM3+BETA*C(J)*XXI*(F2/TAU-TAU*F1)
      SUM4=SUM4-2.*C(J)*F1
      SUM5=SUM5+2.*BETA*C(J)*F2/TAU
      SUM6=SUM6-BETA**2*C(J)*(F2/TAU**2 + F1)
   10 CONTINUE
      JH=NN1+1
      IF(I.LE.NN1) GO TO 18
      CALL DISC2
      J=NN1+1
      XXI=XB(I)+BETA*RB(J-1)-XB(J-1)
      TAU=BETA*RB(I)/XXI
      IF(TAU.GE.1.) TAU=0.999999999
      F1=ARSECH(TAU)
      F2=SQRT(1.-TAU**2)
      SUM1=SUM1+C(J)*XXI**2*((1.+0.5*TAU**2)*F1 -1.5*F2)
      SUM2=SUM2+2.*C(J)*XXI*(F1-F2)
      SUM3=SUM3-BETA*C(J)*XXI*(F2/TAU-TAU*F1)
      SUM4=SUM4+2.*C(J)*F1
      SUM5=SUM5-2.*BETA*C(J)*F2/TAU
      SUM6=SUM6+BETA**2*C(J)*(F2/TAU**2 + F1)
      JH=NN2+1
      IF(I.LE.NN2) GO TO 18
      CALL DISC2
      J=NN2+1
      XXI=XB(I)+BETA*RB(J-1)-XB(J-1)
      TAU=BETA*RB(I)/XXI
      IF(TAU.GE.1.) TAU=0.999999999
      F1=ARSECH(TAU)
      F2=SQRT(1.-TAU**2)
      SUM1=SUM1+C(J)*XXI**2*((1.+0.5*TAU**2)*F1 -1.5*F2)
      SUM2=SUM2+2.*C(J)*XXI*(F1-F2)
      SUM3=SUM3-BETA*C(J)*XXI*(F2/TAU-TAU*F1)
      SUM4=SUM4+2.*C(J)*F1
      SUM5=SUM5-2.*BETA*C(J)*F2/TAU
      SUM6=SUM6+BETA**2*C(J)*(F2/TAU**2 + F1)
      JH=NN3+1
      IF(I.LE.NN3) GO TO 18
      CALL DISC2
```

```
      J=NN3+1
      XXI=XB(I)+BETA*RB(J-1)-XB(J-1)
      TAU=BETA*RB(I)/XXI
      IF(TAU.GE.1.) TAU=0.999999999
      F1=ARSECH(TAU)
      F2=SQRT(1.-TAU**2)
      SUM1=SUM1+C(J)*XXI**2*((1.+0.5*TAU**2)*F1 -1.5*F2)
      SUM2=SUM2+2.*C(J)*XXI*(F1-F2)
      SUM3=SUM3-BETA*C(J)*XXI*(F2/TAU-TAU*F1)
      SUM4=SUM4+2.*C(J)*F1
      SUM5=SUM5-2.*BETA*C(J)*F2/TAU
      SUM6=SUM6+BETA**2*C(J)*(F2/TAU**2 + F1)
   18 XIMX1=XB(I)-XB(1) +BETA*RB(1)
      TAU=BETA*RB(I)/XIMX1
      IF(TAU.GE.1.) TAU=0.999999999
      F1=ARSECH(TAU)
      F2=SQRT(1.-TAU**2)
      ZEO(I)=SUM1+XIMX1*(F2-F1)*C(1)
      ZEOX(I)=SUM2-F1*C(1)
      ZEOR(I)=SUM3+BETA*F2/TAU*C(1)
      ZEOXX(I)=-1./(XIMX1*F2)*C(1)+SUM4
      ZEOXR(I)=BETA/(XIMX1*TAU*F2)*C(1)+SUM5
      ZEORR(I)=-BETA**2/(XIMX1*TAU**2*F2)*C(1)+SUM6
      QB=(1.+ZEOX(I))**2 + ZEOR(I)**2
      CP01=2./(1.4*VOVS**2)*((1.+0.2*VOVS**2*(1.-QB))**3.5 - 1.)
      CPV(I,1)=CP01
      PHIX(I)=ZEOX(I)
      PHIR(I)=ZEOR(I)
      IF(NSHAPE.NE.4) GO TO 503
      IF(I.GT.NN2) GO TO 505
      GO TO 504
  503 IF(I.GT.NN3) GO TO 505
  504 CONTINUE
C    SECOND ORDER AXIAL SOLUTION.
C       A. PARTICULAR SOLUTION
      AN=1.2*VOVS**2/BETA**2
      PSI(I)=VOVS**2*(ZEOX(I)*(ZEO(I)+AN*RB(I)*ZEOR(I))-0.25*RB(I)
     1*ZEOR(I)**3)
      PSIX(I)=VOVS**2*((ZEO(I) +AN*RB(I)*ZEOR(I))*ZEOXX(I) + ZEOX(I)*(
     1ZEOX(I)+AN*RB(I)*ZEOXR(I))-0.75*RB(I)*ZEOR(I)**2*ZEOXR(I))
      PSIR(I)=VOVS**2*((ZEO(I)+AN*RB(I)*ZEOR(I))*ZEOXR(I)+ZEOX(I)*((AN
     1+1.)*ZEOR(I)+AN*RB(I)*ZEORR(I))-0.25*ZEOR(I)**2*(ZEOR(I)+3.*RB(I)
     2*ZEORR(I)))
C       B. COMPLIMENTARY SOLUTION
   20 SUM=0.
      IF(I.EQ.2) GO TO 37
      J3=I-1
      DO 12 J=2,J3
      XI=XB(J-1)-BETA*RB(J-1)
      TAU=BETA*RB(I)/(XB(I)-XI)
      IF(TAU.GE.1.) TAU=0.999999999
      SUM=SUM+BETA*C1(J)*(XB(I)-XI            )*(SQRT(1.-TAU**2)/TAU
     1-TAU*ARSECH(TAU))
   12 CONTINUE
      JH=NN1+1
```

```
      IF(I.LE.JH ) GO TO 37
      CALL DISC3
      J=NN1+1
      XI=XB(J-1)-BETA*RB(J-1)
      TAU=BETA*RB(I)/(XB(I)-XI)
      IF(TAU.GE.1.) TAU=0.999999999
      SUM=SUM-BETA*C1(J)*(XB(I)-XI            )*(SQRT(1.-TAU**2)/TAU
     1-TAU*ARSECH(TAU))
      JH=NN2+1
      IF(I.LE.JH ) GO TO 37
      CALL DISC3
      J=NN2+1
      XI=XB(J-1)-BETA*RB(J-1)
      TAU=BETA*RB(I)/(XB(I)-XI)
      IF(TAU.GE.1.) TAU=0.999999999
      SUM=SUM-BETA*C1(J)*(XB(I)-XI            )*(SQRT(1.-TAU**2)/TAU
     1-TAU*ARSECH(TAU))
      JH=NN3+1
      IF(I.LE.JH ) GO TO 37
      CALL DISC3
      J=NN3+1
      XI=XB(J-1)-BETA*RB(J-1)
      TAU=BETA*RB(I)/(XB(I)-XI)
      IF(TAU.GE.1.) TAU=0.999999999
      SUM=SUM-BETA*C1(J)*(XB(I)-XI            )*(SQRT(1.-TAU**2)/TAU
     1-TAU*ARSECH(TAU))
   37 TAU=BETA*RB(I)/(XB(I)-XB(I-1)+BETA*RB(I-1))
      IF(TAU.GE.1.) TAU=0.999999999
      TAU1=BETA*RB(I)/(XB(I)-XB(1)+BETA*RB(1))
      TT=C1(1)*BETA*SQRT(1.-TAU1**2)/ TAU1
      C1(I)=(RBP(I)*(1.+ZEOX(I))-PSIR(I)-TT-SUM)/(BETA*(XB(I)-
     1XB(I-1)+BETA*RB(I-1))*(SQRT(1.-TAU**2)/TAU-TAU*ARSECH(TAU)))
      IF(IK-2) 94,95,96
   94 JL=NN1
      GO TO 97
   95 JL=NN2
      GO TO 97
   96 JL=NN3
   97 IF(I.LE.JL) GO TO 93
      D=ABS(RBP(JL+1)-RBP(JL))
      IF(D.LE.0.0001) GO TO 92
      D1=PSI(JL+1)-PSI(JL)
      C3=-D1
      C1(JL+1)=(RBP(JL+1)*(1.+ZEOX(JL+1))-PSIR(JL+1)-TT-SUM+3.*C3/
     1(8.*RB(JL+1)))/BETA
      IK=IK+1
      GO TO 93
   92 C1(JL+1)=(RBP(JL+1)*(1.+ZEOX(JL+1))-PSIR(JL+1)-TT-SUM)/BETA
      IK=IK+1
   93 SUM1=0.
      SUM2=0.
      SUM3=0.
      DO 13 J=2,I
      XXI=XB(I)-XB(J-1)+BETA*RB(J-1)
      TAU=BETA*RB(I)/XXI
```

```
      IF(TAU.GE.1.) TAU=0.999999999
      F1=ARSECH(TAU)
      F2=SQRT(1.-TAU**2)
      SUM1=SUM1-C1(J)*XXI**2*((1.+0.5*TAU**2)*F1-1.5*F2)
      SUM2=SUM2-2.*C1(J)*XXI*(F1-F2)
      SUM3=SUM3+BETA*C1(J)*(F2/TAU-TAU*F1)*XXI
   13 CONTINUE
      JH=NN1+1
      IF(I.LE.NN1) GO TO 21
      CALL DISC4
      J=NN1+1
      XXI=XB(I)-XB(J-1)+BETA*RB(J-1)
      TAU=BETA*RB(I)/XXI
      IF(TAU.GE.1.) TAU=0.999999999
      F1=ARSECH(TAU)
      F2=SQRT(1.-TAU**2)
      SUM1=SUM1+C1(J)*XXI**2*((1.+0.5*TAU**2)*F1-1.5*F2)
      SUM2=SUM2+2.*C1(J)*XXI*(F1-F2)
      SUM3=SUM3-BETA*C1(J)*(F2/TAU-TAU*F1)*XXI
      JH=NN2+1
      IF(I.LE.NN2) GO TO 21
      CALL DISC4
      J=NN2+1
      XXI=XB(I)-XB(J-1)+BETA*RB(J-1)
      TAU=BETA*RB(I)/XXI
      F1=ARSECH(TAU)
      F2=SQRT(1.-TAU**2)
      SUM1=SUM1+C1(J)*XXI**2*((1.+0.5*TAU**2)*F1-1.5*F2)
      SUM2=SUM2+2.*C1(J)*XXI*(F1-F2)
      SUM3=SUM3-BETA*C1(J)*(F2/TAU-TAU*F1)*XXI
      JH=NN3+1
      IF(I.LE.NN3) GO TO 21
      CALL DISC4
      J-NN3+1
      XXI=XB(I)-XB(J-1)+BETA*RB(J-1)
      TAU=BETA*RB(I)/XXI
      IF(TAU.GE.1.) TAU=0.999999999
      F1=ARSECH(TAU)
      F2=SQRT(1.-TAU**2)
      SUM3=SUM3-BETA*C1(J)*(F2/TAU-TAU*F1)*XXI
      SUM2=SUM2+2.*C1(J)*XXI*(F1-F2)
      SUM1=SUM1+C1(J)*XXI**2*((1.+0.5*TAU**2)*F1-1.5*F2)
   21 XIMX1=XB(I)-XB(1)  +BETA*RB(1)
      TAU=BETA*RB(I)/XIMX1
      IF(TAU.GE.1.) TAU=0.999999999
      F1=ARSECH(TAU)
      F2=SQRT(1.-TAU**2)
      ZEOP(I)=SUM1+C1(1)*XIMX1*(F2-F1)
      ZEOPX(I)=SUM2-C1(1)*F1
      ZEOPR(I)=SUM3+C1(1)*BETA*F2/TAU
C     TOTAL 2ND ORDER SOLN.=PARTICULAR PLUS COMPLIMENTARY.
      PHI(I)=PSI(I)+ZEOP(I)
      PHIX(I)=PSIX(I)+ZEOPX(I)
      PHIR(I)=PSIR(I)+ZEOPR(I)
      QB=(1.+PHIX(I))**2 + PHIR(I)**2
```

```
      CPV(I,1)=2./(1.4*VOVS**2)*((1.+0.2*VOVS**2*(1.-QB))**3.5-1.)
      CP02=CPV(I,1)
 868  IF(IPRINT.NE.1) GO TO 9
      WRITE(6,42) XB(I),RB(I),RBF(I),CPV(I,1)
 42   FORMAT(1X,4F10.5)
   9  CONTINUE
 35   IF(ABS(AL).GT.0.001) GO TO 116
      DO 117 I=1,NN
      DO 117 J=1,19
      CPV(I,J)=CPV(I,1)
 117  CONTINUE
      GO TO 109
C     FIRST ORDER CROSS FLOW
 116  IF(IPRINT.NE.1) GO TO 120
      WRITE(6,49)
 49   FORMAT(//,30X,16H HYBRID SOLUTION,//)
      WRITE(6,51)
 51   FORMAT(7X,1HX,10X,1HR,8X,6H THETA,8X,2HCP,//)
 120  J=1
      B(1)=2./BETA/(SQRT(1.-BETA**2*TA2)/(BETA**2*TA2)+ARSECH(BETA*TA))
      I=1
      TAU=BETA*TA
      F1=ARSECH(TAU)
      F2=SQRT(1.-TAU**2)
      ZE1(1)=B(1)/2.*(F2/TAU-TAU*F1)
      ZE1X(1)=B(1)*F2/TAU
      ZE1R(1)=-BETA*B(1)/2.*(F2/TAU**2+F1)
      DO 53 IJ=1,19
      UB=COS(AL)*(1.+PHIX(I))+SIN(AL)*COS(THET(IJ))*ZE1X(I)
      VB=COS(AL)*PHIR(I)+SIN(AL)*COS(THET(IJ))*(1.+ZE1R(I))
      WB=-SIN(AL)*SIN(THET(IJ))*(1.+ZE1(I)/TA)
      QB=UB**2+VB**2+WB**2
      CPV(1,IJ)=2./(1.4*VOVS**2)*((1.+0.2*VOVS**2*(1.-QB))**3.5-1.)
      IF(IPRINT.NE.1) GO TO 53
      WRITE(6,42) XB(I),RB(I),THET1(IJ),CPV(1,IJ)
 53   CONTINUE
      IF(NN.NE.2) GO TO 23
      DO 131 IJ=1,19
      CPV(2,IJ)=CPV(1,IJ)
 131  CONTINUE
      GO TO 109
 23   J5=NN
      DO 22 I=2,J5
      SUM=0.
      J6=I-1
      DO 14 J=1,J6
      IF(J.GT.1) GO TO 110
      TAU=BETA*RB(I)/(XB(I)-XB(1)+BETA*RB(1))
      IF(TAU.GE.1.) TAU=0.999999999
      GO TO 111
 110  TAU=BETA*RB(I)/(XB(I)-XB(J-1)+BETA*RB(J-1))
      IF(TAU.GE.1.) TAU=0.999999999
 111  F1=ARSECH(TAU)
      F2=SQRT(1.-TAU**2)
      IF(J.EQ.1) GO TO 107
```

```
      D=ABS(XB(J)-XB(J-1))
      IF(D.LT.0.000001) GO TO 14
  107 SUM=SUM-B(J)*(F2/TAU**2+F1)
   14 CONTINUE
      TAU=BETA*RB(I)/(XB(I)-XB(I-1)+BETA*RB(I-1))
      IF(TAU.GE.1.) TAL=0.999999999
      D=ABS(XB(I)-XB(I-1))
      IF(D.LT.0.000001) GO TO 114
      B(I)=(2./BETA+SUM)/(SQRT(1.-TAU**2)/TAU**2+ARSECH(TAU))
      GO TO 115
  114 B(I)=0.
  115 SUM1=0.
      SUM2=0.
      SUM3=0.
      DO 15 J=1,I
      IF(J.GT.1) GO TO 112
      TAU=BETA*RB(I)/(XB(I)-XB(1)+BETA*RB(1))
      IF(TAU.GE.1.) TAU=0.999999999
      XXI=XB(I)-XB(1)  +BETA*RB(1)
      GO TO 113
  112 XXI=XB(I)-XB(J-1)+BETA*RB(J-1)
      TAU=BETA*RB(I)/XXI
      IF(TAU.GE.1.) TAU=0.999999999
  113 F1=ARSECH(TAU)
      F2=SQRT(1.-TAU**2)
   24 SUM1=SUM1+B(J)/2.*(F2/TAU-TAU*F1)*XXI
      SUM2=B(J)*F2/TAU+SUM2
      SUM3=-BETA/2.*B(J)*(F2/TAU**2+F1)+SUM3
      IF(I.EQ.1) GO TO 46
   15 CONTINUE
   46 ZE1(I)=SUM1
      ZE1X(I)=SUM2
      ZE1R(I)=SUM3
C  HYBRID THEORY
      DO 48 IJ=1,19
      UB=COS(AL)*(1.+PHIX(I))+SIN(AL)*COS(THET(IJ))*ZE1X(I)
      VB=COS(AL)*PHIR(I)+SIN(AL)*COS(THET(IJ))*(1.+ZE1R(I))
      WB=-SIN(AL)*SIN(THET(IJ))*(1.+ZE1(I)/RB(I))
      QB=UB**2+VB**2+WB**2
      CPV(I,IJ)=2./(1.4*VOVS**2)*((1.+0.2*VOVS**2*(1.-QB))**3.5-1.)
      IF(IPRINT.NE.1) GO TO 48
      WRITE(6,42) XB(I),RB(I),THET1(IJ),CPV(I,IJ)
   48 CONTINUE
      IF(N.EQ.2) GO TO 27
   22 CONTINUE
  108 IF(NBLUNT.EQ.2) CALL NEWT
      CALL WAVE
   27 CONTINUE
      RETURN
      END
```

```
      SUBROUTINE INTERP(TX,TY,X,Y,N,J)
      DIMENSION TX(100),TY(100)
      I=0
    1 I=I+1
      IF(TX(I).LE.X) GO TO 1
      IF(I.LE.J) I=J
      IF(I.GT.(N-2)) I=N-2
      CALL INTER5(X,TX(I-2),TX(I-1),TX(I),TX(I+1),TX(I+2),TY(I-2),TY(I-1
     1),TY(I),TY(I+1),TY(I+2),Y)
      RETURN
      END
```

```
      SUBROUTINE INTER5(Y,X1,X2,X3,X4,X5,F1,F2,F3,F4,F5,F)
C     5 POINT LAGRANGE INTERPOLATION SUBROUTINE
C     X1.LE.X.LE.X5
      A1=(X-X2)*(X-X3)*(X-X4)*(X-X5)
      A2=(X-X1)*(X-X3)*(X-X4)*(X-X5)
      A3=(X-X1)*(X-X2)*(X-X4)*(X-X5)
      A4=(X-X1)*(X-X2)*(X-X3)*(X-X5)
      A5=(X-X1)*(X-X2)*(X-X3)*(X-X4)
      D1=(X1-X2)*(X1-X3)*(X1-X4)*(X1-X5)
      D2=(X2-X1)*(X2-X3)*(X2-X4)*(X2-X5)
      D3=(X3-X1)*(X3-X2)*(X3-X4)*(X3-X5)
      D4=(X4-X1)*(X4-X2)*(X4-X3)*(X4-X5)
      D5=(X5-X1)*(X5-X2)*(X5-X3)*(X5-X4)
      C1=A1/D1
      C2=A2/D2
      C3=A3/D3
      C4=A4/D4
      C5=A5/D5
      F=C1*F1+C2*F2+C3*F3+C4*F4+C5*F5
      RETURN
      END
```

```
      SUBROUTINE NEWRAP(C7,RN,C6,F,CF1)
C     THIS SUBROUTINE USES NEWTON RAPHSON METHOD TO SOLVE FOR MEAN
C         SKIN FRICTION COEFFICIENT.
      CF=0.0025
      J=0
    1 F=C7/SQRT(CF)-ALOG10(RN*CF) +C6
      DFDCF=-.5*C7/(CF**1.5)-.43429/CF
      J=J+1
      CF1= CF
      CF=CF-F/DFDCF
      IF(CF.LE.0.0001) CF=0.0001
      DCF=CF-CF1
      IF(ABS(DCF)-1.E-05) 2,2,4
    4 IF(J-50) 1,1,2
    2 CONTINUE
      RETURN
      END
```

```
      SUBROUTINE NEWT
      COMMON/GEOM/RP(6),X(30),R(30),C2,N,NSHAPE,N1,N2,XB(225),RB(225)
      COMMON/GEO1/ RBP(225),BETA
      COMMON/GEO2/NN1,NN2,NN3,NN4,NFL,NBLUNT,NN,NNI,IPRINT,NN1A
      COMMON/GEO3/VOVS,AL,XM,YM,XINT,YINT,NNIA
      COMMON/GEO4/K,F,RR,RREF
      COMMON/WAVE/CABL,CNBL,CMBL,CAW,CNW,CMW
      COMMON/CPV/ CPV(225,20),JA,JB
      DIMENSION PH(20),PHI(20)
      PLPI=(1.2*VOVS**2)**3.5*(6./(7.*VOVS**2-1.))**2.5
      IF(NFL.EQ.1) GO TO 2
      CP0= (0.90F*PLPI-1.)/(0.7*VOVS**2)
      IF(IPRINT.NE.1) GO TO 19
      WRITE(6,6) CP0
    6 FORMAT(1X,40HPRESSURE COEFFICIENT ON TRUNCATED NOSE =,F10.5)
   19 CA=CP0*(R(1)/RREF)**2
      CN=0.
      CM=0.
      CABL=CA
      CNBL=0.
      CMBL=0.
      XCP=0.
      CL=-CA*SIN(AL)
      CD=CA*COS(AL)
      IF(NFL.EQ.2) GO TO 20
      NNI=2
      GO TO 99
    2 CP0=(PLPI-1.)/(0.7*VOVS**2)
      CS=COS(AL)
      SS=SIN(AL)
      PH(1)=0.
      PHI(1)=0.
      IF(AL.GT.0.0001) GO TO 9
      NM=1
      GO TO 10
    9 DO 3 I=2,19
      PHI(I)=PHI(I-1)+10.
      PH(I)=PHI(I)/57.29583
    3 CONTINUE
      NM=19
   10 IF(IPRINT.NE.1) GO TO 18
      WRITE(6,8)
    8 FORMAT(1X,39HPRESSURE COEFFICIENTS ON SPHERICAL NOSE)
   18 X1=0.
      DX=(RR+XM  )/6.
      DO 4 I=1,7
      X2=X1-RR
      R2=SQRT(RR**2-X2**2)
      DO 11  L=1,NM
      A=(1.-X1   /RR)**2
      CP   =CP0*(A*CS**2+(X1   /RR-1.)*SQRT(1.-A)*COS(PH(L))*SIN(2.*AL)
     1+(1.-A)*COS(PH(L))**2*SS**2)
      IF(IPRINT.NE.1) GO TO 11
      WRITE(6,5) X2,R2,PHI(L),CP
   11 CONTINUE
```

```
      X1=X1+DX
    4 CONTINUE
      D=CP-CPV(2,19)
      D2=D
      DO 12 I=3,NN1
      X2=XB(I)
      IF(X2.GE.XINT) GO TO 15
      X1=RR+X2
      IF(X1.GE.RR) X1=RR
      IF(X1.GE.RR) X2=RR
      R2=SQRT(RR**2-X2**2)
      DO 13 L=1,NM
      A=(1.-X1/RR)**2
      CP    =CP0*(A*CS**2+(X1    /RR-1.)*SQRT(1.-A)*COS(PH(L))*SIN(2.*AL)
     1+(1.-A)*COS(PH(L))**2*SS**2)
      IF(IPRINT.NE.1) GO TO 13
      WRITE(6,5) X2,R2,PHI(L),CP
   13 CONTINUE
      IF(D.GT.0.) GO TO 14
      D1=D2
      D2=CP-CPV(I,19)
      IF(D2.LE.0.) GO TO 12
      SLOPE=(D2-D1)/(XB(I)-XB(I-1))
      XNV= XB(I-1)-D1/SLOPE
      NNI=I
      GO TO 15
   14 D1=D2
      D2=CP-CPV(I,19)
      IF(D2.GE.0.)GO TO 12
      SLOPE=(D2-D1)/(XB(I)-XB(I-1))
      XNV=XB(I-1)-D1/SLOPE
      NNI=I
      GO TO 15
   12 CONTINUE
   15 IF(I.GE.NN1) XNV=XINT
      NNI=I
      IF(X2.GE.XINT) XNV=XINT
      IF(I.GE.NN1) NNI=I-1
      YNV=SQRT(RR**2-XNV**2)
      TH2=ATAN(-YNV/XNV)
      SH=SIN(TH2)
      CH=COS(TH2)
      RA=(RR/RREF)**2
      CA=CP0/2.*RA*(CS**2*(1.-CH**4)+.5*SS    **2*SH**4)
      CN=CP0*RA*SIN(2.*AL)*SH**4/4.
      CM=-CP0/2.*RA*SIN(2.*AL)*(SH**4/4.+SH**2*CH**3/5.+2./15.*(CH**3
     1-1.))
      CABL=CA
      CNBL=CN
      CMBL=CM
      CL=CN*CS-CA*SS
      CD=CA*CS+CN*SS
      XCP=-CM/CN
   20 CONTINUE
    5 FORMAT(1X,4F10.5)
```

```
   99 RETURN
      END
```

```
      SUBROUTINE NORMFC
      COMMON/GEOM/PP(6),X(30),R(30),C2,N,NSHAPE,N1,N2,XB(225),RB(225)
      COMMON/GEO1/ RBP(225),BETA
      COMMON/GEO2/NN1,NN2,NN3,NN4,NFL,NBLUNT,NN,NNT,IPRINT,NN1A
      COMMON/GEO3/VOVS,AL,XM,YM,XINT,YINT,NNIA
      COMMON/GEO4/K,F,RR,RREF
      COMMON/WAVE/CABL,CNBL,CMBL,CAW,CNW,CMW
      COMMON/VOL/ VOL,CAF,CNF,CMF,RN,DIA,XP,AP,VOLN
      COMMON/LENG/BL,ANL,ALA
      DIMENSION A1(10),A2(10),AM(10),F1(10),G1(10),F2(10),G2(10),FA(10)
     1,D04(10),D06(10),D07(10),D08(10),D09(10),D10(10),D12(10)
     2,D11(10),XCPLA(10)
      DATA(A1(I),I=1,10)/1.75,1.82,1.9,1.96,2.05,2.6,3.5,3.65,3.7,3.35/
      DATA(A2(I),I=1,10)/1.8,1.83,1.89,1.95,1.97,2.15,2.45,2.44,2.4,2.2/
      DATA(AM(I),I=1,10)/0.,.2,.4,.6,.68,.8,.94,.97,1.05,1.2/
      DATA(F1(I),I=1,10)/0.,.1,.2,.3,.45,.6,.75,.85,.925,1./
      DATA(G1(I),I=1,10)/3.35,3.48,3.6,3.65,3.5,2.6,1.75,1.46,1.35,1.28/
      DATA(F2(I),I=1,10)/0.,.25,.5,.65,.82,1.,1.25,1.5,2.,2.5/
      DATA(G2(I),I=1,10)/3.35,3.,2.5F,2.25,1.93,1.3,1.02,.95,.85,.75/
      DATA(FA(I),I=1,10)/0.,.5,1.,1.5,2.,2.5,3.,4.,6.,8./
      DATA(D04(I),I=1,10)/0.,0.,0.,0.,0.,0.,0.,0.,0.,0./
      DATA(D06(I),I=1,10)/0.,.03,.043,.05,.05,.05,.05,.05,.05,.05/
      DATA(D07(I),I=1,10)/0.,.08,.113,.133,.143,.148,.15,.15,.15,.15/
      DATA(D08(I),I=1,10)/0.,115,.16,.186,.207,.223,.235,.248,.25,.252/
      DATA(D10(I),I=1,10)/0.,.175,.23,.265,.293,.31,.325,.337,.34,.34/
      DATA(D11(I),I=1,10)/0.,.097,.138,.16,.176,.186,.19,.195,.197,.197/
      DATA(D12(I),I=1,10)/0.,.097,.138,.16,.176,.186,.19,.195,.197,.197/
      DATA(XCPLA(I),I-1,10)/.5,.4,.342,.31,.29,.272,.26,.248,.245,.245/
      IF(BL.GE.0.02) GO TO 6
      CNALB=0.
      GO TO 2
    6 IF(VOVS.GT.1.) GO TO 1
      F11=SQRT(1.-VOVS**2)
      CALL INTERP(F1,G1,F11,G11,10,3)
      CNALB=-G11*(1.-4.*RB(NN)**2)
      GO TO 2
    1 F12=SQRT(VOVS**2-1.)
      CALL INTERP(F2,G2,F12,G12,9,3)
      CNALB=-G12*(1.-4.*RB(NN)**2)
    2 THE=ABS(RBP(NN1))
      IF(NN1A.EQ.2) THE=ABS(RBP(NN2))
      IF(NBLUNT.EQ.2) THE=ABS(RBP(NN2))
      CALL INTERP(AM,A1,VOVS,A11,10,3)
      CALL INTERP(AM,A2,VOVS,A22,10,3)
      CNALN=-A11*THE +A22
      IF(ALA.GT.0.01) GO TO 9
      CNALA=0.
      GO TO 4
    9 CALL INTERP(FA,D07,ALA,D071,10,3)
      CALL INTERP(FA,D08,ALA,D081,10,3)
      CALL INTERP(FA,D10,ALA,D101,10,3)
      CALL INTERP(FA,D06,ALA,D061,10,3)
      IF(VOVS.GE.0.8) GO TO 5
      D041=0.
      CALL INTER5(VOVS,.4,.6,.7,.8,1.,D041,D061,D071,D081,D101,CNALA)
```

```
      IF(VOVS.LT.0.6) CNALA=5.*D061*(VOVS-0.4)
      IF(VOVS.LT.0.4) CNALA=0.
      GO TO 4
    5 CALL INTERP(FA,D12,ALA,D121,10,3)
      D111=D121
      CALL INTER5(VOVS,.7,.8,1.,1.1,1.2,D071,D081,D101,D111,D121,CNALA)
    4 CNAL=CNALA+CNALN+CNALB
      XCPN=ANL-VCLN/(3.14159*RREF**2)
      XCPB=XP(NN)-PL/2.
      XCPB=BL*(1.-3.14159*(RREF**2-RREF*BL*ABS(RBP(NN))+BL**2/3.*
     1RBP(NN)**2))+ANL+ALA
      XCPA=ANL+ALA/2.
      CALL INTERP(FA,XCPLA,ALA,XCP1,10,3)
      XCP=XCP1*ALA
      XCPA=ANL+XCP
      CMAL=-(CNALN*XCPN+CNALA*XCPA+CNALB*XCPB)
      CNW=CNAL*AL
      CMW=CMAL*AL
      RETURN
      END
```

```
      SUBROUTINE RBAND
      COMMON/BAND/CAP,CNP,CMP,HB
      COMMON/GEO3/VOVS,AL,XM,YM,XINT,YINT,NNI4
      DIMENSION AM(15),DCAP(15)
      DATA(AM(I),I=1,12)/0.,.5,.7,.8,.9,.95,1.1,1.2,1.5,2.,2.5,3.0/
      DATA(DCAP(I),I=1,12)/0.,0.,0.,.001,.005,.01,.0092,.0079,.0067,
     1.0055,.0052,.005/
      CALL INTERP(AM,DCAP,VOVS,CAP1,12,3)
      CAP=CAP1*HB/0.01
      CNP-0.
      CMP=0.
      RETURN
      END
```

```
      SUBROUTINE SIMP
      COMMON/GEOM/PP(6),X(30),R(30),C2,N,NSHAPE,N1,N2,XB(225),RB(225)
      COMMON/GEO1/ RBP(225),BETA
      COMMON/CPV/ CPV(225,20),JA,JB
      COMMON/DIS2/SUM1,SUM2,SUM3,SUM4,SUM5,SUM6
      COMMON/GEO4/K,F,RR,RREF
      DIMENSION F1(225),G(225),G1(225)
      DO 1 I=JA,JB
      A1=       CPV(I,1)+2.*(CPV(I,3)+CPV(I,5)+CPV(I,7)+CPV(I,9)
     1+CPV(I,11)+CPV(I,13)+CPV(I,15)+CPV(I,17)) +CPV(I,19)
      A2=      4.*(CPV(I,2)+CPV(I,4)+CPV(I,6)+CPV(I,8)+CPV(I,10)
     1+CPV(I,12)+CPV(I,14)+CPV(I,16)+CPV(I,18))
      F1(I)=0.05818*(A1+A2)*RB(I)
      B1= CPV(I,1)-CPV(I,19) +2.*(.93969*(CPV(I,3)-CPV(I,17))+.76604*(
     1CPV(I,5)-CPV(I,15))+.5*(CPV(I,7)-CPV(I,13))+.17365*(CPV(I,9)-
     2CPV(I,11)))
      B2=4.*(.98481*(CPV(I,2)-CPV(I,18))+.86603*(CPV(I,4)-CPV(I,16))+
     1.64279*(CPV(I,6)-CPV(I,14))+.34202*(CPV(I,8)-CPV(I,12)))
      G(I)=0.05818*(B1+B2)*RB(I)
      G1(I)=G(I)*XB(I)
    1 CONTINUE
      IF(JA.NE.JB) GO TO 2
      SUM1=0.
      SUM2=0.
      SUM3=0.
      GO TO 99
    2 JBB=JB-1
      DO 3 I=JA,JBB
    7 H=(RB(I+1)-RB(I))/6.
      X12=(XB(I+1)+XB(I))/2.
      IF((JB-JA).LT.5) GO TO 4
      J=JA+2
      CALL INTERP(XB,F1,X12,F12,JB,J)
      CALL INTERP(XB,G,X12,G12,JB,J)
      CALL INTERP(XB,G1,X12,G112,JB,J)
      GO TO 5
    4 F12=(F1(I)+F1(I+1))/2.
      G12=(G(I)+G(I+1))/2.
      G112=(G1(I)+G1(I+1))/2.
      IF(JB.GT.2) GO TO 5
      F1(3)=F1(2)
      G(3)=G(2)
      G1(2)=2./3.*G1(2)
      G1(3)=G1(2)
      G112=2./3.*G112
    5 SUM1=SUM1+H*(F1(I)+4.*F12+F1(I+1))
      H1=(XB(I+1)-XB(I))/6.
      SUM2=SUM2+H1*(G(I)+4.*G12+G(I+1))
      SUM3=SUM3+H1*(G1(I)+4.*G112+G1(I+1))
    3 CONTINUE
      SUM3=SUM3+SUM2*RR
   99 RETURN
      END
```

```
      SUBROUTINE SKINF
      COMMON/GEOM/ P(6),X(30),R(30),C2,N,NSHAPE,N1,N2,XB(225),RB(225)
      COMMON/GE01/ PBP(225),BETA
      COMMON/GE02/NN1,NN2,NN3,NN4,NFL,NBLUNT,NN,NNI,IPRINT,NN1A
      COMMON/GE03/VOVS,AL,XM,YM,XINT,YINT,NNIA
      COMMON/GE04/ K,F,RR,RREF
      COMMON/DIS2/ SUM1,SUM2,SUM3,SUM4,SUM5,SUM6
      COMMON/CPV/ CPV(225,20),JA,JB
      COMMON/VOL/ VCL,CAF,CNF,CMF,RN,DIA,XP,AP,VOLN
      IF(NBLUNT.EQ.1) GO TO 5
      IF(NFL.EQ.2) GO TO 5
      SUM1=6.28318*RR*YINT
      SUM2=3.14159*YINT**2*(RR-YINT/3.)
      THE=ATAN(-YINT/XINT)
      SUM3=RR**2*THE/2.-RR**2*SIN(THE)/2.
      AB=ACOS((RR+XINT)/RR)
    4 SUM4=SUM3*2./3.*RR**3*(1.-SIN(AB)**3)
      GO TO 6
    5 SUM1=0.
      SUM2=0.
      SUM3=0.
      SUM4=0.
    6 CF3=0.
C     THIS SUBROUTINE CALCULATES THE AXIAL FORCE COEFFICIENT DUE TO SKIN
C     FRICTION ON THE BODY (CDF).
      PI=3.14159
      AREF=PI*RREF**2
      GAMA=1.4
      TWOTI=1.+0.9*(GAMA-1.)*(VOVS**2/2.)
      C=GAMA-1.
      A=SQRT(C*VOVS**2/(2.*TWOTI))
      B=(1.+.5*C*VOVS**2)/TWOTI-1.
      D=SQRT(B**2+4.*A**2)
      D1=(2.*A**2-B)/D
      D2=B/D
      D3=.242/(A*SQRT(TWOTI))
      D4=ASIN(D1)
      D5=ASIN(D2)
      C6=(1.+2.*.76)/2.*ALOG10(TWOTI)
      C7=D3*(D4+D5)
      RN3=RN*XB(NN)*DIA
      CALL NEWRAP(C7,RN3,C6,H,CF3)
      IF(NBLUNT.EQ.1) GO TO 1
      K=NNIA
      K1=NN1
      K2=NN2
      K3=NN3
      K4=NN4
      GO TO 2
    1 K=1
      K1=NN1
      K2=NN2
      K3=NN3
      K4=NN4
    2 JA=K
```

```
      JB=K1
      IF(JB.EQ.NN) JB=NN-1
      CALL TRAPE
      VOLN=SUM2
      IF(NN1.EQ.NN) GO TO 99
      JA=K1+1
      JB=K2
      IF(JB.EQ.NN) JB=NN-1
      CALL TRAPE
      IF(NBLUNT.EQ.2) VOLN=SUM2
      IF(NN1A.EQ.2) VOLN=SUM2
      IF(NN2.EQ.NN) GO TO 99
      JA=K2+1
      JB=K3
      IF(JB.EQ.NN) JB=NN-1
      CALL TRAPE
      IF(NN3.EQ.NN) GO TO 99
      JA=K3+1
      JB=NN-1
      CALL TRAPE
   99 SB =SUM1
      VOL=SUM2
      AP=SUM3
      XP=SUM4/SUM3
      CDFB=CF3*SB/AREF
      CAF=CDFB
      CNF=0.
      CMF=0.
      RETURN
      END
```

```
      SUBROUTINE TRANS
      COMMON/GEOM/RF(6),X(30),R(30),C2,N,NSHAPE,N1,N2,XB(225),RB(225)
      COMMON/GEO1/ RBP(225),BETA
      COMMON/GEO2/NN1,NN2,NN3,NN4,NFL,NBLJNT,NN,NNI,IPRINT,NN1A
      COMMON/GEO3/VOVS,AL,XM,YM,XINT,YINT,NNIA
      COMMON/GEO4/K,F,RR,RREF
      COMMON/CPV/ CPV(225,20),JA,JB
      COMMON/DIS2/ SUM1,SUM2,SUM3,SUM4,SUM5,SUM6
      COMMON/LENG/BL,ANL,ALA
      COMMON/WAVE/CABL,CNBL,CMBL,CAW,CNW,CMW
      DIMENSION AM(10),CA15(10),CA2(10),CA25(10),CA3(10),CA4(10)
      DATA(AM(I),I=1,8)/.85,.9,.95,1.,1.05,1.1,1.15,1.2/
      DATA(CA15(I),I=1,8)/.01,.072,.13,.177,.215,.247,.277,.3/
      DATA(CA2(I),I=1,8)/0.,.036,.073,.107,.14,.169,.191,.205/
      DATA(CA25(I),I=1,8)/0.,.01,.04,.07,.098,.122,.138,.143/
      DATA(CA3(I),I=1,8)/0.,0.,.024,.048,.073,.092,.102,.097/
      DATA(CA4(I),I=1,8)/0.,0.,.01,.032,.047,.055,.055,.04/
      IF(RBP(NN).LE.0.) GO TO 87
      CB0=0.
      GO TO 88
   87 VOV=VOVS-.0498
      IF(VOV.LT.1.) GO TO 89
      AREF=3.14159*RREF**2
      IF(NSHAPE.NE.4) GO TO 1
      IF(NN1A.EQ.2) GO TO 1
      J=NN2+1
      GO TO 2
    1 J=NN3+1
    2 DO 10 L=J,NN
      XX=XB(L)-XB(J)
      DELTA=ATAN(1./(2.*ANL))
      IF(RBP(J-3).LT.RBP(1)) DELTA=ATAN(.2/ANL)
      GAMA=1.4
      C1=1.+GAMA
      C0=SQRT(C1)
      C3=VOV **2
      C4=1.-C3
      C5=C4/(C1*C3)
      C6=3.*DELTA/(2.*C0)
      C7=25.*C1*VOV **(2./3.)
      C8=.5*C4/(C1*C3)
      C9=1.25*C5**2
      C10=2.*C5/(VOV **(2./3.))*C6**(2./3.)
      C11=(C6/VOV )**(4./3.)
      CSQ=C7*(C8+(C9+C10+C11)**(.5))
      C=SQRT(CSQ)
      Y=2.*ALA  +2.*XX
      CP1      =.4*(Y-C)/SQRT(C1*VOV **(2./3.))*(.04*(Y-C)**2/(C1*VOV **
     1(2./3.))-C4/(C1*C3))**.5
      IF(Y.GT.C) CP1=0.
      DELTA=-RBP(L)
      GAMA=1.4
      C1=1.+GAMA
      C0=SQRT(C1)
      C3=VOV **2
```

```
      C4=1.-C3
      C5=C4/(C1*C3)
      C6=3.*DELTA/(2.*C1)
      C7=25.*C1*VOV **(2./3.)
      C8=.5*C4/(C1*C3)
      C9=1.25*C5**2
      C10=2.*C5/(VOV **(2./3.))*C6**(2./3.)
      C11=(C6/VOV )**(4./3.)
      CSQ=C7*(C8+(C9+C10+C11)**(.5))
      C=SQRT(CSQ)
      Y=XX*2.
      CPV(L, 1)=.4*(Y-C)/SQRT(C1*VOV **(2./3.))*(.04*(Y-C)**2/(C1*VOV **
     1(2./3.))-C4/(C1*C3))**.5-DELTA**2+CP1
      IF(Y.GT.C) CPV(L,1)=CP1
      IF(IPRINT.NE.1) GO TO 15
      WRITE(6,13) XB(L),CPV(L, 1),CP1
   13 FORMAT(1X,3F10.5)
   15 DO 10 K1=1,19
      CPV(L,K1)=CPV(L,1)
   10 CONTINUE
      JA=J
      JB=NN
      SUM1=0.
      SUM2=0.
      SUM3=0.
      CALL SIMP
      CB0=2.*SUM1/AREF
      V0=VOV-1.
      IF(V0.LE.0.06) CB1=CB0
      V1=VOVS
   89 CONTINUE
      IF(VOVS.GT.0.95) GO TO 90
      CB0=0.
      GO TO 88
   90 CB0=CB1*(VOVS-.95)/ (V1-.95)
   88 CONTINUE
      CALL INTERP(AM,CA15,VOVS,A0,8,3)
      CALL INTERP(AM,CA2 ,VOVS,A1,8,3)
      CALL INTERP(AM,CA25,VOVS,A2,8,3)
      CALL INTERP(AM,CA3 ,VOVS,A3,8,3)
      CALL INTERP(AM,CA4 ,VOVS,A4,8,3)
      IF(ANL.LE.4.) GO TO 16
      CAN=A4*(1.-.2*(ANL-4.))
      GO TO 17
   16 CALL INTERS(ANL,1.5,2.,2.5,3.,4.,A0,A1,A2,A3,A4,CAN)
   17 CAN=CAN+CB0
   99 RETURN
      END
```

```
      SUBROUTINE TRAPE
      COMMON/GEOM/RP(6),X(30),R(30),C2,N,NSHAPE,N1,N2,XB(225),RB(225)
      COMMON/GEO1/ RBP(225),BETA
      COMMON/CPV/ CPV(225,20),JA,JB
      COMMON/JIS2/ SUM1,SUM2,SUM3,SUM4,SUM5,SUM6
C     THIS SUBROUTINE INTEGRATES THE SURFACE AREA,PLANFORM AREA AND
C    VOLUME BY TRAPEZOIDAL RULE.
      PI=3.14159
      IF(JB.NE.1) GO TO 2
      SUM1=PI*RB(2)*SQRT(RB(2)**2+XB(2)**2)
      SUM2=PI/3.*RB(2)**2*XB(2)
      SUM3=.5*RB(2)*XB(2)
      SUM4=SUM3*2./3.*XB(2)
      GO TO 99
    2 DO 1 I=JA,JB
      DX=XB(I+1)-XB(I)
      SUM1=SUM1+PI*DX*(RB(I)*SQRT(1.+RBP(I)**2)+RB(I+1)*SQRT(1.+RBP(I+1
     1)**2))
      SUM2=SUM2+PI/2.*DX*(RB(I)**2+RB(I+1)**2)
      SUM3=SUM3+DX*(RB(I+1)+RB(I))
      SUM4=SUM4+DX*(XB(I+1)*RB(I+1)+XB(I)*RB(I))
    1 CONTINUE
   99 RETURN
      END
```

```
      SUBROUTINE WAVE
      COMMON/WAVE/CABL,CNBL,CMBL,CAW,CNW,CMW
      COMMON/GEOM/RP(6),X(30),R(30),C2,N,NSHAPE,N1,N2,XB(225),RB(225)
      COMMON/GEO1/ RBP(225),BETA
      COMMON/GEO2/NN1,NN2,NN3,NN4,NFL,NBLUNT,NN,NNI,IPRINT,NN1A
      COMMON/DIS2/SUM1,SUM2,SUM3,SUM4,SUM5,SUM6
      COMMON/CPV/ CPV(225,20),JA,JB
      COMMON/GEO4/K,F,RR,RREF
      COMMON/GEO3/VOVS,AL,XM,YM,XINT,NNIA
      DIMENSION F0(6),F1(6),F2(6),XN(6),RN(6),CPN(6,7),PH(7),RNP(6),AM(9
     1),CP0(9)
      CA2=0.
      CA3=0.
      CA4=0.
      CN2=0.
      CN3=0.
      CN4=0.
      CM2=0.
      CM3=0.
      CM4=0.
      SUM1=0.
      SUM2=0.
      SUM3=0.
      AREF=3.14159*RREF**2
      IF(NBLUNT.EQ.1) GO TO 1
      K=NNI
      K1=NN1
      K2=NN2
      K3=NN3
      K4=NN4
      GO TO 2
    1 K=1
      K1=NN1
      K2=NN2
      K3=NN3
      K4=NN4
      CABL=0.
      CNBL=0.
      CMBL=0.
    2 JA=K
      JB=K1
      CALL SIMP
      CA1= 2.*SUM1/AREF
      CN1=-2.*SUM2/AREF
      CM1= 2.*SUM3/(AREF*2.*RREF)
      SUM1=0.
      SUM2=0.
      SUM3=0.
      IF(NN1.EQ.NN ) GO TO 99
      JA=K1+1
      JB=K2
      CALL SIMP
      CA2= 2.*SUM1/AREF
      CN2=-2.*SUM2/AREF
      CM2= 2.*SUM3/(AREF*2.*RREF)
```

```
      SUM1=0.
      SUM2=0.
      SUM3=0.
      IF(NN2.EQ.NN ) GO TO 99
      JA=K2+1
      JB=K3
      CALL SIMP
      CA3= 2.*SUM1/AREF
      CN3=-2.*SUM2/AREF
      CM3= 2.*SUM3/(AREF*2.*RREF)
      SUM1=0.
      SUM2=0.
      SUM3=0.
      IF(NN3.EQ.NN ) GO TO 99
      JA=K3+1
      JB=K4
      CALL SIMP
      CA4= 2.*SUM1/AREF
      CN4=-2.*SUM2/AREF
      CM4= 2.*SUM3/(AREF*2.*RREF)
   99 CAW= CABL+CA1+CA2+CA3+CA4
      CNW= CNBL+CN1+CN2+CN3+CN4
      CMW=CMBL+CM1+CM2+CM3+CM4
      RETURN
      END
```

E. SAMPLE INPUT DATA SET

The sample case below is the input data cards for the improved 5"/54 projectile[38]. The Formats and parameter locations and definitions have been discussed previously.

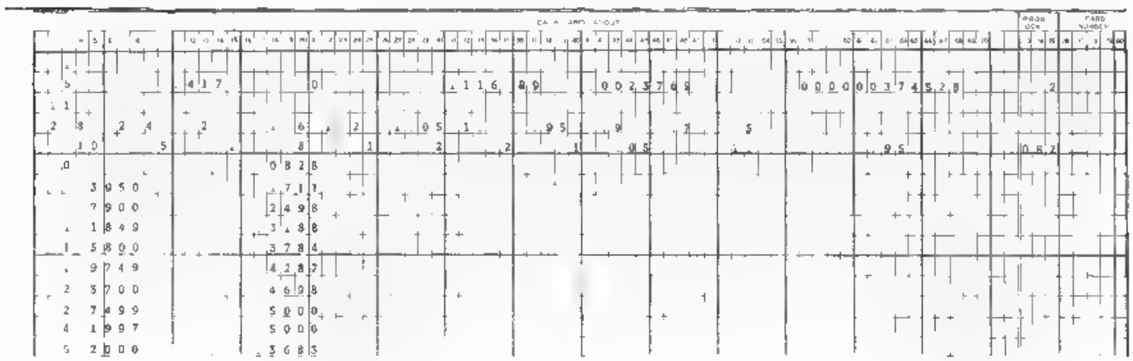

F. SAMPLE OUTPUT

The resulting output for the above input data case is shown below. The reference conditions are printed first followed by the input body coordinates. The last output quantity is a table listing the individual axial force contribution and a table listing the force coefficients.

CASE NO. 1

ANGLE OF ATTACK = .500EGS   REFERENCE DIAMETER = .417FT

REFERENCE CONDITIONS

SPEED OF SOUND = 1116.890 FT/SEC
DENSITY = .0023769 SLUGS/FT3
ABSOLUTE VISCOSITY = .000000374528 LB-SEC/FT2

BODY COORDINATES

X	R
0.0000	.0828
.3950	.1711
.7900	.2498
1.1849	.3188
1.5800	.3784
1.9749	.4287
2.3700	.4698
2.7499	.5000
4.1997	.5000
5.2000	.3683

AXIAL FORCE CONTRIBUTIONS

MACH NO.	SKIN FRICTION	BASE PRESSURE	PRESSURE	PROTRUSIONS	TOTAL
2.800	.0274	.0585	.1063	0.0000	.1922
2.400	.0302	.0666	.1169	0.0000	.2155
2.000	.0332	.0842	.1286	0.0000	.2460
1.600	.0369	.1023	.1415	0.0000	.2397
1.200	.0409	.1227	.1569	0.0000	.3205
1.050	.0426	.1232	.1527	0.0000	.3195
1.000	.0432	.1176	.0921	0.0000	.2529
.950	.0438	.1037	.0304	0.0000	.1779
.900	.0444	.0866	.0030	0.0000	.1540
.700	.0472	.0731	0.0000	0.0000	.1204
.500	.0507	.0698	0.0000	0.0000	.1204

FORCE COEFFICIENTS

MACH NO.	CD	CN	CL	CM	CNAL	CMAL	XCP/D
2.800	.1924	.0246	.0230	-.049	2.823	-5.032	1.9951
2.400	.2158	.0227	.0208	-.040	2.605	-4.622	1.7743
2.000	.2462	.0205	.0184	-.030	2.350	-3.458	1.4717
1.600	.2618	.0171	.0147	-.017	1.961	-1.953	.9957
1.200	.3206	.0131	.0103	-.003	1.496	-.389	.2604
1.050	.3186	.0126	.0099	.004	1.448	.494	-.3409
1.000	.2530	.0120	.0090	.009	1.372	.972	-.7128
.950	.1780	.0116	.0101	.011	1.332	1.301	-.9772
.900	.1341	.0118	.0107	.010	1.357	1.163	-.8610
.700	.1205	.0119	.0109	-.002	1.366	-.222	.1527
.500	.1205	.0120	.0110	-.005	1.376	-.526	.3822

APPENDIX C

DISTRIBUTION

Commander, Naval Ordnance Systems Command
Washington, D. C. 20360
Attn: ORD-03, Mr. Oscar Seidman
Mr. Lionel Pasiuk
Mr. Zeig Levinstein
ORD-55, Mr. W. Greenlease
Technical Library (2)

Commander, Naval Material Command
Washington, D. C. 20360
Attn: Dr. John Huth
Technical Library (2)

Commander, Naval Air Systems Command
Washington, D. C. 20360
Attn: Mr. William Volz
Technical Library (2)

Commander, Naval Ordnance Laboratory
White Oak, Silver Spring, Maryland 20910
Attn: Dr. J. Anderson
Dr. A. Seigler
Mr. Sam Hastings
Mr. Frank Regan
Technical Library (2)

Commander, Naval Weapons Center
China Lake, California 93555
Attn: Dr. W. R. Haseltine
Mr. Ray Van Aken
Mr. D. Meeker
Technical Library (2)

Commanding Officer, Naval Missile Center
Point Mugu, California 93041
Attn: Technical Library (2)

Commander, Naval Ship Research and Development Center
Washington, D. C. 20007
Attn: Dr. T. C. Tai
Mr. E. N. Brooks
Technical Library (2)

Commander, Naval Weapons Center
Corona Laboratories
Corona, California 91720
Attn: Technical Library (2)

Office of Naval Research
Pentagon
Washington, D. C.
Attn: Mr. Mort Cooper
Technical Library (2)

Commanding Officer and Director
Naval Ship Research & Development Center
Carderock, Maryland
Attn: Technical Library (2)

Deputy Chief of Naval Operations
(Development)
The Pentagon
Washington, D. C. 20350
Attn: Technical Library (2)

Commanding Officer
Naval Air Development Center
Warminster, Pa. 18974
Attn: Technical Library (2)

Commanding Officer
Naval Air Development Center
Aeronautical Structures Department
Philadelphia, Pa. 19112
Attn: Technical Library (2)

Chief of Naval Research
Department of the Navy
Washington, D. C. 20360
Attn: Technical Library (2)

Commander
Pacific Missile Range
U. S. Naval Missile Center
Point Mugu, California 93041
Attn: Technical Library (2)

Director
Naval Strategic Systems Projects Office (PM-1)
Department of the Navy
Washington, D. C. 20360
Attn: Technical Library (2)

Superintendent
U. S. Naval Academy
Annapolis, Maryland 21402
Attn: Head, Weapons Department
Head, Science Department
Technical Library (2)

Superintendent
U. S. Naval Postgraduate School
Monterey, California 95076
Attn: Head, Mechanical Engineering Dept.
Head, Department of Aeronautics
Technical Library (2)

Officer in Charge
U. S. Naval Scientific and Technical Intelligence Center
U. S. Naval Observatory
Washington, D. C. 20360
Attn: Technical Library (2)

Commander
Naval Undersea Warfare Center
3203 East Foothill Blvd.
Pasadena, California 91107
Attn: Technical Library (2)

Commanding Officer
Naval Ordnance Station
Indian Head, Maryland 20640
Attn: Technical Library (2)

Commandant of the Marine Corps
Headquarters, Marine Corps
Washington, D. C. 20380
Attn: Code AX (2)
Code A04F (2)
Code A03H
Technical Library (2)

Director, Development Center
Marine Corps Development and Education Command
Quantico, Virginia 22134

Chief of S and R Division
Development Center
Marine Corps Development and Education Command
Quantico, Virignia 22134

Chief of Air Operations Division
Development Center
Marine Corps Development and Education Command
Quantico, Virginia 22134

Chief of Ground Operations Division
Development Center
Marine Corps Development and Education Command
Quantico, Virginia 22134

Marine Corps Liaison Officer
Field Artillery Board
Fort Sill, Oklahoma 73503
Attn: Technical Library (2)

Commanding General, Ballistic Research Laboratory
Aberdeen Proving Ground, Maryland 21005
Attn: Dr. C. H. Murphy
Mr. L. McAllister
Mr. B. McCoy
Technical Library (2)

Commanding General, Picatinny Arsenal
Dover, New Jersey
Attn: Mr. A. Loeb
Technical Library (2)

Commanding General, U. S. Army Missile Command
Redstone Arsenal, Alabama 35809
Attn: Mr. Ray Deep
Dr. D. J. Spring
Technical Library (2)

Commanding General,
U. S. Army Material Command AMCRD-TP
Washington, D. C. 20315
Attn: Mr. Joseph M. Hughes
Technical Library (2)

Office of Chief of Research and Development
Washington, D. C. 20310
Attn: Major R. A. Burns
Technical Library (2)

Commanding Officer
Army Chemical Center
Edgewood, Maryland 21040
Attn: Technical Library (2)

Chief of Ordnance
U. S. Army
Washington, D. C. 20310
Attn: Technical Library (2)

Commanding General
Frankford Arsenal
Philadelphia, Pa. 19104
Attn: Technical Library (2)

Commanding Officer
Harry Diamond Laboratories
Washington, D. C. 20013
Attn: Mr. R. Warren
Technical Library (2)

CO of U. S. Army Combat Development Command
Field Artillery Agency
Fort Sill, Oklahoma
Attn: Technical Library (2)

President of U. S. Army Field Artillery Board
Fort Sill, Oklahoma 73503
Attn: Technical Library (2)

Aeronautical Research Laboratory
Wright-Patterson AF Base
Dayton, Ohio 45433
Attn: Technical Library (2)

Aeronautical System Division
USAF
Wright-Patterson AF Base
Dayton, Ohio 45433
Attn: Technical Library (2)

AF Office of Scientific Research
Washington, D. C. 20330
Attn: Technical Library (2)

Arnold Engineering Development Center
USAF
Tullahoma, Tennessee 37389
Attn: Technical Library (2)

Ballistic Systems Division
USAF
AF Unit PO
Los Angeles, California 90053
Attn: Technical Library (2)

Headquarters, USAF
Systems Command
Andrews AF Base, Md. 20331
Attn: Technical Library (2)

Headquarters, USAF
Washington, D. C. 20330
Attn: Technical Library (2)

Flight Research Center
Edwards AF Base, California 93523
Attn: Technical Library (2)

Space Systems Division
USAF
AF Unit PO
Los Angeles, California 90053
Attn: Technical Library (2)

U. S. Air Force Systems Command Regional Offices
c/o Department of the Navy
Washington, D. C. 20360
Attn: Technical Library (2)

AFATL (ADLRA)
Eglin Air Force Base, Florida 32542
Attn: Mr. C. Butler
Mr. F. Burgess
Mr. C. Matthews
Technical Library (2)

USAF Academy
Colorado Springs, Colorado 80912
Attn: Technical Library (2)

Wright Air Development Center
Wright-Patterson AF Base, Ohio 45433
Attn: Technical Library (2)

Applied Physics Laboratory
The Johns Hopkins University
8621 Georgia Avenue
Silver Spring, Maryland 20910
Attn: Dr. L. L. Cronvich
Mr. Freeman K. Hill
Mr. Edward T. Marley
Dr. Gordon Dugger
Technical Library (2)

Advanced Research Projects Agency
Department of Defense
Washington, D. C. 20305
Attn: Technical Library (2)

Director, Defense Research & Engineering
Department of Defense
Washington, D. C. 20305
Attn: Technical Library (2)

George C. Marshal Space Flight Center
Huntsville, Alabama 35804
Attn: Technical Library (2)

NASA Goddard Space Center
Greenbelt, Maryland 20771
Attn: Technical Library (2)

NASA Lewis Research Center
Cleveland, Ohio 44101
Attn: Technical Library (2)

NASA
Washington, D. C. 20546
Attn: Technical Library (2)

NASA Ames Research Center
Moffett Field, California
Attn: Mr. Vic Peterson
Mr. John Rakich
Dr. E. Murman
Technical Library (2)

NASA Langley Research Center
Langley Station, Hampton, Virginia
Attn: Mr. Leroy Spearman
Mr. C. M. Jackson, Jr.
Mr. W. C. Sawyer
Technical Library (2)

Virginia Polytechnic Institute and State University
Department of Aerospace Engineering
Blacksburg, Virginia
Attn: Prof. J. A. Schetz
Technical Library (2)

Stanford Research Institute
Menlo Park, California 94025
Attn: Dr. Milton Van Dyke
Technical Library (2)

North Carolina State University
Department of Mechanical and Aerospace Engineering
Box 5246
Raleigh, North Caroline 27607
Attn: Prof. F. R. DeJarnette
Technical Library (2)

The University of Tennessee Space Institute
Tullahoma, Tennessee
Attn: Dr. B. H. Goethert
Dr. J. M. Wu
Technical Library (2)

Defense Documentation Center
Cameron Station
Alexandria, Virginia 21314 (12)

LOCAL:

D
G
K
F
E
T
C-2
GT
ET
FT
GR
GX
GP
GA
GB (5)

GC
GW
KB
GBA
GBC
GBJ (5)
GBW
GBR
GBJ (Moore) (40)
KBB (5)
Technical Library (2)

UNCLASSIFIED
Security Classification

DOCUMENT CONTROL DATA - R & D

(Security classification of title, body of abstract and indexing annotation must be entered when the overall report is classified)

1. ORIGINATING ACTIVITY (Corporate author) Naval Weapons Laboratory Dahlgren, Virginia 22448	2a. REPORT SECURITY CLASSIFICATION UNCLASSIFIED 2b. GROUP

3. REPORT TITLE

BODY ALONE AERODYNAMICS OF GUIDED AND UNGUIDED PROJECTILES AT SUBSONIC, TRANSONIC AND SUPERSONIC MACH NUMBERS

4. DESCRIPTIVE NOTES (Type of report and inclusive dates)

5. AUTHOR(S) (First name, middle initial, last name)

Frank G. Moore

6. REPORT DATE November 1972	7a. TOTAL NO. OF PAGES	7b. NO. OF REFS
8a. CONTRACT OR GRANT NO. b. PROJECT NO. c. d.	9a. ORIGINATOR'S REPORT NUMBER(S) TR-2796 9b. OTHER REPORT NO(S) (Any other numbers that may be assigned this report)	

10. DISTRIBUTION STATEMENT

Distribution approved for public release, distribution unlimited.

11. SUPPLEMENTARY NOTES	12. SPONSORING MILITARY ACTIVITY

13. ABSTRACT

Several theoretical and empirical methods are combined into a single computer program to predict lift, drag, and center of pressure on bodies of revolution at subsonic, transonic, and supersonic Mach numbers. The body geometries can be quite general in that pointed, spherically blunt, or truncated noses are allowed as well as discontinuities in nose shape. Particular emphasis is placed on methods which yield accuracies of ninety percent or better for most configurations but yet are computationally fast. Theoretical and experimental results are presented for several projectiles and a computer program listing is included as an appendix.

U.S. NAVAL WEAPONS LABORATORY
SCIENTIFIC, TECHNICAL and ADMINISTRATIVE PUBLICATIONS

TECHNICAL REPORTS: Scientific and technical information on the work of the Laboratory for general distribution.

TECHNICAL NOTES: Preliminary or partial scientific and technical information, or information of limited interest, for distribution within the Laboratory.

CONTRACTOR REPORTS: Information generated in connection with Laboratory contracts and released under NWL auspices.

ADMINISTRATIVE REPORTS: Administrative information on the work, plans and proposals of the Laboratory.

ADMINISTRATIVE NOTES: Preliminary or partial administrative information, or information of limited interest, for distribution within the Laboratory.

Details on the availability of these publications may be obtained from:

TECHNICAL LIBRARY
U. S. NAVAL WEAPONS LABORATORY
DAHLGREN, VIRGINIA 22448